3-10-2010

Increasing the Sensitivity of Surface Acoustic Wave (SAW) Chemical Sensors and other Chemical Sensing Investigations

Nina R. Smith

INCREASING THE SENSITIVITY OF SURFACE ACOUSTIC WAVE (SAW) CHEMICAL SENSORS AND OTHER CHEMICAL SENSING INVESTIGATIONS

THESIS

Nina R. Smith, 2nd Lieutenant, USAF

AFIT/GE/ENG/10-28

DEPARTMENT OF THE AIR FORCE

AIR UNIVERSITY

AIR FORCE INSTITUTE OF TECHNOLOGY

Wright-Patterson Air Force Base, Ohio

The views expressed in this thesis are those of the author and do not reflect the official policy or position of the United States Air Force, Department of Defense, or the U.S. Government.

AFIT/GE/ENG/10-28

INCREASING THE SENSITIVITY OF SURFACE ACOUSTIC WAVE (SAW) CHEMICAL SENSORS AND OTHER CHEMICAL SENSING INVESTIGATIONS

THESIS

Presented to the Faculty

Department of Electrical and Computer Engineering

Graduate School of Engineering and Management

Air Force Institute of Technology

Air University

Air Education and Training Command

In Partial Fulfillment of the Requirements for the

Degree of Master of Science in Electrical Engineering

Nina R. Smith, BSEE

2nd Lieutenant, USAF

March 2010

AFIT/GE/ENG/10-28

INCREASING THE SENSITIVITY OF SURFACE ACOUSTIC WAVE (SAW) CHEMICAL SENSORS AND OTHER CHEMICAL SENSING INVESTIGATIONS

Nina R. Smith, BSEE

2nd Lieutenant, USAF

Approved:

//SIGNED//	8 Mar 10
Ronald A. Coutu, Jr., Ph.D., P.E. (Chairman)	Date
//SIGNED//	8 Mar 10
LaVern A. Starman, Maj, Ph.D., USAF (Member)	Date
//SIGNED//	8 Mar 10
Yong C. Kim, Ph.D. (Member)	Date

Abstract

The work involves the fabrication and testing of three different surface acoustic wave (SAW) device designs, an investigation of nanowires sensitive to chemicals and preconcentrator prototypes to include with chemical sensors. SAW devices are microelectromechanical systems (MEMS) that use a piezoelectric substrate to propagate a surface wave. The propagation of the surface wave is affected by chemicals in the air if the surface of the substrate is coated with a chemically sensitive polymer.

The SAW chemical sensor designs include modifications to a basic SAW device to see if sensitivity is increased. The modifications consist of etched trenches between the two transducer fields of the device, coating the device with carbon nanotubes (CNTs) under the chemically sensitive layer and coating CNTs on top of the chemically sensitive layer. SAW devices are coated with Nafion®, a polymer sensitive to ethanol. The devices are tested in a sealed probe chamber that is flooded with ethanol. The comparison of frequency shifts of the magnitude and phase responses indicates that trenches etched between the transducer fields increase the sensitivity of the SAW devices. The increase of sensitivity is signified by a shift of peak frequency of an extra 100kHz over the unaltered device after five minutes of flowing ethanol. The CNT coatings make the SAW devices less sensitive to chemical concentrations in the air.

Another aspect of the research involves the investigation of nanowires that have been shown to be sensitive to chemicals. Testing of the nanowires involves measuring the

resistance of palladium, polypyrrole and polyaniline nanowires. The nanowires need to be measured with currents of less than 5μA and 10mV. Investigation of the nanowires indicates that they are less suited to detecting chemicals in a non-ideal measurement circumstance than SAW devices.

Preconcentrators are another way to improve the sensitivity of chemical sensors. Some preconcentrator prototypes fabricated in the polysilicon multi-user MEMS process (PolyMUMPs™) system are tested and evaluated for heating characteristics and abilities. Fabricating preconcentrators with the PolyMUMPs™ system is an effective way to produce many preconcentrators that exhibit small feature sizes and good heating capabilities. A grid pattern presents the best way to heat a large surface area the most uniformly. Coating the devices with CNTs also increases the heat to which devices can be heated and decreases the amount of time that it takes to heat the devices.

Acknowledgments

I would like to thank the members of my thesis committee for their guidance and inputs and the various labs at AFIT and AFRL that allowed me to use their facilities and equipment for fabrication and testing of my devices. I would also like to thank my Mother, my Father, and all my family members for their continued support and guidance throughout the years. Without the values they instilled in me from the beginning, I would never have accomplished this thesis. In addition, thanks go to my fiancé for his support and confidence in me. Congratulations also go to him for finishing his thesis. I wish to acknowledge all my friends and family who believe in me and love me. Thank you all for your smiles and friendships. I also wish I could acknowledge all of the researchers who have worked in this field. If not for their work, I would not have accomplished so much. So thank you to researchers in the MEMS and chemical sensing sciences, you are all very talented and dedicated to the field and will continue to influence the research of others. Also, thanks to my peers and coworkers for sharing pictures of the equipment and providing support to finish this document.

Nina R. Smith

Table of Contents

	Page
Abstract	iv
Acknowledgments	vi
Table of Contents	vii
List of Figures	ix
List of Tables	xii
List of Acronyms	xiii
I. Introduction	1
1.1 Motivation	1
1.2 Goals and Objective	3
1.3 Approach	4
1.4 Thesis Overview	7
II. Literature Review	8
2.1 Chemical Sensor Overview	8
2.2 SAW Chemical Sensors	14
2.3 Preconcentrators	19
2.4 Nanowires	25
2.5 Microfabrication Processes	26
2.6 Previous Work at AFIT	30
2.7 Summary	31
III. Models and Methodology	32
3.1 System Boundaries	32
3.2 System Output	35
3.3 Workload	36
3.4 Performance Metrics	37
3.5 System Parameters	38
3.6 Factors Under Investigation	40
3.7 Evaluation Technique	42

3.8 Methodology Summary 45
IV. Cleanroom Fabrication 46
4.1 Introduction 46
4.2 Overview of SAW Device Fabrication 46
4.3 Cleaning and Photoresist Deposition 47
4.3 Mask Layer 1: IDT Fields Exposing and Developing 49
4.4 Metal Deposition and Lift Off 53
4.5 Mask Layer 2: Trenches Etching and Aligning 55
4.6 Chemical Sensitive Layer and CNT Deposition 58
4.7 Nanowire Fabrication 61
4.8 Fabrication Summary and Results 63
V. Results and Analysis 66
5.1 Experimental Set-Up Data Gathering 66
5.2 Results from Large 3μm Devices 69
5.3 Analysis of SAW Device Tests 73
5.4 Nanowire Test Results 76
5.5 Results of Preconcentrator Tests 80
VI. Conclusions and Recommendations 92
6.1 Summary of Contributions 94
6.2 Suggestions for Future Study 95
Appendix A: SAW Fabrication Process 97
Section A1: L-edit Patterns 97
Section A2: Fabrication Steps 100
Appendix B: Network Analyzer Data 103
Section B1: 3μm Size Comparisons 103
Section B2: 2μm Device Graphs 110
Section B3: AFRL Device Data 112
Section B4: Large 3μm Devices, Propagation Field Alterations 113
Appendix C Lessons Learned 126
Bibliography 127

List of Figures

Figure		Page
1.	Modifications to SAW devices under investigation	5
2.	Schematic sketches of the four types of acoustic sensors	9
3.	Schematic for the µChemLab™ gas-phase chemical analysis system	12
4.	Micromachined gas chromatograph used for µChemLab™	13
5.	SAW Operation	15
6.	A Chromatogram showing successful separation of 30 organic vapors	22
7.	Preconcentrator with three stages to absorb different types of particles	23
8.	Preconcentrator patterns depicted as Poly0 layer of MUMPs	24
9.	PolyMUMPs™ fabrication process	25
10.	Photolithography process.	28
11.	DRIE process	30
12.	Surface acoustic wave chemical sensor system diagram	33
13.	Nanowire system diagram	34
14.	Preconcentrator system diagram	34
15.	Preconcentrator designs	42
16.	Illustration of four point probe method of resistance measurement	44
17.	Photolitography and metal lift off process	47
18.	Spinner and hot plate station in AFIT clean room	48
19.	AFIT EVG 620 Mask Aligner	50
20.	Development	52
21.	Plasma Asher	53
22.	AFIT Denton DV-502A E-Beam Evaporator for thin metal deposition	54
23.	Karl Suss MJB3 mask aligner in AFIT cleanroom	57
24.	Nanowire Channel and Electrode Gap	62
25.	Nanowire of Sample 504, a PANI nanowire	62
26.	Two images of the final product, devices with a Nafion® coating	64
27.	MMR Technologies Inc, probe station chamber model LTMP-4	66
28.	Owlstone OVG, Chamber, Network Analyzer and Keithley 4200	67

29. Owlstone OVG-4 used to regulate the flow of nitrogen 68
30. Schematic of SAW connection to network analyzer 69
31. Magnitude traces for an unmodified SAW device during ethanol exposure 70
32. Phase traces for an unmodified SAW device during ethanol exposure 71
33. Magnitude traces of an unaltered SAW device recovery 72
34. Phase traces of an unaltered SAW device recovery 72
35. Two point probe measurement of PPy nanowire 78
36. Four point probe measurement of PPy nanowire 78
37. QFI Multi-Sensor Microscope System to provide IR images 82
38. Lines of Poly1-Poly2 stack 83
39. Bowtie Pattern, Poly1-Poly2 stack 84
40. Bowtie Pattern, Poly1-Poly2 stack 84
41. Grid Pattern, Poly 85
42. Ladder Pattern, Poly 0 86
43. 6µm Spiral, Poly1-Poly2 stack 87
44 Bowties with CNTs, Poly1-Poly2 stack 88
45. Ladder Pattern with CNTs, Poly2 89
46. Bars pattern, Poly1 after heating 90
47. Broken Poly1 bars due to heating and bending of Poly1 layer 90
A1. 2µm Finger SAW Device Pattern 97
A2. 2µm Finger Device, Bond Pad and Finger Intersection 98
A3. Medium 3µm Finger SAW Device Pattern 99
A4. Development Photographs 101
A5. Metalized Sample Images 102
A6. Example of IDT Pattern 102
B1. 3µm Small, Sample M, 5% wt Nafion®, Magnitude 104
B2. 3µm Small, Sample M, 5% wt Nafion®, Phase 105
B3. 3µm Medium, Sample M, 5% wt Nafion®, Magnitude 106
B4. 3µm Medium, Sample M, 5% wt Nafion®, Phase 107
B5. 3µm Large, Sample M, 5%wt Nafion®, Magnitude 108
B6. 3µm Large, Sample M, 5% wt Nafion®, Phase 109

B7. 2μm Fingers, Sample H, no Nafion®, Magnitude 111
B8. 2μm Fingers, Sample H, no Nafion®, Phase 112
B9. Sample N Magnitude and Phase Traces 115
B10. Sample F Magnitude and Phase Plots 117
B11. Sample M Magnitude and Phase Plot 119
B12. Sample Z4, a zinc oxide sample with no trenches 121
B13. Sample Z1, Six Trench Device 123
B14. Sample Z1 a Twelve Trench Device 125

List of Tables

Table		Page
1.	SAW device pattern sizes on masks for fabrication	39
2.	Factor levels and values for SAW devices	41
3.	Nanowire Samples	63
4.	Samples Tested	64
5.	Frequency and Magnitude Differences for Samples	74
6.	Frequency and Phase Differences for Samples	76

List of Acronyms

Acronym	Definition
AC	Alternating Current
AFIT	Air Force Institute of Technology
AFRL	Air Force Research Laboratory
BOE	Buffered Oxide Etch
CNT	Carbon Nanotube
DC	Direct Current
DRIE	Deep Reactive Ion Etching
HCl	Hydrochloric Acid
HF	Hydrofluoric Acid
IC	Integrated Circuit
IR	Infrared
ITO	Indium Tin Oxide
$LiNbO_3$	Lithium Niobate
MEMS	Microelectromechanical Systems
OVG-4	Owlstone Vapor Generator Model Number
PANI	Polyaniline
Pd	Palladium
PolyMUMPs™	Polysilicon Multi-User MEMS Process
PPy	Polypyrrole
SAW	Surface Acoustic Wave
SNL	Sandia National Laboratory
TSM	Thickness-Shear Mode
QFI	Quantum Focus Instruments

Increasing the Sensitivity of Surface Acoustic Wave (SAW) Chemical Sensors and other Chemical Sensing Investigations

I. Introduction

The work in this thesis focuses on testing of Surface Acoustic Wave (SAW) devices by measuring their frequency responses while ethanol is run through a chamber. Other investigations include the investigation of nanowires and their sensitivity to chemicals by measuring their resistance. Some preconcentrator prototypes are also investigated for their heating characteristics by using thermal imaging equipment. This chapter describes the motivation for the work, the goals and objective, the approach to the work and a thesis overview.

1.1 Motivation

Chemicals are present in everyday life and can be one of the first indicators of harmful toxins in the air. Recognizing harmful chemicals at lower levels provides earlier warnings. The ability to identify specific chemicals allows for better knowledge and situational awareness. If warfighters or medical personnel know better what sort of chemicals are present, they can better defend and work against the chemicals.

For humans, sensing chemicals is usually dependent on a sense of smell. Humans often use dogs to detect substances because of a dog's superior sense of smell; however, a dog's capability is also limited. Dogs cannot specifically identify the level of chemical present, relay exactly what the chemical is and cannot be introduced to known dangerous

environments. Much like other tasks, humans are finding ways to use technology to fill the gaps in their knowledge of the world.

Optical characteristics of chemicals have often been used for chemical identification through spectroscopy practices. However, for use with computer technologies, the chemical information must be converted into an electrical equivalent. One transducing technology that is very popular for many different applications are microelectromechanical systems (MEMS) technologies. The small size of MEMS makes them sensitive to minute changes and low concentrations of chemicals. Nevertheless, the mechanical parts are not sensitive to chemicals on their own. A chemically reactive polymer or substance must coat the mechanical piece so that chemicals will accumulate on the piece and cause a physical change to the system. The changes in the mechanical piece affect a change to electrical signals.

Work at the Air Force Research Laboratory (AFRL) focuses on using SAW devices to detect chemicals. The devices depend on the propagation of surface waves, an input of oscillating waves and measuring the output wave. Coating the devices with polymers or biological substances makes the SAW devices sensitive to chemicals because the chemicals change the characteristics of the coating substance, which changes the propagation of the wave. Different coatings make the devices sensitive to different chemicals. The changes in the output wave are observed and relate to the chemical varieties and concentrations to which the device is exposed.

Requirements for the thesis included experimenting with alterations to the SAW propagation field. The thesis work includes fabrication and testing of the devices with

different levels of chemical concentration and testing nanowire chemical sensors fabricated at the University of Pittsburgh. The measurements of detection levels of the SAW devices and nanowires qualitatively and quantitatively compare the various configurations and chemical sensing methods. The work also introduces some preconcentrator designs that may help the sensors detect lower concentration levels.

1.2 Goals and Objective

The primary goal of the work is to increase the sensitivity of the SAW device developed at the Air Force Institute of Technology (AFIT) and AFRL and perform multiple tests that verify the ability to sense chemicals. SAW devices under investigation are patterned with 3μm finger widths and 85, 150, and 300μm apertures. Some devices with 2μm finger widths and 400μm apertures are briefly investigated because of past work done at AFIT [1]. Increased sensitivity is recognized as an identifiable change in the output wave at a lower chemical concentration level.

In an effort to increase the sensitivity of SAW devices this work investigates some modifications to the basic SAW device design. The changes include etching trenches parallel to the surface wave propagation, coating carbon nanotubes (CNTs) under the chemically sensitive layer and coating CNTs on top of the sensitive layer. The objective is to produce testing results that show if the structure of the propagation field affects the sensitivity of the device and if the sensitivity is improved by the adjustments to the propagation field. The SAW devices are fabricated in the AFIT cleanroom and tested in a sealed probe station into which chemicals are introduced. Some changes to the

fabrication process laid out in previous work are made to reduce the time and increase device yield [1].

A second objective of the work is the testing of several nanowire configurations developed and fabricated at the University of Pittsburgh. Nanowires have been shown to exhibit changes in resistance when exposed to different chemical environments [2]. The testing aims to determine the changes in resistance of nanowires when exposed to various chemicals. By including some tests of nanowires with this chemical sensing work, one can see how the two different sensing methods compare.

A final objective is to look at the possibility of adding a preconcentrator to the SAW device system. Preconcentrators require a different type of absorbent coating and direct current (DC) voltage input to heat them. The investigation of preconcentrators focuses on what pattern is best for uniformly heating a preconcentrator plate and what affect coating the preconcentrators with carbon nanotubes (CNTs) has on the heating characteristics. Most preconcentrator coatings are carbon based, but have too big of feature sizes for the preconcentrators prototyped, so CNTs are used to mimic a carbon coating on the preconcentrators. Work by other researchers, shows that CNTs exhibit absorptive and desorptive properties, so they are a possible coating for future preconcentrator devices [3, 4].

1.3 Approach

Two principle ideas to make chemical sensors more sensitive are investigated; both deal with altering the characteristics of the propagation field. Changes to the propagation field include etched trenches parallel to wave propagation and the inclusion

of carbon nanotubes (CNTs) on the surface of the substrate and on the surface of the chemically sensitive coating, as shown in Figure 1. The modifications are an attempt to increase the surface area of the chemically sensitive coating so that it can absorb more chemical particles and therefore cause a larger shift in the resonant frequency of the propagating wave.

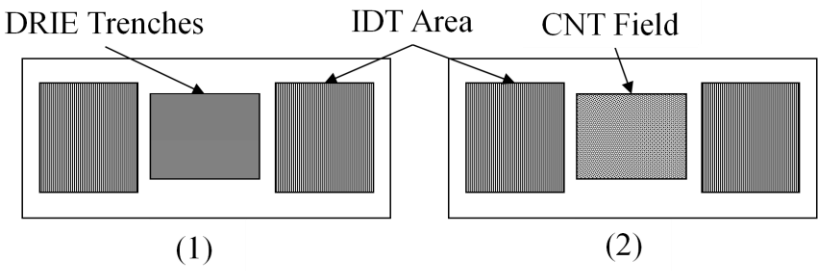

Figure 1 Modifications to SAW devices under investigation, (1) Trenches etched between IDT fields, (2) CNTs deposited on surface of device

Work with the nanowires involves testing the nanowires fabricated by the University of Pittsburgh in the probe station available for SAW device testing. The nanowires are tested for sensitivity to ethanol by measuring the resistance with a semiconductor analyzer. Testing of the nanowires in a different testing set up provides a greater understanding of the new technology and provides a comparison between the SAW technique of chemical sensing and the nanowire chemical sensing device.

Another idea is to include a preconcentrator with the SAW device. Therefore, some preconcentrator designs are prototyped and tested for heating characteristics. Preconcentrators are often used in other chemical detection systems to collect analytes in the air and then introduce the chemicals in a higher concentration to detectors [5]. When concentrated levels of the chemical reach the propagation field for absorption, larger

changes in the propagating wave occur. The result is that the sensors will detect the chemicals even if they exist at low concentrations in the environment. Various preconcentrator designs are available; however, few microscale preconcentrators exist because the carbon coatings used for preconcentrators have feature sizes on a 100μm scale [5]. In addition, preconcentrators benefit from large surface areas for absorbing particles [6]. The carbon and polymer coatings on preconcentrators collect chemicals and then release them when heated. Releasing the chemicals that are absorbed over a period of time in a short pulse introduces the chemicals to the sensor at a higher concentration. In other words, preconcentrators need to heat a large surface area quickly and uniformly because the quicker the heating and the larger the surface area uniformly heated to a high temperature, the higher the concentration of particles released.

Preconcentrators in this work are fabricated using a multi-user MEMS process (MUMPs), specifically the PolyMUMPs™ fabrication process which uses polysilicon layers [7]. The designs are based on a hotplate preconcentrator design. Some of the preconcentrators are coated with CNTs which are meant to mimic other carbon coating materials to absorb and then release the absorbed chemicals when heated. Direct testing of the preconcentrators and the concentrations of chemicals they release is not possible with the testing configurations available at AFIT and AFRL. In addition, due to the limitations of the probe station the preconcentrator patterns cannot be tested individually with the sensors. Testing of the preconcentrators includes heating the preconcentrator prototypes with DC voltage while observing the thermal characteristics of the patterns with an infrared imaging device.

1.4 Thesis Overview

Chapter 2 discusses existing chemical sensing systems, SAW device operation and fabrication, preconcentrator designs and nanowire basics. The discussions of existing technologies include research by Sandia National Laboratories and other colleges. Chapter 3 discusses the methodology for testing of the devices. The chapter provides a description of the system under test and the tests conducted. Chapter 4 shows some of the fabrication steps and clean room work the used in the fabrication of SAW devices under test in this work, includes some pictures of the resulting samples and discusses fabrication difficulties. Chapter 5 presents the results of the tests and an analysis of the findings, discusses the affects of the changes to the propagation field and shows that trenches between the transducer fields of the SAW device increase its sensitivity. Finally, Chapter 6 presents the conclusions and findings of this work and some recommendations for future work. Important findings are that trenches increase the sensitivity of the SAW devices tested by causing an extra 100kHz shift in resonant frequency of the SAW, a grid pattern produces the most uniform heating of a large surface area of a preconcentrator prototype and carbon nanotubes cause a large spike in heating. Additionally, tests on the nanowires show that their sensitivity needs to be tested in various environments and testing configurations to fully understand the changes that occur in nanowires when exposed to chemicals.

II. Literature Review

The following review covers background information relevant to chemicals sensors that use acoustic waves, vapor chemical sensor SAW devices, preconcentrators and nanowires. Section 2.5 describes MEMS fabrication processes and specifically the fabrication processes used in the production of the devices tested in this research such as photolithography, e-beam evaporation, metal lift-off and PolyMUMPs™. Section 2.6 includes a brief description of the work already completed at AFIT relevant to SAW devices.

2.1 Chemical Sensor Overview

2.1.1 Quantifiable Device Characteristics

Important sensor parameters are sensitivity, selectivity, specificity, resolution, reversibility and durability. Sensitivity is a measure of the amount of change to the output signal produced in response to a given concentration of a chemical. Selectivity characterizes the degree to which a sensor distinguishes one chemical from another. Specificity refers to the number of chemicals that a sensor detects or can differentiate between. Resolution is a measure of the minimum change of input quantity to which they can respond. Reversibility relates to how well the device recovers to a neutral state [8].

2.1.2 Sensing Methods

There are many methods of using acoustic waves for sensing applications. Some of the devices include thickness-shear mode resonators, surface acoustic wave devices,

acoustic plate mode devices and flexural plate wave devices. Each device uses a particular acoustic mode.

Acoustic wave sensors are classified by the type of wave propagation mode they use. If the wave propagates through the substrate, it is a bulk wave device. Thickness-Shear Mode (TSM) devices use bulk waves. Waves propagating on the surface of surface wave devices. The number of ports the devices use also distinguishes them from one another. TSM resonators use one port for both input and output, but SAW and flexural plate wave devices use two ports. Figure 2 depicts four of the most common acoustic wave sensors [8].

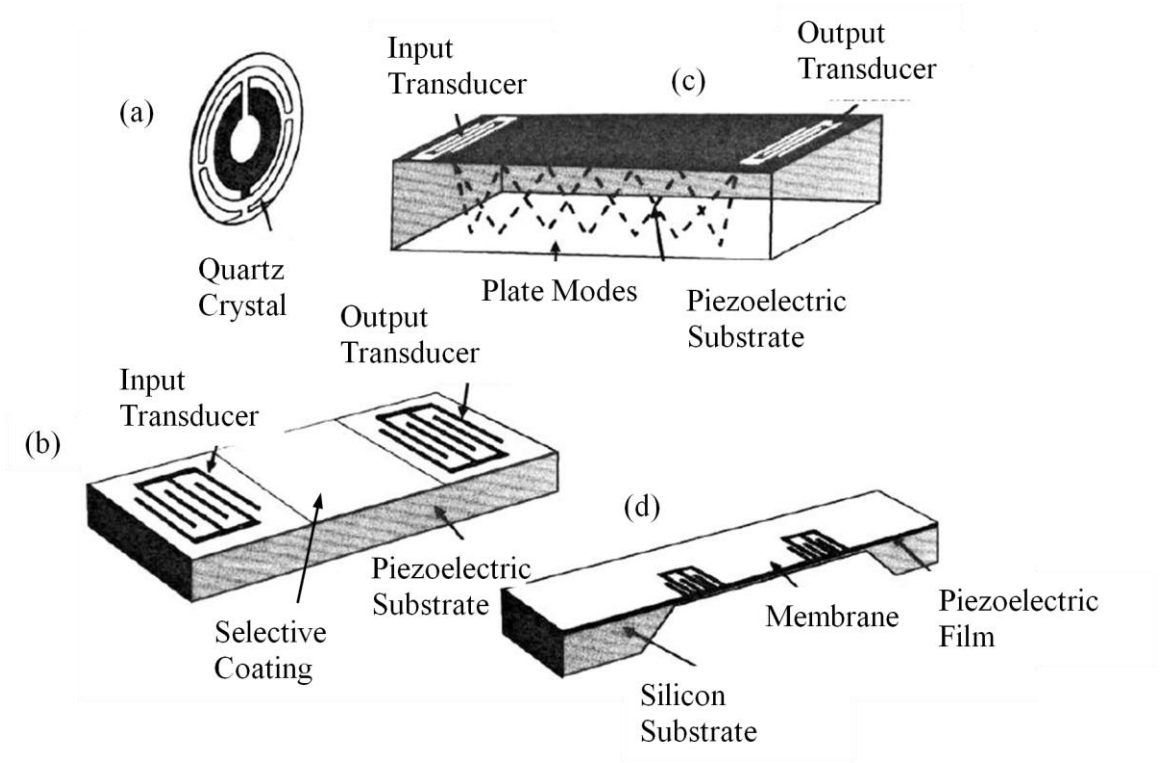

Figure 2 Schematic sketches of the four types of acoustic sensors. (a) Thickness-Shear Mode (TSM) resonator; (b) Surface-Acoustic-Wave (SAW) sensor; (c) Shear-Horizontal Acoustic-Plate_Mode (SH-APM) sensor; and (d) Flexural-Plate-Wave (FPW) sensor [8]

Acoustic wave sensors become chemical sensors when they are coated with a film that serves as a chemical-to-physical transducer. Films have traditionally been polymer substances, but biological coatings have been experimented with for increased selectivity [8, 9]. The films exhibit a change to one or more of their physical properties in response to the presence of the chemical species to be detected. Commonly, chemicals result in an increase in the mass density of the film, a change that arises from accumulation of the chemical species; other possible changes include elastic and electrical properties [8]. Most acoustic devices experience excessive damping when in a liquid environment and function only in a gaseous or vacuum ambient environment. SAW devices are the focus of this thesis, therefore they are the only acoustic wave sensing devices discussed in detail.

2.1.3 Commercial Products

Researchers are continually working on microfabricated chemical sensing systems. Systems are being researched for improvements and better reliability. Some existing systems based on SAW devices include VaporLab, made by Microsensor Systems, and the zNose, made by Electronic Sensor Technology. Other systems include the SAM system by Daimler Chrysler Aerospace and Fox, Centauri by Alpha M.O.S. [9]. One of the most relevant systems for the SAW device research at AFRL is the MicroChemLab developed at Sandia National Laboratory (SNL).

Microsensor Sytems, Inc. is a SAW device developer that has been investigating SAW devices since 1979. The company makes a device known as VaporLab. VaporLab is a handheld, battery-powered chemical vapor identification system that is typically used

for environmental, food and beverage, fragrance and cosmetics, safety exposure and personal monitoring, as well as medical and dental applications [9]. The system uses an array of polymer-coated SAW sensors to accurately detect a broad spectrum of chemical vapors, such as benzene, acrylonitrile, vinyl chloride, 1,3-butadiene and ethylene oxide and costs $10,000 [10]. The company also has other portable devices that detect nerve agents, blood agents and other chemical warfare hazards.

The zNose, developed by Electronic Sensor Technology, is specifically designed to detect explosives. The zNose is a portable system that utilizes a heated column to separate particles and SAW detectors. The detector can analyze samples in 10 seconds and is sensitive to parts per billion [11]. Electronic Sensor Technology also sells a remote sampler designed to collect and preconcentrate air samples. The samples are stored in tubes so that they can be introduced to the detector when the user desires.

Sandia National Laboratory initiated the MicroChemLab program in 1996 to produce a battery-operated, hand-held microanalytical system to detect gas-phase analytes that would provide high-confidence analytical techniques to the field. Also known as the MicroHound^{TM}, the system originally focused on the selective detection of chemical warfare agents; the system now also detects pharmaceutical solvents, petrochemicals, toxic industrial chemicals and tri-halo-methanes [12]. The MicroChemLab system consists of a micromachined preconcentrator (PC), a gas chromatography channel (GC), and a quartz surface acoustic wave array detector. Figure 3 shows a schematic of the MicroChemLab [13].

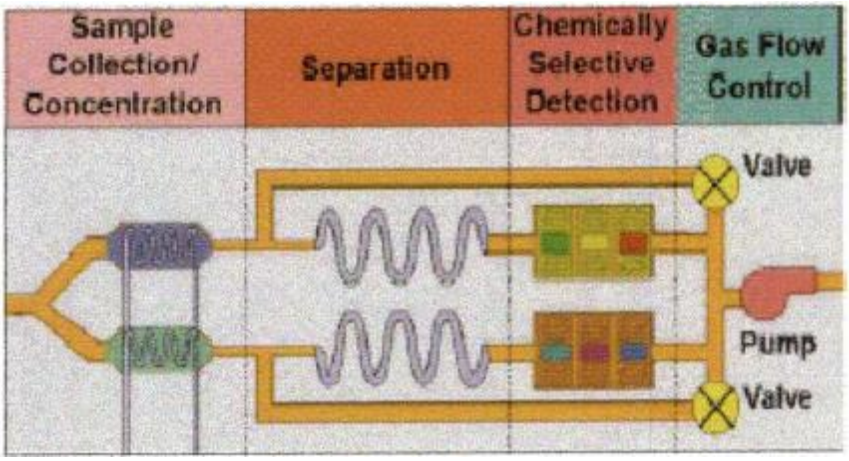

Figure 3 Schematic for the µChemLab™ gas-phase chemical analysis system [13]

In the MicroChemLab, integration of the preconcentrator and gas chromatography channel requires that a magnetically-actuated flexural plate wave sensor (magFPW) array replace the quartz SAW sensor because a magFPW can be fabricated on silicon. SNL uses a 5-layer polysilicon MEMS process known as SwIFT (Surface micromachining with Integrated Fluidic Technology) to fabricate, package and coat a monolithically-integrated MicroChemLab with a PC, GC and magnetically-actuated flexural plate wave sensors.

The MicroChemLab preconcentrator consists of a hotplate design of free-standing silicon nitride membrane and thin-film heater. The chromatography channel reduces the amount of humidity in the sample that reaches the SAW device to reduce the interference of humidity with the SAW. After further development, the MicroChemLab adopted a 3D preconcentrator to increase the surface area on the preconcentrator while maintaining a comparable thermal conductivity [12].

The gas chromatography channels, shown in Figure 4, consists of deep reactive ion etched (DRIE) columns that allow for high volumetric flow rates at reduced gauge pressures [12]. The walls of the GC are coated with a stationary phase that separates chemicals.

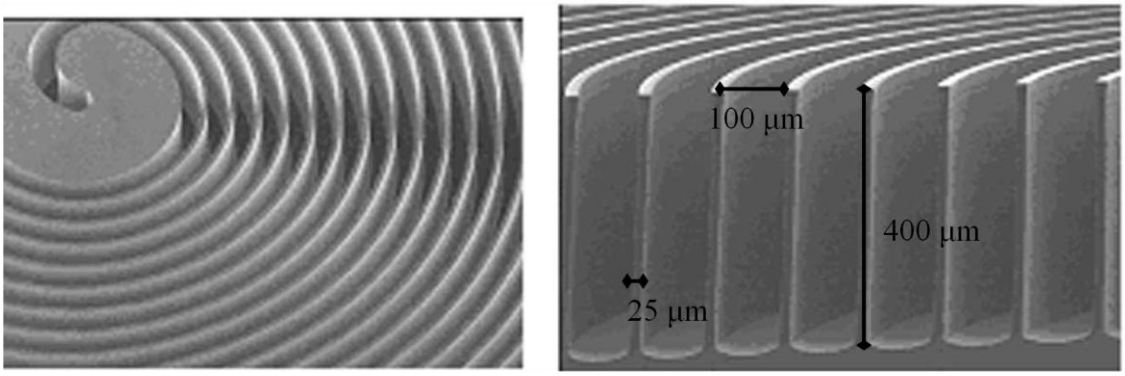

Figure 4 Micromachined (open column) gas chromatograph used for separating analytes in the μChemLab™ chemical analysis system [12]

More details about stationary phases can be found in [12]. Selectivity is determined by the coatings. The SAW sensor devices are monolithically produced with gold evaporation and liftoff on a quartz substrate. Four SAW devices created an array that detected various chemicals based on three coated devices and one uncoated device used as a reference.

The combination of the preconcentrator and chromatography channels reduces the number of false positive readings that are common in field sensing devices. Further developments will involve more powerful detectors and selective materials as well as reduced dead volume and further miniaturization [12].

2.2 SAW Chemical Sensors

Surface acoustic wave chemical sensors use the surface of piezoelectric substrates for wave propagation between two interdigital transducer (IDT) regions. The wave type is also known as Rayleigh wave because Lord Rayleigh discovered the propagation mode in 1887 [8]. Surface electrodes on piezoelectric materials excite waves, which become sensitive to surface perturbations. Most of the acoustic energy of the wave remains confined to within one wavelength of the surface of an isotropic solid. The shorter wavelengths associated result in more acoustic energy closer to the surface, and therefore increased sensitivity. Wave amplitude also affects sensitivity.

R.M. White at the University of California, Berkeley, first showed that lithographically patterned interdigital electrodes on a piezoelectric crystal excite surface acoustic waves [8]. Because of his work, SAW devices are now used in signal-processing applications such as frequency filters, resonators, delay lines, convolvers and correlators. Figure 5 shows a typical electrode pattern for SAW devices [8]. Applying a voltage between alternately connected electrodes causes a periodic electric field on the crystal. The periodic electric field results in movement of the electrodes, which causes a surface acoustic wave on piezoelectric substrates.

SAW devices are used for sensing many different things such as temperature, pressure, torque, mass, dew-point and chemical vapors sensors [14]. Chemical sensing SAW devices use chemically specific coatings that absorb particular chemicals and affect the propagation of surface waves. These coatings are typically polymers that experience a change in mass density due to their absorption of chemical particle in the air.

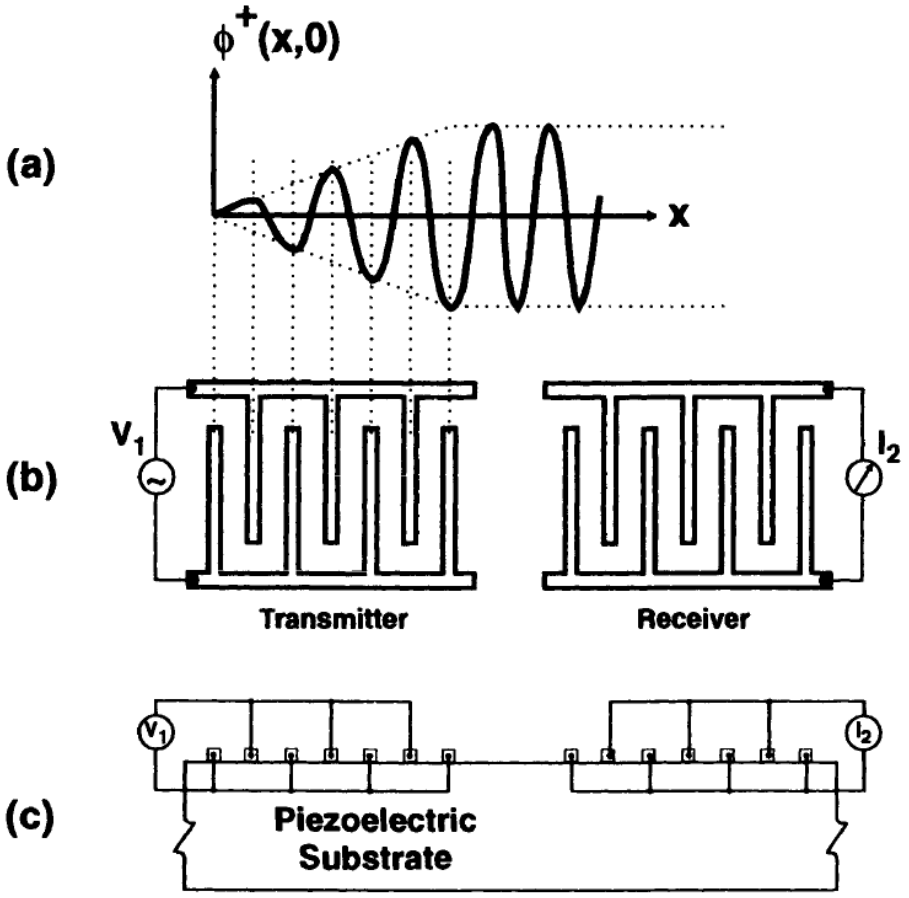

Figure 5 SAW Operation (a) shows the production of a surface acoustic wave due to the transducer field shown in (b), (b) shows the interdigital transducers (IDTs), (c) shows how the IDT inputs and outputs are connected for measurements [8]

2.2.1 Piezoelectric Properties

Wave propagation depends on piezoelectric properties of the substrate. Piezoelectric materials experience stresses and strains when introduced to an electric signal and produce electric signals when they are stressed or strained. Some piezoelectric substrates commonly used for SAW devices are quartz, lithium niobate and gallium

arsenide. Each material propagates waves at a different velocity based on the substrate cut and orientation [8]. SAW devices in this work are on a lithium niobate substrate.

2.2.2 Wave Propagation

A thin film deposited between the transmitter and receiver IDT allows for adsorption of a particular molecule and sensing of mass changing. The mass-induced change in propagation of SAW depends on the input frequency, density of the substrate and propagation velocity of the substrate. Surface particle velocities are dependent on the substrate. Transducer periodicity affects the frequency of waves, given by Equation 1 [15]:

$$f = \frac{v}{\lambda} \tag{1}$$

Where v is the velocity of SAW propagation and λ is the transducer periodicity. Changes in wave propagation can be caused by mass loading, viscoelectic properties of a thin film and electrical conductivity changes induced by sorbed species in a thin film coating. SAW devices are compatible with integrated circuit (IC) fabrication and have good temperature stability and ruggedness [15]. However, when immersed in a liquid, excessive attenuation of surface waves disrupts a SAW device's sensing ability.

The changes in mass produce a change in the velocity. The mass-induced change in SAW propagation velocity is given by Equation 2 [8].

$$\frac{\Delta v}{v_o} = -c_m f_o \rho_s \tag{2}$$

In Equation 2, c_m is the mass sensitivity factor, which depends on the orientation of the substrate and piezoelectric coefficients. The f_0 term in the equation represents the operating frequency and ρ_s is the surface mass density. Ballantine provides greater details and an in depth discussion of sensing mechanics [8].

2.2.3 Interdigital Transducer Fields

The pattern of metal on the device produces the IDT fields. The transducer fingers are modeled as a discrete source for the generation of surface waves in the piezoelectric medium [8]. Performance of the sensor is maximized by altering the length, width, position and thickness of the IDT.

The width of transducer fingers affects the frequency of SAW and shorts between transducer arms causes the transducers not to oscillate, which means that the fingers cannot produce any acoustic activity. Most SAW sensors operate from 25 to 500MHz with wave amplitudes of 10Å [14].

The bandwidth of the SAW is inversely proportional to the number of fingers, N_p, in the IDT field. Equation 3 explains the relationship [8].

$$B=\frac{2}{N_p} \tag{3}$$

A narrow bandwidth is desirable for oscillator applications in order to improve stability [8]. The length of the fingers represents an aperture size which relates to the amount of area affected by the propagating wave.

2.2.4 Chemically Sensitive Coatings

To be chemical sensors, devices depend on a polymer coating that reacts to specific chemicals and changes the way acoustic waves propagate. The changes are measured by a port and interpreted by computations. The thin film coating between transducers determines the type of chemicals the sensor can measure. Forming arrays of sensors coated with different types of polymers allows for detection of many different kinds of chemicals in vapors or solutes [9].

The magnitude of change generally depends on the amount of analyte that reaches the polymer to change its characteristics. One way to increase the amount of analyte that reaches the sensor is to utilize a preconcentrator. Preconcentrators collect certain particles depending on the coating on the preconcentrator. The preconcentrator collects particles and then releases them when heated to provide a chemical sensor with pulses of a concentrated dose of analyte for sensing. This can increase the sensitivity of a chemical sensor and improve the ability of sensors to detect low levels of chemicals in gaseous vapors based on the preconcentrator's concentration factor [16].

The work at AFRL focuses on using a biologically active agent that reacts to chemicals better than polymer coatings. Coating SAW devices is a post processing step that adds time and cost to device manufacturing. The coating used in these experiments is Nafion®, a polymer that is sensitive to ethanol and other alcohols. The name, Nafion®, is a registered trademark of E.I. DuPont de Nemours who first developed the perfluorosulfonic membrane [17].

2.3 Preconcentrators

One of the methods for increasing the sensitivity of a SAW device is to pair it with a preconcentrator. A preconcentrator is designed to collect chemical molecules and then release the molecules as a pulse to provide the SAW device with a higher concentration of chemical molecules. Preconcentrators use a large surface area to trap analytes on a collecting surface, then use a pulse of heat to release the analyte molecules so that there is a higher concentration of analyte molecules in the volume of vapor that reaches the sensor [16].

Various microfabricated preconcentrators exist and are being researched to improve the sensitivity and selectivity of micro-scale chemical sensors. Designs of microfabricated preconcentrators depend on whether the analytical system is meant to detect complex organic mixtures or a specific analyte such as an explosive or a chemical warfare agent. The concentration factor is one of the most significant measures of merit for a preconcentrator [16]. Preconcentrators must be kept small to minimize the energy needed to heat the trap rapidly. Geometry of a preconcentrator must provide low resistance to airflow, but provide enough sorbent bed depth to prevent breakthrough[1] of the vapor. And the sorbent material must be able to efficiently trap and release the target vapors over the operating temperature range of the device [8]. Researchers have found

[1] Breakthrough is defined as when a particular solute pumped continuously through a column will begin to be eluted. It is related to the column volume and the retention factor of the solute. It helps determine the sample capacity of a concentrator for a particular solute [28].

multiple ways to meet these requirements and are experimenting with additional ways to design preconcentrators.

There are some limits to preconcentrators. Some low molecular weight molecules, such as methane, ethane, and propane are not readily trapped by any sorbent layer and cannot be enriched in such a manner [8]. Additionally, high molecular weight vapors are not easily desorbed from a coating and a preconcentrator will diminish the concentration of such particles.

2.3.1 Designs and Stages

The designs of preconcentrators can be based on planar, three dimensional, serpentine microchannel or phased heater arrays. Preconcentrators can also be single stage or multi-stage [16]. Analyte flow can be directed parallel or perpendicular to the preconcentrating device.

Voiculescu et. al has a thorough description of the different types of preconcentrator designs that concludes multi-stage preconcentrators coated with different types of adsorbent materials enhance the efficiency of collection and concentration of organic compounds. Multiple stage preconcentrators also have the highest concentration factor of the preconcentrators that Voiculescu investigated. However, the multiple stage preconcentrators required a more complicated fabrication technique than planar preconcentrators [16].

Voiculescu looks at specific preconcentrators used in different applications and draws comparisons between the devices considered. Each design has trade-offs and

balances between size and heating capacity and speed must be considered for integrating a preconcentrator into a sensing system. 3D structures allow for heating of a larger amount of sorbent material, but may require more energy for heating. Smaller, single-stage devices may provide shorter pulses of concentrated analyte. For example, a preconcentrator based on a perforated polyimide hotplate that is 6mm x 6mm uses less power than a multiple-stage preconcentrator with dimensions of 9mm x 3mm and still offers a high concentration factor and an easy fabrication process. In contrast, the preconcentrator fabricated with CMOS technology has dimensions of 3.4mm x 3.4mm and a low fabrication cost and electric power, but a lower concentration factor. Preconcentrator designs chosen should depend on the sensing system with which it is being integrated [16].

Researchers at the University of Michigan have multiple publications on a multiple-stage microfabricated preconcentrator-focuser for micro gas chromatography system [18-20]. Their work involves a three stage device designed to capture compounds spanning four orders of magnitude in volatility. The goal of the system is to analyze 30 to 50 compounds in 10 minutes with a small sample of volume (50ml) and a power consumption of 10mW [19]. Figure 6 shows a graph of the detection response of a gas chromatography system in conjunction with the three-stage preconcentrator.

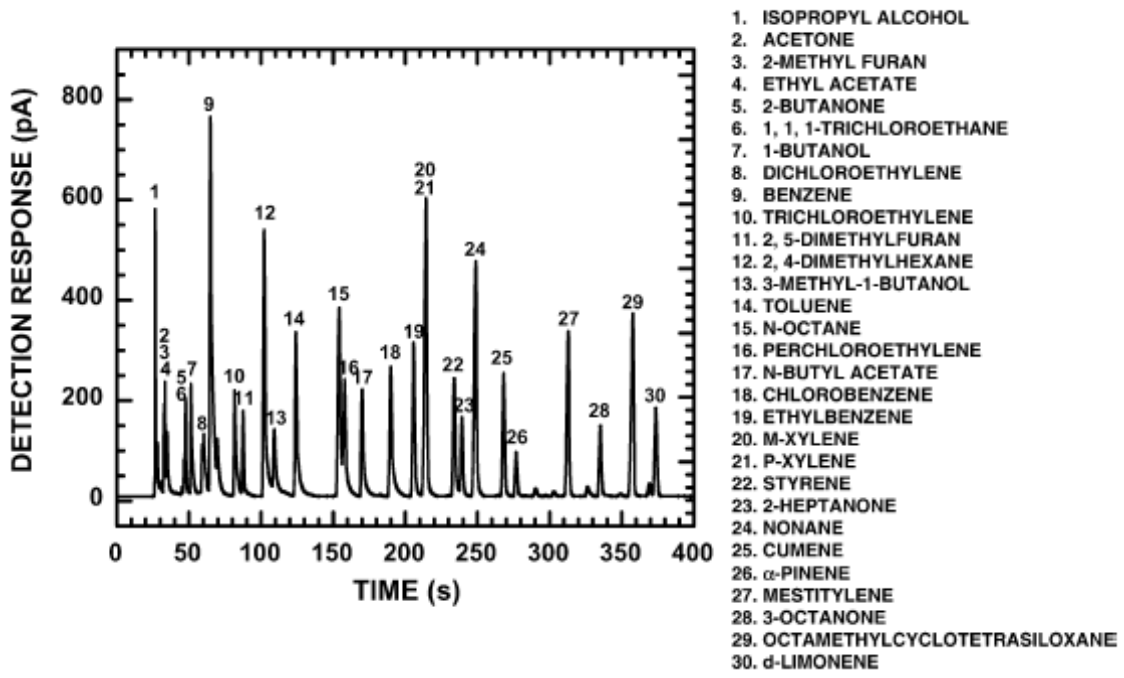

Figure 6 A Chromatogram showing successful separation of 30 organic vapors using three-stage microfabricated preconcentrator-focuser with a conventional gas chromatography system [20]

2.3.2 Coatings

Preconcentrators need a selective coating, such as a polymer, that absorbs particular particles for collection and then releases the particles without changing the particles. The particles can then be detected by the sensor in the system. Most preconcentrators release particles when heated with a pulse of voltage. The faster a preconcentrator can uniformly heat its absorptive coating, the better the sensor can observe the particles released. Adding a preconcentrator to a system can slow its measurement response time because of the delay in waiting for absorption and then heating of the preconcentrator to release absorbed particles, but often the increased sensitivity outweighs this added delay. A multi-stage preconcentrator developed by

students at The University of Michigan exhibits three different granular materials, Carbopack B, Carbopack X, and Carboxen 1000, depicted in Figure 7. The materials trap compounds with different volatilities [19].

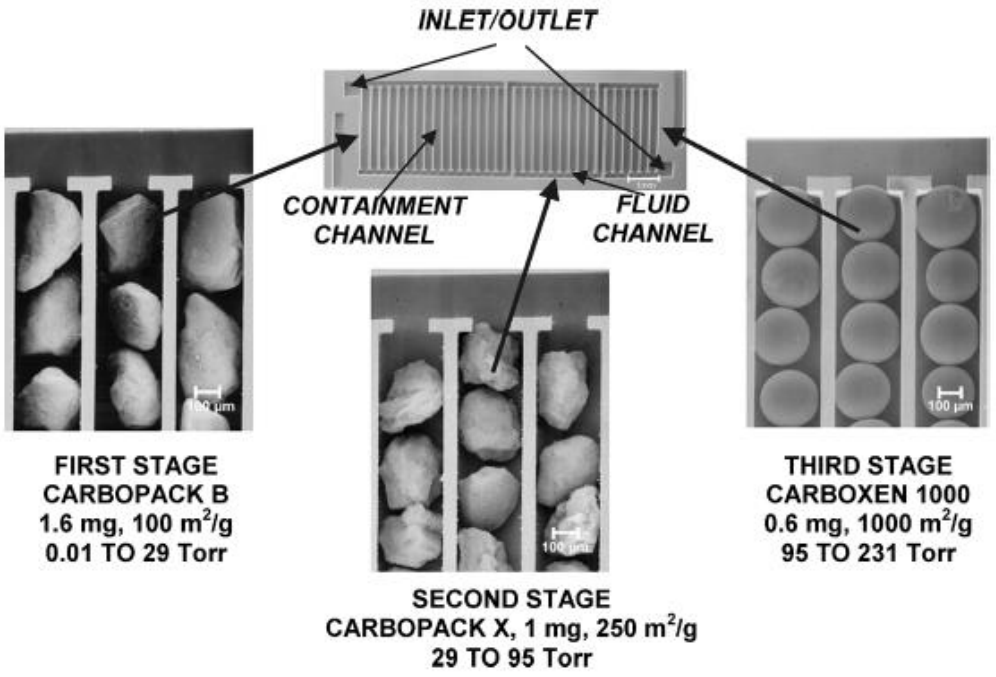

Figure 7 Preconcentrator with three stages to absorb different types of particles based on their respective vapor pressure ranges [19]

Three-stage microfabricated preconcentrator-focuser using thick microheater (upper center) packed with three carbon adsorbents to cover a wide range of compound volatilities [19]. The adsorbents have a large surface area and have been tested with a wide range of vapors and vapor pressures [16]. Other coatings include porous polymers such as Tenax^{TM}, Chromosorb^{TM}, Porapak^{TM}, and Carbotrap^{TM} [8]. Polymers such as these are commonly used by gas chromatographers, but must be tested and scaled down

for use on microfabricated preconcentrators. Gardner et. al provides a discussion about polymer energies and chemical structures [21].

2.3.3 PolyMUMPs™ Fabrication for Preconcentrators

The polysilicon multi-user MEMS process (polyMUMPs) fabrication is one option for the fabrication of MEMS devices. PolyMUMPs allows for the fabrication of many devices at once and saves time and money by combining patterns from many people onto one mask to save space on a silicon substrate. The preconcentrators in this work were fabricated using PolyMUMPs™ to save time and resources.

Several designs were submitted for fabrication and tested for heating characteristics. Figure 8 shows some of the preconcentrator designs tested. The patterns shown are drawn in the Poly0 layer of MUMPs but actual designs submitted included other PolyMUMPs™ layers.

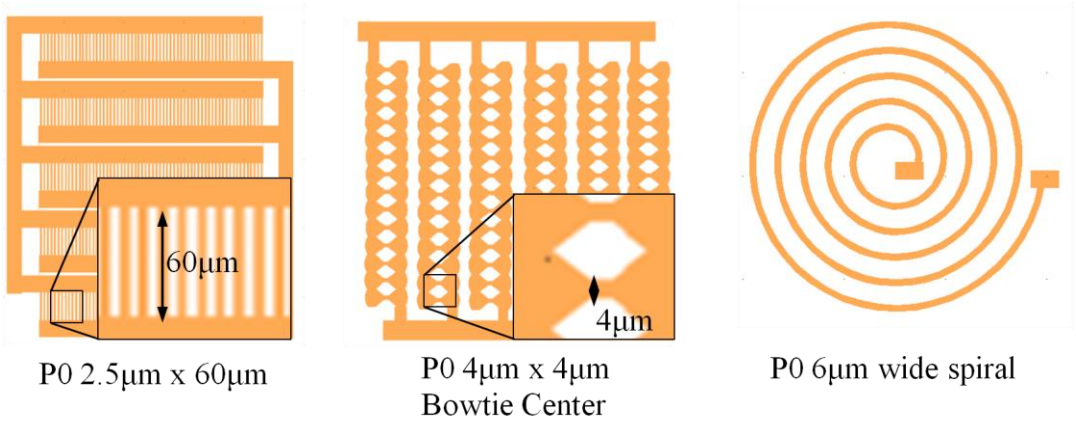

Figure 8 Preconcentrator patterns depicted as Poly0 layer of MUMPs

The process uses polysilicon layers for device patterns and includes three polysilicon layers and one gold layer on a silicon substrate, shown in Figure 9 [7]. Two

polysilicon layers are deposited on sacrificial silicon oxide layers that can be removed to create free standing structures. Preconcentrators in this work are prototyped using the PolyMUMPs™ process fabrication.

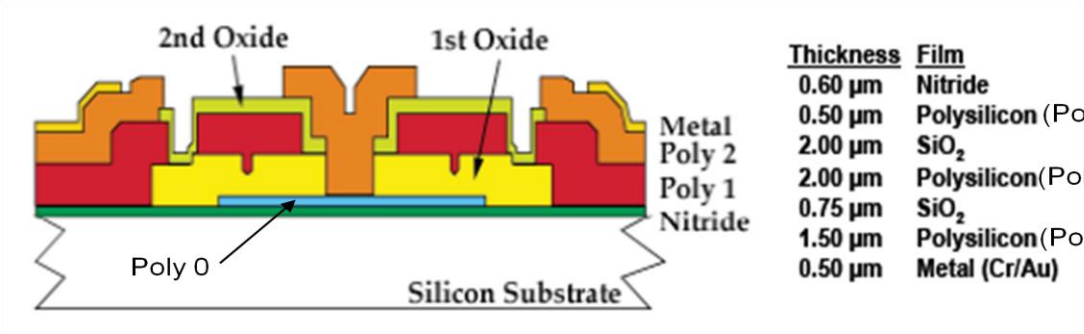

Figure 9 PolyMUMPs™ fabrication process, film layers listed in order of deposition and growth and labels correspond to layers [7]

Preconcentrator patterns have been laid out in all of the polysilicon layers to test each for heating characteristics. Arrays of preconcentrator patterns utilize different layers of the PolyMUMPs™ process for different designs so that many heating configurations can be tested. The designs are intended to provide efficient heating of a large surface area. The designs investigated in this work show a proof of concept for preconcentrators paired with SAW devices and provide a variety of designs to investigate the best heating configuration.

2.4 Nanowires

Nanowire sensors are an up-and-coming method for sensing chemicals. Nanowires have been shown to experience a change in resistance when exposed to various chemicals. The advantage of nanowires is that no chemically active coating added as a post-processing step is needed. The University of Pittsburgh has been doing

work with nanowires as chemical sensors and part of this thesis involves collaboration with the University of Pittsburgh for nanowire testing. Researchers at the University of Pittsburgh have demonstrated that nanowire arrays are sensitive to chemicals and may be sensitive to explosives and biomarkers [22].

The nanowires fabricated at the University of Pittsburgh are single nanowires that use an electrochemical method of growth between two electrodes. First, fabricators clean a (100)-oriented silicon wafer, deposit a 1μm thick layer of thermal SiO_2, a 25Å titanium adhesion layer, and a 975Å thick gold layer for the electrodes. The layers are patterned and etched in a lift-off manner to form the contact electrodes. E-beam lithography forms the electrolyte channels. The electrolyte channels provide a pattern guide for the electroplating solution. The method of fabrication requires no post-assembly process. The nanowires produced exhibit diameters as small as 30nm to 50nm with good uniformity [2, 23].

2.5 Microfabrication Processes

Acoustic wave devices in this research are fabricated using a photolithography process and thin film metal deposition. Photoresist creates a pattern for the application of multiple layers of metal that form the IDT fingers.

Microfabrication processes are categorized into three basic types: surface micromaching, bulk micromaching and micromolding. Surface micromachining involves adding thin layers on top of a substrate surface. The layers can create free standing elements by using a sacrificial layer that is selectively removed. Bulk micromachining

involves the removal of part of the substrate to produce three-dimensional structures. Micromolding involves injecting a material into a pattern or filling gaps with a material and is typically larger in scale than surface micromachining. The following sections discuss the processes for creating SAW devices, nanowires and the preconcentrator designs under investigation.

2.5.1 Photolithography

Photolithography is a technique for patterning thin films so that materials can be deposited in particular patterns or etches can be made according to designated shapes. Photolithography depends on photoresist polymers that coat a substrate. The polymers react to UV energy. The energy changes the solubility of the photoresist. Photoresists are either positive or negative. A positive photoresist stays in place if it is not exposed to light, leaving a pattern of photoresist in the same place as the pattern on the mask. A negative photoresist stays in place where it is exposed to light, leaving a gap in the photoresist where the pattern on the mask blocks light from the photoresist. Figure 10 depicts this process.

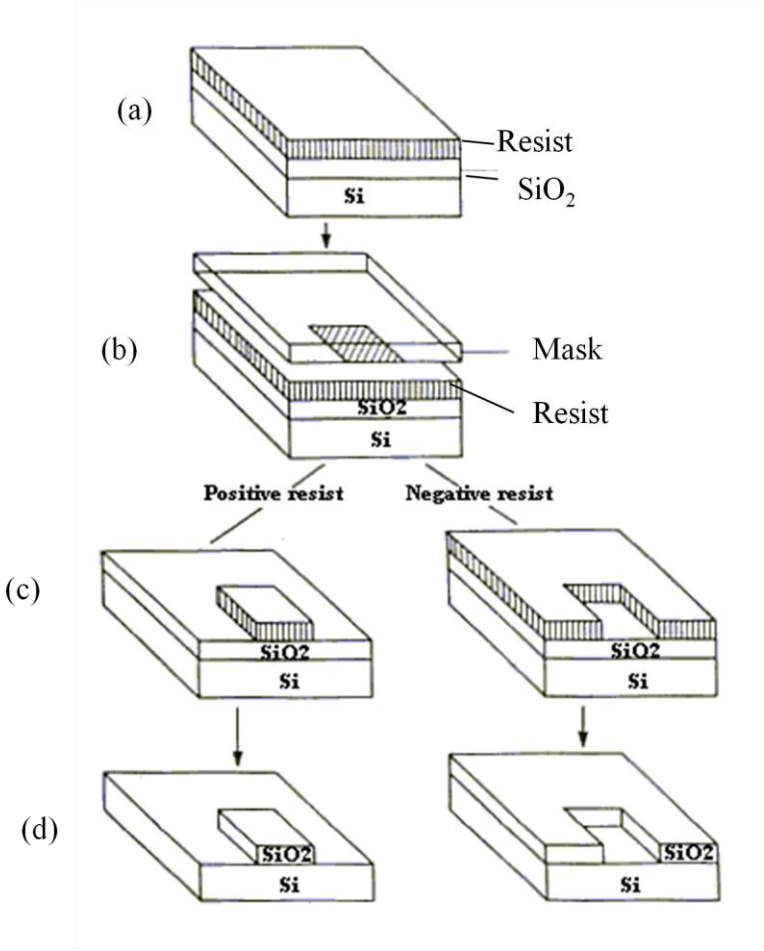

Figure 10 Photolithography process. (a) Oxidized substrate is coated with photoresist. (b) Resist is selectively exposed through a mask. (c) Developing creates a pattern. (d) Photoresist acts as a protective layer during etch. The resist is removed with an organic solvent, leaving a pattered layer [24]

2.5.2 Evaporation of Metals

Metals are deposited on the substrate through an evaporation process. The material to be coated on the chips is heated in a vacuum environment. The heated material travels outward from the heated area and adheres to the surface of the sample. Directional coverage is obtained by placing the substrate a particular distance away from the heating element. Other methods of thin-film coating exist, but evaporation is used in

the research. Gold, nickel, aluminum and titanium are coated on the chips in layers to create the electric signals in transducer field fingers that cause the stresses and strains to create surface waves that propagate across the piezoelectric surface.

2.5.3 Deep Reactive Ion Etching

Deep Reactive Ion Etching (DRIE) is a particular form of plasma etching. Plasma etching is a form of dry etching in which ionization and fragmentation of gasses take place and produce chemically active species known as oxidizers and/or reducing agents. A high-voltage radio frequency AC signal between two parallel electrodes generates plasma. The high electric fields ionize the gas molecules and produce active species. Two forms of reactions then occur between the wafer and gas: chemical and physical etching. Ion species react chemically with silicon or other thin-films, forming a gaseous compound, which gas circulation removes. The species also bombards the substrate and physically removes atoms. This physical etching is generally more directional and anisotropic than chemical etching because of the protection of the sidewalls [24].

Specific off-shoots of plasma etching are defined by the state of the electrode holding the wafer. If the electrode is grounded, the etch is known as a plasma etch. If the wafer is attached to an electrode with an AC bias applied to it, the etch is referred to as a reactive ion etch.

DRIE is a process that allows for high-aspect ratios and produces features with near vertical sidewalls. DRIE uses repeated cycles of an etching step and a step to coat the side walls of the etch with an inhibiting polymer film, as seen in Figure 11 [25]. The inhibition film is preferentially removed from the bottom of etched trenches with ion

bombardment but prevents etching of the sidewalls to create a deep, vertical wall trench. DRIE provides a room temperature process for the etching of vertical sidewalls which provides the ability to correlate the mask with three-dimensional structures. Etch selectivity is also a benefit of DRIE. The process uses photoresist, silicon oxide, silicon nitride, or metal as a masking material.

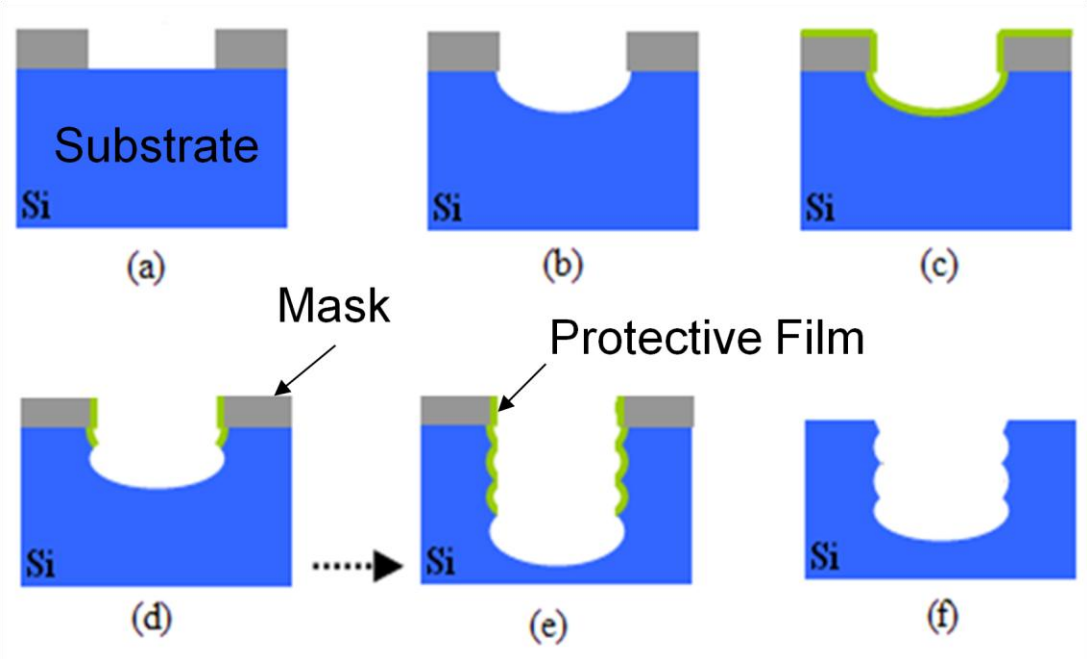

Figure 11 DRIE process (a) shows the mask on the substrate, (b) is the initial etch, (c) shows the coating of a film to protect the sidewalls, (d) an etchant removes the film from horizontal surfaces and etching occurs again, (e) the process is repeated for the desired length of time to reach a particular depth, (f) the mask is cleaned of and a deep etch remains [25]

2.6 Previous Work at AFIT

In Gallagher's AFIT Thesis, he generated the mask for 2μm wide IDT field with 400 fingers, the chamber for testing, and measurement of SAW activity [1, 26]. The thesis provided a fabrication process with an LOR3A photoresist and S1818 photoresist

stack. However, that process is modified to reduce the fabrication time and the finger width is changed to make device fabrication easier for a novice fabricator. Gallagher also presented some initial tests of SAW devices and evidence of chemical sensing but provided no comparisons between different devices for sensitivity [1]. The work recommended investigation of a preconcentrator, but provided no guidance for its design.

2.7 Summary

Microfabricated products are making great strides in the chemical sensing world. Microfabrication practices allow for the production of very sensitive devices and a wide variety of devices. Many of the applications of the devices are still being discovered and modified. The scale of MEMS makes them particularly well-suited to chemical applications because the small features are sensitive to the small features of chemical molecules. Knowing the past work that has been done in the field is an important aspect of the research so that there is no duplication of efforts. In addition, to begin working with MEMs, knowledge of the fabrication processes and the types of devices that each process produces is important. The research of previous work ensures that no duplication of efforts occurs. The work at AFIT on SAW devices paved the way so this thesis effort could focus on testing and refining the fabrication process, determining the proper substrate to use, and setting up a testing station.

III. Models and Methodology

The set up for an experiment is an important factor in any testing situation. How the system is defined, the parameters under consideration and the factors that are varied require discussion and definitions. Chapter 3 discusses the boundaries of the system under test, such as the inputs to the system, factors and parameters that affect the system, and outputs of the system. Services of the system enumerate the reason the system is used and what the system can provide to other systems. The system's workload is the inputs and the conditions that cause system to perform or affect its performance. Performance metrics show how well the system works and provide the quantifiable data for comparisons between two different devices. System parameters are elements that affect how the system works. Parameters can be factors that are varied to produce different outcomes, or they can be controls to narrow the scope of tests. A table of the factors that are varied for experiments and the level of the factors is included and discussed. The evaluation technique discusses how the experiments are run.

3.1 System Boundaries

For the SAW devices, the system under test consists of two IDT fields and a propagation field. IDTs are fabricated on a lithium niobate substrate because of its piezoelectric properties. The component under test for this research is the propagation field. IDT fields, optimal finger widths and separation are not part of this research. Also not part of the research is device materials and fabrication processes. Different propagation field coatings are used to detect different chemicals as well as various preconcentrator coatings for absorbing different chemicals. Figure 12 shows a block

diagram of the system. Inputs to the system include the driving signal for the IDTs and the vapor containing the chemicals for detection.

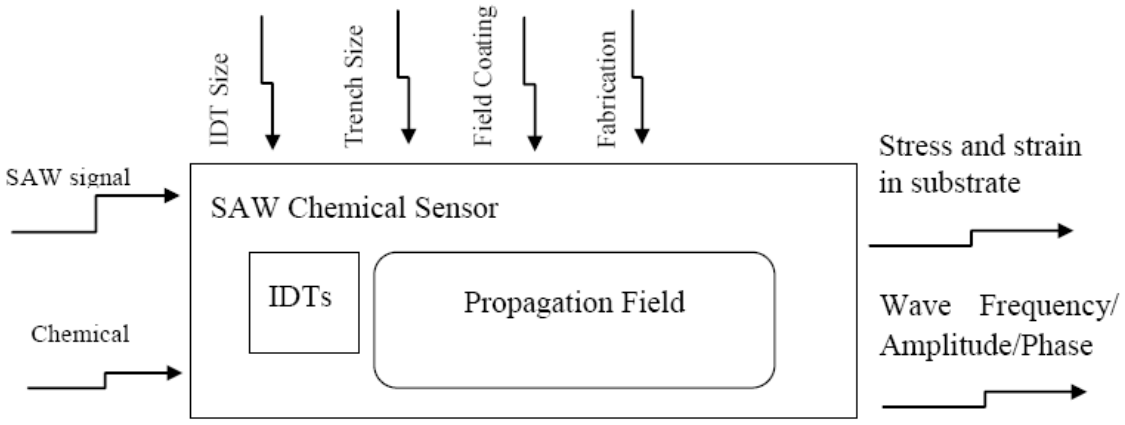

Figure 12 Surface acoustic wave chemical sensor system diagram, items inside the box are components of the system, items on the left are inputs, items on the top are parameters and items on the right are outputs

Nanowire systems depend on the fabrication and production of the nanowires. The scale of the nanowires makes them fragile and sensitive to shock and high voltage. The system is quite similar to the chemical sensor system because the wires require an input signal whose changes due to the introduction of a chemical are measured. Figure 13 shows a visual representation of the nanowire system.

Preconcentrator designs are another aspect of the research. The preconcentrator system consists of a preconcentrator pattern that receives a DC voltage input. The observable outputs are the heat characteristics of the preconcentrator and the temperatures it can reach at particular voltages. Other aspects of the preconcentrator system are the chemical concentration input and output; however, they are not measured and tested in the work because the prototypes are not tested for concentration factors

because it is outside the scope of this research effort. Figure 14 depicts the preconcentrator system.

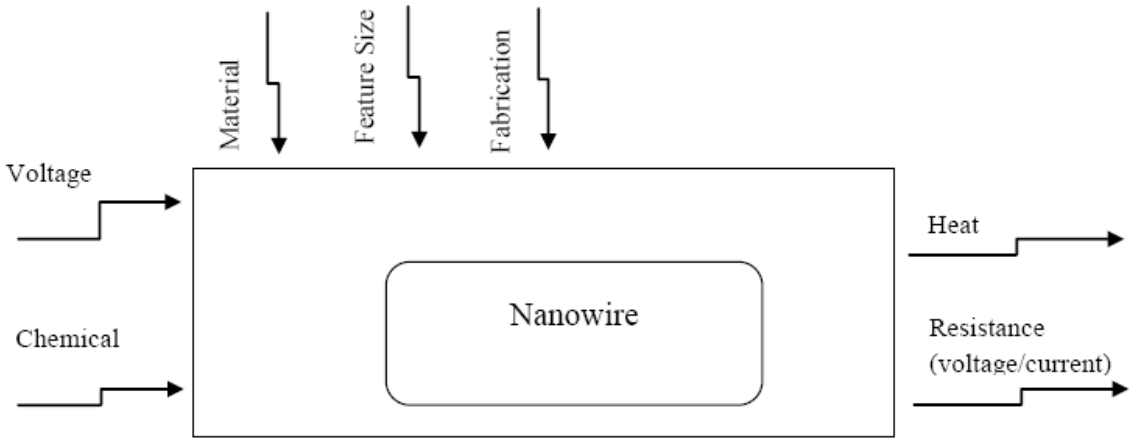

Figure 13 Nanowire system diagram items inside the box are components of the system, items on the left are inputs, items on the top are parameters and items on the right are outputs

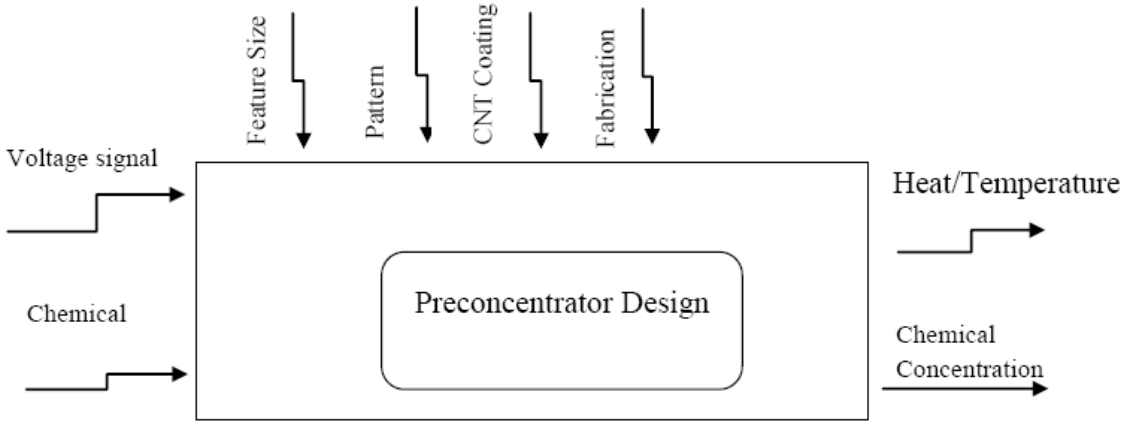

Figure 14 Preconcentrator system diagram items inside the box are components of the system, items on the left are inputs, items on the top are parameters and items on the right are outputs

3.2 System Output

The SAW chemical sensor system provides an output waveform that is modulated due to exposure to chemicals. The output waveform is compared with the input waveform, a comparison that shows how the wave propagates. A signal causes stresses and strains in the piezoelectric substrate due to the input IDT field. The stresses produce a propagating surface wave. The propagated wave moves to the output IDTs, which results in an output wave measured by a network analyzer. The analyzer detects the frequency, amplitude and phase of the input and output wave. If the system does not exhibit acoustic activity, no output wave is detected and measured.

The long term goal for the system is to detect a variety of chemicals by creating an array of SAW devices coated with a variety of substances. The various coatings allow for the detection of explosives and various harmful substances. The immediate goal of the research is to determine which configuration of propagation field coating surface provides the highest sensitivity. Higher sensitivity in sensors means earlier detection of explosives and less exposure to harmful chemicals. This increases safety for individuals investigating explosive devices and chemicals.

Nanowire chemical sensors exhibit the changes in resistance when exposed to chemicals. The smaller scale of nanowires means that they have the potential to respond to low concentrations of a chemical. In addition, nanowires do not require a polymer coating, a post-processing step that SAW devices require.

The preconcentrator gathers a chemical from the air over a period of time and then releases the chemical in a short period of time, creating a higher concentration. The

release of a higher concentration to the chemical sensor allows the sensor to show a response when there is actually a lower concentration of the chemical than the sensor would normally detect.

3.3 Workload

Chemical inputs are the workload of the SAW device and nanowire systems. Chemicals can be introduced at different rates and different levels. Different types of chemicals can be introduced into the probe station, but the ability of the device to detect the particular chemical depends on the substance coated on the propagation field because different substances react to different chemicals. Preconcentrator coatings have the same attribute; they collect particular chemicals and are not affected by other chemicals.

Ethanol is used as the workload on the SAW devices and nanowires in this research. A Nafion® coating collects ethanol molecules on the SAW device. Chemicals are introduced into the probe station by bubbling nitrogen through 200 proof ethanol. The nitrogen and ethanol flow rates are regulated by an Owlstone OVG-4 device. The device is intended to provide a flow control element in chemical testing. The device can be used for calibration because it has the ability to release a particular concentration or flow rate of a chemical within its heated chamber; however, at the time of the tests the OVG-4 is being calibrated for use with ethanol and is not used for an ethanol concentration regulator.

For the preconcentrators, the workload is the voltage input into the pattern. The preconcentrators will be evaluated based on the heating pattern caused by the voltage and the temperatures the preconcentrators reach.

3.4 Performance Metrics

Performance metrics include frequency change, amplitude changes and phase response of the output wave. A larger change in the resonant frequency of the propagating wave or phase shift after a particular period of time after exposure to ethanol signifies a more sensitive device.

Measurements of the nanowires include the resistance of the wire. The measurement of sensitivity of the nanowires is based on the amount of time after ethanol flows into the chamber that the resistance changes and how much the resistance changes. The resistive heating of the nanowires is an output of the system, but is not a metric for observation in this study.

Metrics of the preconcentrator devices are uniformity of heating and power consumption. Uniform heating of the preconcentrator provides for better release of the chemicals absorbed. The amplitude of voltage applied to the preconcentrator, the current required to heat it and the uniformity of temperature in the pattern are metrics to evaluate preconcentrators. Low voltage and low current are better if heating and temperature levels of the preconcentrator still exhibit uniformity and reach high temperatures in a short period of time.

3.5 System Parameters

Parameters of the system that affect its performance include the size of the IDT field, trench size, field coating, preconcentrator, materials, and fabrication. Major parameters of the IDT field include finger length, width, and the number of fingers. The finger width determines the frequency of the propagating wave. The number of fingers determines the amplitude of propagating wave, but also affects attenuation of the wave. The trench size in the propagation field affects the surface area for coating and the propagation of the wave and its interaction with the surface.

Materials that coat the propagation field affect the chemical absorbed. The thickness of the coating can affect wave propagation. Pieces tested in this work have a coating of 5% wt. Nafion®. The Nafion® is spun on at 500 rpm for 10 seconds and 4000 rpm for 30 seconds. The coating procedure results in a Nafion® thickness of approximately 0.3μm.

Input values also affect operation. For example, the rate at which a chemical is introduced affects the change that occurs in the wave. The input voltage frequency must align with the IDT field resonant frequency to generate a SAW. The amplitude of this voltage also affects propagation and form of the SAW. The input voltage for the preconcentrator affects concentrator operation and how well the substance on the preconcentrator releases the absorbed chemical. Measurements are taken from four different size SAW devices, as described in Table 1.

Table 1 SAW device pattern sizes on masks for fabrication

Finger width (μm)	Number of fingers	Finger length (μm)	Center to center spacing (μm)
2	100	400	2000
3	17	85	400
3	33	150	500
3	65	300	1000

Testing focuses on the largest 3μm device. Most of the analysis within Chapter 5 focuses on these devices. However, Appendix B includes results from other sizes. The different devices represent an attempt to make fabrication IDT fields easier. The difference in waveforms from the different sizes is not a focus of the tests or analysis but is a notable observation seen in the graphs in Appendix B.

Nanowire sensitivity to chemicals depends on the material that composes the wire. Nanowires sensitive to methanol and ethanol are composed of Polypyrrole (PPy) and Polyaniline (PANI). Palladium (Pd) nanowires are sensitive other particles such as hydrogen [2, 22]. The feature size of nanowires affects their initial resistance and is affected by fabrication of the devices. Nanowires in this study are grown in a 15μm long, 100nm wide channel and span a gap between electrodes 5μm long. All of the nanowires are grown through the same process but have a variable resistance and a variable shape.

The resistance and shape are affected by the fabrication but are not controllable at this point because of the idiosyncratic nature of the nanowire fabrication.

Preconcentrator operation depends on concentrator design and surface area. Preconcentrators release the chemicals they absorbed as a pulse when heated to the proper temperature, the steeper the rise in heat, the smaller the pulse width of release and the larger the surface area heated, the more particles that are released. Increased surface area can also increases the power consumption of the preconcentrator. Preconcentrator coatings dictate the type of particles that preconcentrators absorb and range from polymers to carbon based substances.

3.6 Factors Under Investigation

Factors tested in this study include propagation field properties, nanowire reactions to chemicals and preconcentrator designs. Experiments focus on the inclusion of etched trenches in the propagation field and CNTs coated on the propagation field to determine if their added surface area makes the sensors more sensitive. CNTs are coated onto the samples before the Nafion® deposition by adding the CNTs to a methanol, DI water solution, which is then sonicated for 3 minutes. The solution is deposited on the chip, which is spun at 500rpm for 30 seconds after spinning, the methanol solution evaporates, leaving CNTs on the surface of the substrate. CNTs are also deposited after the Nafion® coating by directly placing CNTs on the surface and then carefully spreading the CNTs to coat the entire surface.

Table 2 shows the factors altered for the experiments and the values used for SAW devices. Input signals are varied with respect to amplitude and frequency to find the best output wave.

Table 2 Factor levels and values for SAW devices

Factor	Levels	Values
Propagation Field	Unaltered	Smooth propagation field
Propagation Field	Trenches	6 Trenches, 300µm Long, 3µm Wide 12 Trenches, 300µm Long, 3µm Wide
Propagation Field	CNT Field, Under Nafion®	300µm x 300µm
Propagation Field	CNTs Deposited on Nafion®	Dry coated with CNTs
Propagation Field	CNTs mixed with Nafion®	Spin coat Nafion® with CNTs
IDT Field Size	Large	Finger length: 300µm Number of Fingers: 65

Three different nanowire materials are tested, palladium (Pd), PANI and PPy. The resistance of each nanowires varies and has some affect on the ability of the nanowire to sense chemicals, but is not a controllable factor that can be easily tested. The shape of the nanowire also affects its sensing capabilities, but again is not a controllable factor to test.

Experiments with preconcentrators require the identification of the voltage for the best temperature to release the absorbed chemicals. Factors under investigation for the preconcentrators are the shape of the preconcentrator and the material that composes the preconcentrator. Preconcentrator tests include preconcentrators in a ladder shape, a grid, a spiral, bowties and bars, as seen in Figure 15.

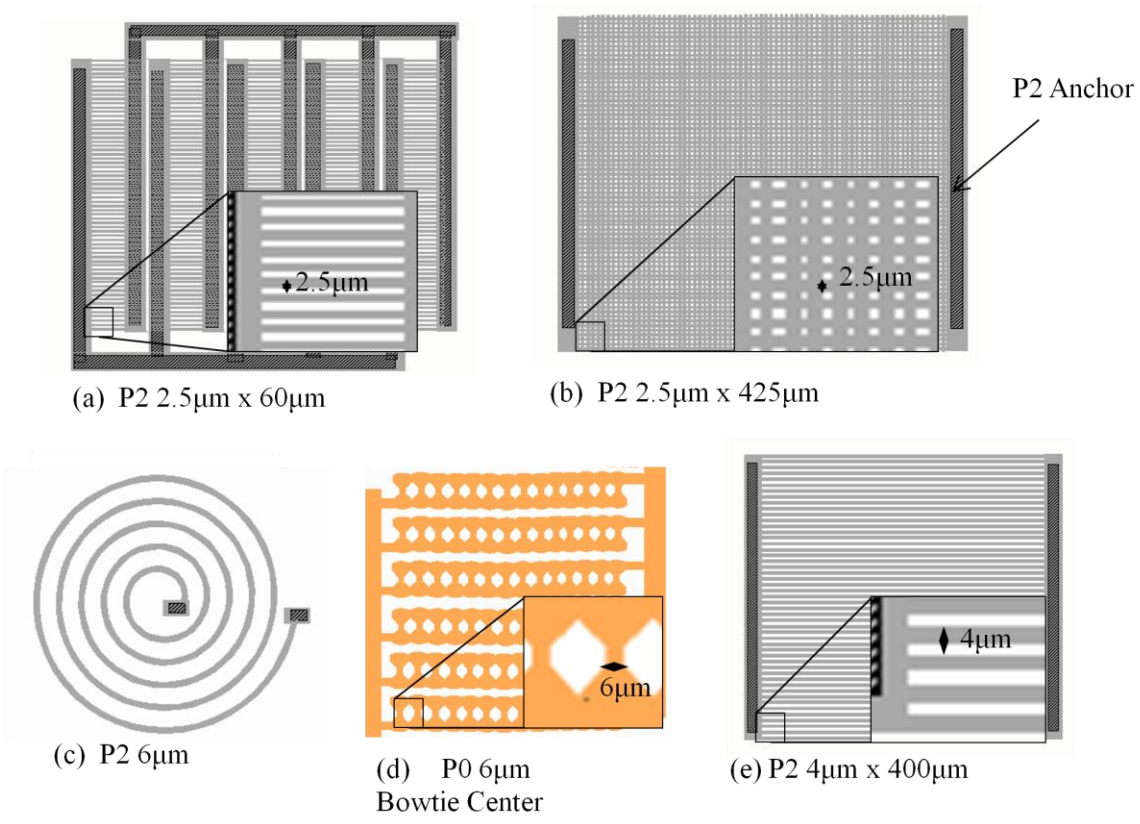

Figure 15 Preconcentrator designs: (a) Ladder shape, (b) Grid, (c) Spiral, (d) Bowties, (e) Bars. Gray patterns are the Poly2 layer and orange is a Poly0 layer pattern

The gray in the designs is a Poly2 layer of MUMPs and the orange is Poly0. The patterns for test occur in Poly0, Poly1, Poly2, stacked Poly1 and Poly2, and stacked Poly0, Poly1, Poly2. Stacking the polysilicon layers means that no sacrificial oxide layers are present.

3.7 Evaluation Technique

For evaluation of the SAW devices, an Agilent E5070B vector network analyzer measures the output wave detected by the output IDT field. The two-port device with N-type connectors measures the magnitude and phase of transmitted frequencies from

300kHz to 3GHz. Using an S_{12} or S_{21} parameter measurement displays the difference between the input and output IDT activity. A probe station connects the network analyzer to the SAW devices. The station is sealed for vapors to pass through the chamber and around the sensing device.

The data collection during SAW device testing includes baseline data taken while nitrogen is flowing through the chamber when the probes are first connected to the device. The introduction of ethanol into the chamber occurs and a measurement is taken every 2 or 3 minutes to show the effect of ethanol in the chamber. When the device appears to reach an equilibrium state, nitrogen is again introduced to the chamber and measurements are taken every 3 to 5 minutes to show the recovery abilities of the device. All of the variations of the device are tested in the same manner. The flow of both nitrogen and ethanol is regulated by the OVG system so that comparisons between the device reactions can be made.

The nanowires are tested by measuring their resistance and then flooding the chamber with ethanol. A Keithley 4200 Semiconductor Characterization System measures the resistance of the nanowire using a four point probe method. A two point probe method to measure resistance is used by the University of Pittsburgh, and therefore a comparison between a two probe and a four probe measurement is performed. The four probe measurement is more accurate because it eliminates the contact resistance added by the probes. Using four probes, two probes measure the voltage value on either side of the nanowire and the values are subtracted from one another to produce the voltage drop. One probe acts as a current source and the fourth probe is the current ground, as shown in

Figure 16. In a two probe measurement, the current source probe also measures the voltage value, which is taken as the voltage across the nanowire because the second probe is the current and voltage ground.

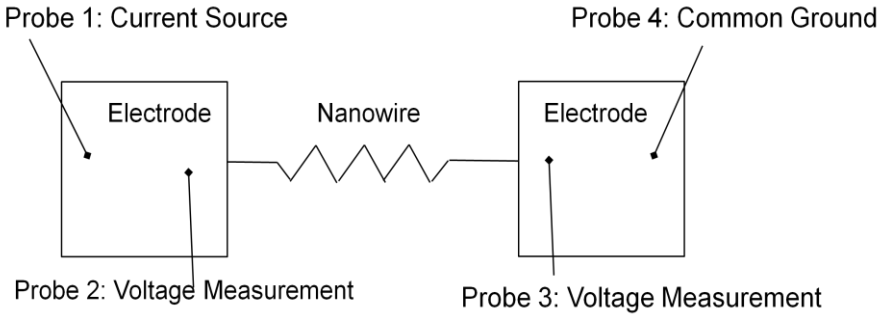

Figure 16 Illustration of four point probe method of resistance measurement. Probe 1 is the current source, probe 4 is the common ground and probes 2 and 3 measure voltage levels to produce a voltage difference measurement

For tests at AFIT, current is driven through the nanowire at values from 0.1μA to 6μA in 0.1μA steps and then 1μA steps. The voltage and current are then plotted to produce a current verses voltage line where the resistance is the slope of the line. Ethanol and nitrogen are flooded into the chamber using the OVG system and measurements are taken to coincide with particular times, similar to the SAW device measurements.

Testing at the University of Pittsburgh is done by connecting the resistor to a Keithley 428 current amplifier. The amplifier supplies a current to the nanowire and provides a voltage measurement to a Keithley 2701 Ethernet Multimeter and Data Acquisition device. A LabView program made by the researchers then records the voltage reading as the gas flow changes.

The preconcentrators are tested using a QFI Multi-Sensor Microscope System, a machine at the Sensors Directorate of AFRL that provides IR imaging. QFI is an

abbreviation of the company who makes the system, Quantum Focus Instruments Corporation. The system has a number of different imaging options, one of which is infrared for heat imaging. A preconcentrator is connected to a DC voltage source. The data collection includes an image of the heat transfer at a particular voltage and the temperature readings of various places on the heated element. Transient characteristics are noted, but not directly recorded.

3.8 Methodology Summary

The methodology chapter describes the boundaries and important parameters of the system and the components of the system that are under test. The components to be tested include modifications to the propagation field of a SAW chemical sensor, the heating characteristics of various patterns of preconcentrators and various nanowires. Each system has a unique evaluation and measurement technique for quantitative data collection and analysis, the results of which are in Chapter 4.

IV. Cleanroom Fabrication

4.1 Introduction

The AFIT clean room contains a number of machines for creating MEMS devices. The EVG620 mask aligner, spinners and metal evaporation machines are used most for the processing of SAW devices in this work. This chapter discusses the processes for fabricating a SAW device in the AFIT cleanroom and some of the post-processing steps that occur at AFRL. The chapter also includes a discussion about the deposition of CNTs onto the PolyMUMPs™ fabricated preconcentrators and a short section about how the University of Pittsburgh fabricates the nanowires.

4.2 Overview of SAW Device Fabrication

Creating a SAW device requires cleaning the substrate chips, spinning on photoresist and baking the photoresist, then exposing the photoresist while masking off a pattern and developing the photoresist. Once the photoresist is developed away, the chip is inspected for development and pattern quality, then the chips are plasma ashed[2] to provide an ideal surface for metal adhesion. Metal is deposited by thin-film evaporation, which is non-conformal, so that a metal lift off can occur. After the metal lift off, chips are cleaned again and taken to AFRL for the spin on of a chemically sensitive coating. The chemically sensitive coating completes the fabrication of the SAW device. Appendix A lists the fabrication steps to make the SAW devices and Figure 17 shows a profile of

[2] Plasma ashing or plasma stripping is the removal of organic matter by an oxygen plasma.

the substrate and layers through the process. The following sections discuss each step of the process in greater detail.

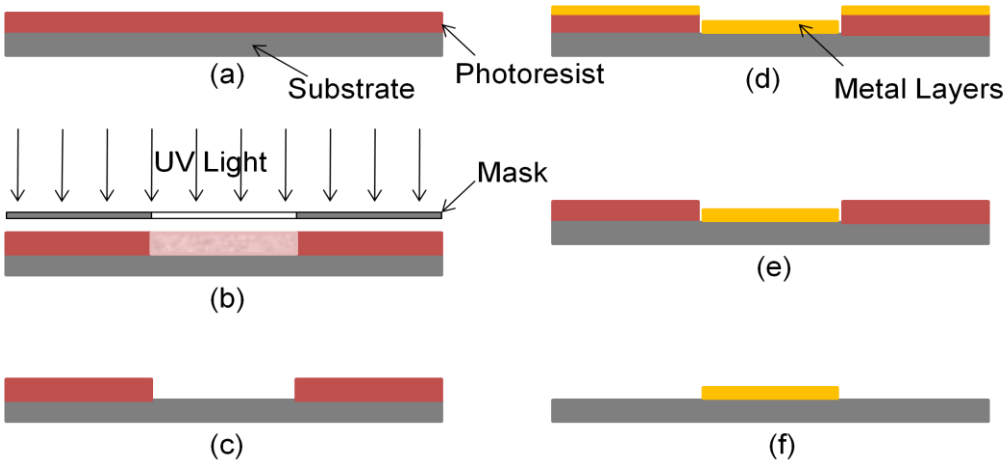

Figure 17 Photolitography and metal lift off process (a) photoresist deposition, (b) phototresist exposure, (c) photoresist development, (d) metal deposition, (e) metal lift off (f) finished product

4.3 Cleaning and Photoresist Deposition

SAW devices are made on lithium niobate substrates. AFRL dices the three inch wafers into smaller samples with a diamond tipped saw blade. The samples in this study are 5/8 inches square. Before dicing, the substrates are coated with a layer of S1818 photoresist spun at 3000 or 4000 rpm for 30 seconds. The photoresist coating protects the substrate from particles created during dicing. Figure 18 shows part of the spinner station in the AFIT cleanroom. Not shown in the image are the spinner controller and acetone, methanol, and photoresist bottles to the right of the spinner, and a sink to the left of the hotplates. The equipment is under a fume hood. The aluminum foil on the spinner keeps photoresist from coating the spinner bowl.

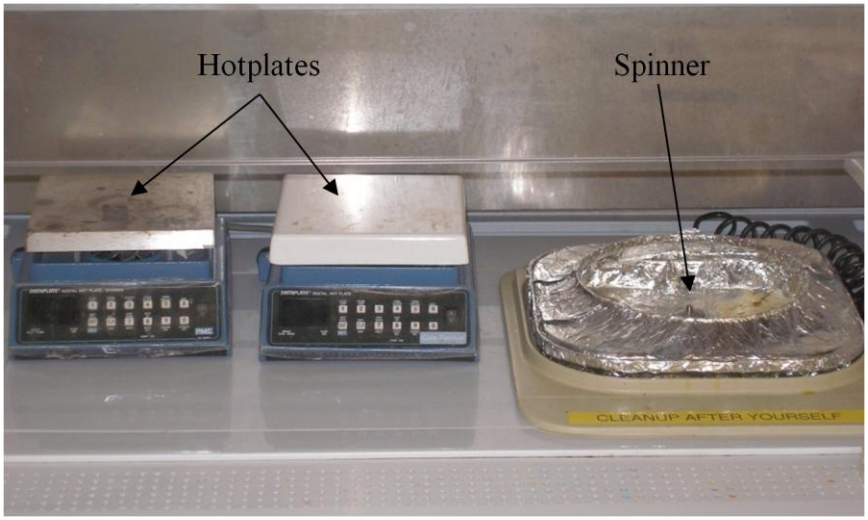

Figure 18 Spinner and hot plate station in AFIT clean room

Sample chips are cleaned for 30 seconds with acetone and 25 seconds with methanol. Cleaning removes shards of substrate from the dicing process and any remaining photoresist on the chip. The chips are placed on a 110˚C hotplate to dry for two minutes. When the two minutes expires, the chips are moved to an aluminum cooling block. After cooling, the chips are coated with 1805 photoresist. The S1805 photoresist is spun on the chips, then the chip is again baked at 110˚C for two minutes. Spinning of the photoresist includes a five second spread at 500 rpm, then a 30 second spin at 3000 or 4000 rpm. The difference in speed results in a slightly different photoresist height, but both speeds provide sufficient thickness (more than 4/3 of the height of the deposited metal) for a metal lift-off and do not significantly affect development. After the chip cools, it receives another layer of photoresist. This photoresist layer is an S1818 photoresist which is spun at the same speed as 1805 and bakes at 110˚C for 2 minutes.

4.3 Mask Layer 1: IDT Fields Exposing and Developing

4.3.1 Exposure

The exposure step is important for proper photoresist development because it is the UV energy that properly loosens the bonds of the photoresist so that the 351 developer can remove it. The energy of the bulb and the filters of the mask aligner affect the proper time of exposure. For the 350 watt bulb in the AFIT EVG620 mask aligner, five to ten seconds of exposure time is enough for one layer of S1818 and one layer of S1805.

Figure 19 shows the AFIT cleanroom EVG620 mask aligner. The aligner gives step-by-step instructions to walk the user through a recipe. The user manual in the cleanroom gives instructions for the creation of a recipe. The exposure recipe uses information such as the mask thickness, substrate thickness, type of alignment needed, contact type desired and exposure time. Creating an accurate recipe is very important for proper exposure. If the incorrect mask and substrate thickness are entered, the machine can crack the substrate or can leave the two pieces too far apart for good alignment. The alignment style specifies top side manual and backside alignment for different applications. The contact type is important for proper contact between the substrate and mask, which affects the pattern definition and development.

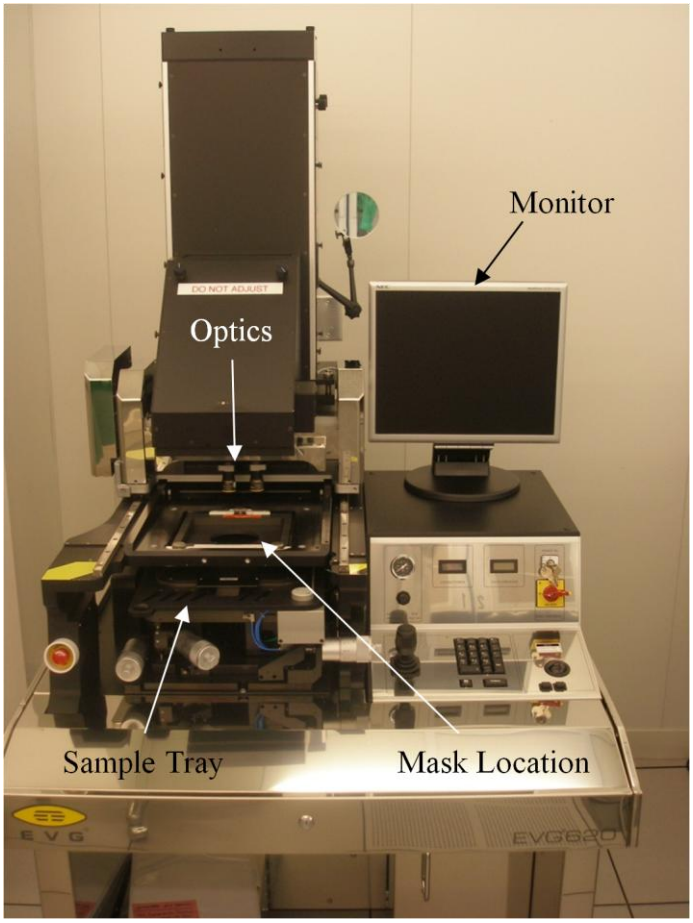

Figure 19 AFIT EVG 620 Mask Aligner

The exposure time affects how well the photoresist develops and how defined the lines of the pattern are. Differences such as the thickness of the photoresist, the substrate, the developing solution and the pattern all affect the exposure time needed. Most devices are fabricated with an exposure time of 7 seconds. Different mask aligner models have different exposure times because of differences in light filtering and bulb power.

S1818 is a positive photoresist, which means that when exposed to UV light, the photoresist will develop away when sprayed with 351 developer. In other words, the dark portions of the pattern that appear on the mask will be the areas where the photoresist

stays. Such development means that in the metal deposition step, the metal can adhere to the substrate and the pattern that results after metal deposition and lift off matches the clear patterns for windows of light that appear on the mask.

4.3.2 Development

S1805 and S1818 photoresist are developed with 351 developer. The developing process represents an area of development that has a lot of opportunity for variation and seemingly small changes sometimes affect how well a pattern develops. For example, the person developing can chose many methods and combinations of spraying, resting and spinning the chip. A general development process includes spraying the chip without spinning it for about 5 seconds, then resting while the developer puddles for 5 seconds, starting a flow of developer again with spinning, and continuing that for 30 seconds. The developer is then rinsed away with water while the chip spins at 500 rpm for 30 seconds.

Exposure and development become qualitative processes which researchers eventually tweak to their own process. There are many factors that affect how well the exposure and development steps create the desired pattern. Feature sizes also affect exposure and development processes. Small feature sizes become difficult to produce, especially the long, narrow fingers of the 2μm SAW devices. Figure 20 show some of the pictures of the development process. The images show what constitutes poor development and good development of patterns.

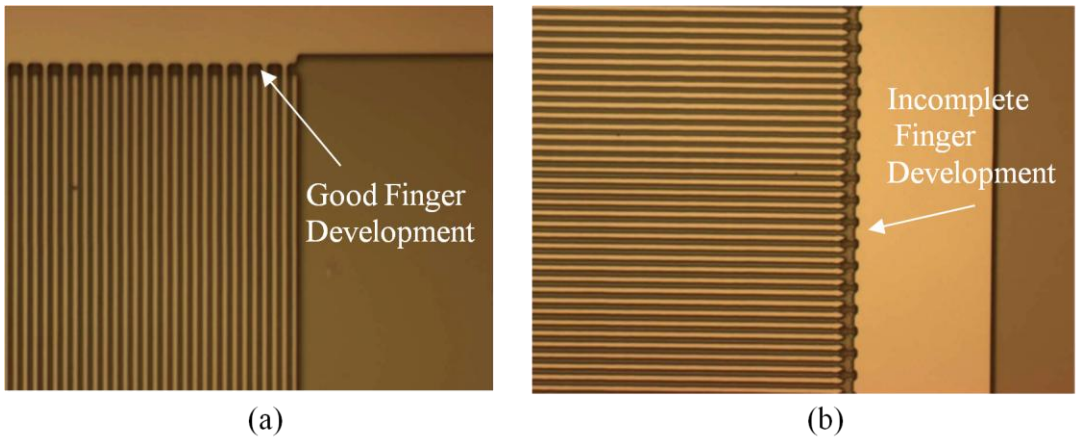

Figure 20 Development Photographs: (a) shows good development of 2 µm fingers. (b) shows good development of fingers, but photoresist still pooled at ends of fingers

In Figure 20(a) shows fingers made from two layers of LOR3A photoresist and one layer of S1818 photoresist. The extra layers of photoresist are different from the process outlined because it is a process left over from past work. LOR3A is harder to remove than S1818, but the extra layers may allow for the longer development time needed for the long, skinny fingers the 2µm SAW devices require. Figure 20(b) is a picture of a chip with S1805 and S1818 photoresist. The difficulties in fabricating the 2µm finger devices necessitates that most of the research is done with 3µm devices. The patterns on the mask for 3µm devices exhibit shorter and wider fingers, which makes the development process easier. The 3µm patterns still produce SAW activity and still effectively show any effects of the modifications to the propagation field, which is the component of study in this work.

4.4 Metal Deposition and Lift Off

4.4.1 Plasma Ash

Placing samples in the oxygen plasma asher before metal deposition makes the lift off process much easier. The plasma asher removes excess carbon and other organic matter that adheres to the surface of samples. Figure 21 shows a picture of the Anatech SP 100 plasma asher in the AFIT cleanroom that was used in SAW device fabrication. The user interface is a touch screen in the top left corner and the dial in the bottom right is the adjustment for reflected power. The reflected power is a product of the RF signals used in the plasma ashing process. The dial set is so that the reflected power can be as close to zero as possible. The samples in this work are plasma ashed with the power at 75 watts for four minutes. If the samples are plasma ashed for too long the plasma will remove all of the photoresist.

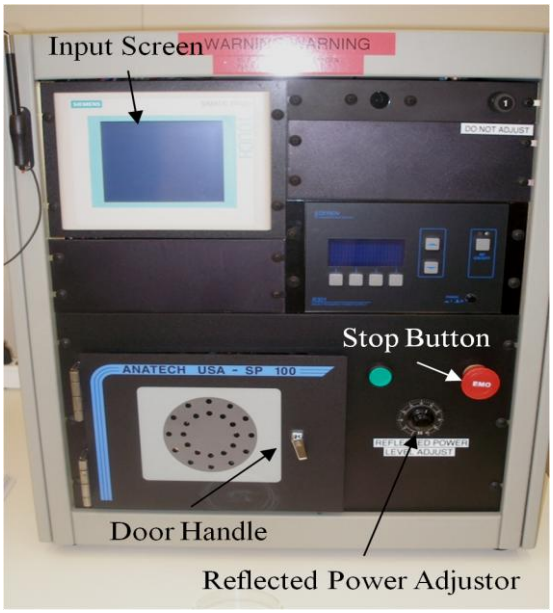

Figure 21 Plasma Asher

4.4.2 Metal Deposition

In this work, metals are deposited on the samples with a Torr EB-4P-6KW E-Beam Evaporator, which is quite similar to the Denton DV-502A E-Beam evaporator shown in Figure 22. The metals are deposited in a particular order so that the metals will adhere to one another and create the electric fields that are needed to produce the SAW waves. The evaporation process takes about 11 minutes total, not including the time for switching the metals. The thickness of metal correlates to the amount of time it stays in the machine and the power settings of the machine. The metal for SAW devices is 100 Å Titanium for an adhesion layer, 750 Å Aluminum, 100 Å Nickel, and 150 Å Gold. The deposition times and powers that correspond to each metal are 2 minutes at 65mA for Ti, 4 minutes 20 seconds at 36mA for Al, 2 minutes 45 seconds at 68mA for Ni, and 1 minute 30 seconds at 62mA for Au.

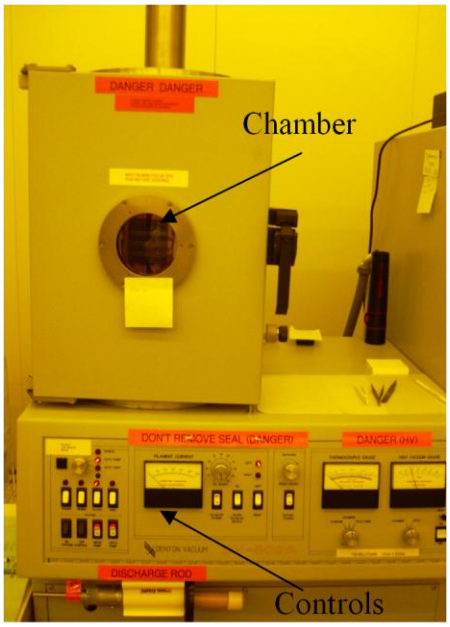

Figure 22 AFIT Denton DV-502A E-Beam Evaporator for thin metal deposition

4.4.3 Metal Lift Off

After the metal is deposited, the unwanted metal is removed. Evaporation is a non-conformal deposition process, which means the metal that falls into the patterns to the substrate is not connected to the metal on top of the photoresist. The metal on the photoresist is unwanted and is removed with a tape lift-off process. A piece of transparent adhesive tape is placed on top of the metalized chip and the air bubbles are patted out, then the tape is peeled off the piece, bringing the metal that is deposited on top of the photoresist with it.

Any remaining unwanted metal is removed by soaking the sample in acetone and placing the sample submerged in acetone into a sonicator. The sonication helps the acetone remove the photoresist from all crevices and corners. To use the sonicator, a thin layer of water is placed in the tub and a glass container with the sample submerged in acetone is placed in the water. The machine is turned on and the sample vibrates due to sonic vibrations. The sample is sonicated for 1 to 5 minutes, or until inspection of the sample reveals that all unwanted metal is removed.

4.5 Mask Layer 2: Trenches Etching and Aligning

The changes to the propagation field that involve putting trenches on the field require an additional fabrication step. One method of fabricating trenches on lithium niobate ($LiNbO_3$) samples is etching trenches into a thin film layer deposited on the chips. Zinc oxide is a piezoelectric material that can propagate SAWs and is therefore the thin film chosen to deposit on the samples. Another way to include trenches on the SAW

device is to DRIE trenches into the lithium niobate substrate. The etching process requires equipment at AFRL, and is therefore subject to the AFRL timeline. In addition, lithium niobate is a difficult substrate to etch and requires extra processing of the $LiNbO_3$ sample.

4.5.1 Zinc Oxide

Chips are coated with zinc oxide through a sputtering process. The samples are sputtered for 1 hour at 100 watts. After coating, the thickness of the zinc oxide on a piece of silicon coated with the lithium niobate chips is measured. Profilometer measurements indicate that the thickness of zinc oxide is 0.15μm.

Zinc oxide coated pieces are patterned through a photolithography process. The holes in the photoresist allow for etching of the exposed zinc oxide. Patterning of the zinc oxide with trenches is done through a chemical etching process with a buffered oxide etch (BOE), which etches zinc oxide at a rate of 0.06μm per minute. The first and second chips are etched for 2 minutes and 45 seconds. The results of the etch are not entirely consistent over the entire chip. On some places of the chip the trenches are well etched, but other areas of the chip show no sign of etching. The difference in etching may be due to uneven sputtering of the chip, residual photoresist or how the chip is agitated in the etchant. The third chip is etched for 3 minutes and 15 seconds, which produces a more complete etching of the entire chip.

The large 3μm SAW devices have two different trench fields. The first field has six trenches that are 2μm wide and 500μm long. The second has twelve trenches that are 2μm wide and 500μm long. The twelve trenches provide a 0.97% increase in surface area

and the six trenches provide a 0.49% increase in surface area based on the additional surface of a 0.15µm sidewall of the trenches.

After the trenches are etched, the chips are patterned for metal deposition. The patterning process is the same, except before exposure the chip must be aligned with the mask so that the trenches line up with the propagation field of the SAW device. The alignment process is difficult on the EVG620 because the chips are 5/8 of an inch square and only one optic can be used for alignment. The older mask aligner in the AFIT clean room, a Karl Suss MJB3, has a smaller magnification, which makes it possible to view the entire chip and align the whole chip at once. The exposure time for the older mask aligner is slightly longer (20-30 seconds) due to the lower power of the UV bulb, but the development process is the same. Figure 23 shows the Karl Suss MJB3 mask aligner in the AFIT cleanroom.

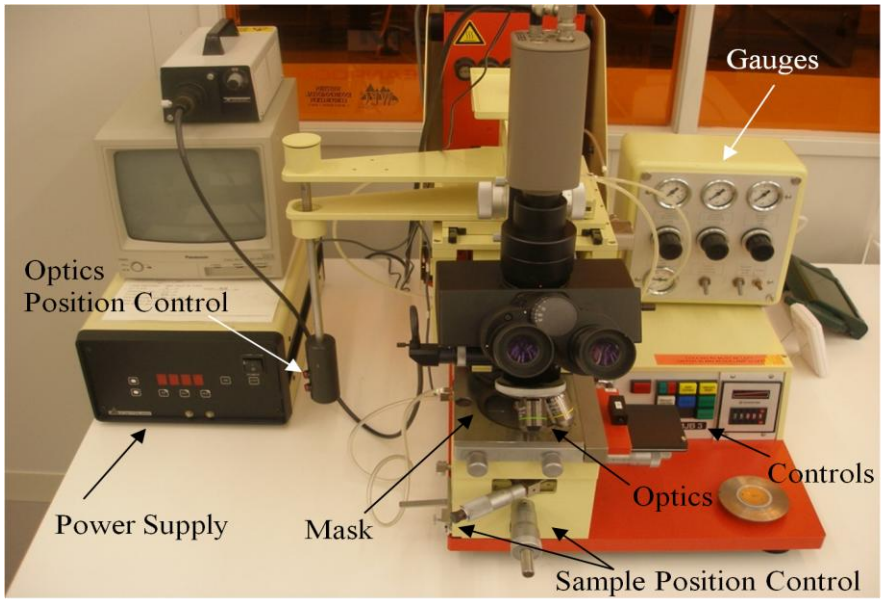

Figure 23 Karl Suss MJB3 mask aligner in AFIT cleanroom

4.5.2 Lithium Niobate Etching

Etching the lithium niobate substrate is a bulk micromachining process. Lithium niobate is a difficult substrate to etch and requires an Indium Tin Oxide (ITO) layer as a mask. Sputtering the $LiNbO_3$ samples with ITO leaves a 1.5μm layer of ITO for patterning. Hydrofluoric acid (HF) and Hydrochloric acid (HCl) are supposed to etch ITO, but trials of this etching produce undesirable results. The etchants cause the ITO to flake off in pieces and the small trench widths show no sign of etching. Therefore, the ITO needs to be DRIE as well. A mask for the ITO is SU-8 photoresist, which is a thick photoresist that can be used to create the 10μm thick mask desired. SU-8 is a negative photoresist that is patterned using a photolithography process. The spaces in the SU-8 then produce spaces in the ITO in the etching process. The SU-8 is removed by the etching process, leaving a pattern of ITO, which then masks the $LiNbO_3$ and is removed by the DRIE process. Due to timing issues with the AFRL DRIE processing, no $LiNbO_3$ samples with trenches etched into the substrate are available for testing at the time of this thesis.

4.6 Chemical Sensitive Layer and CNT Deposition

4.6.1 CNT Deposition

The chips that receive a CNT deposition have CNTs deposited on them before having the Nafion® deposited on them. The CNTs are commercially grown at SES Research Inc., they are single-walled and range in length from 5μm to 15μm with an outer diameter of less than 2nm. The CNTs come in an ash-like form that makes

deposition of them a challenge. After CNT deposition, evaluating the evenness and the quality of deposition is difficult because unless the CNTs group together, they are too small to see with the naked eye, or see well under the microscope; adhesion of the CNTs is assumed because of the adherence of groupings of CNTs.

Initial deposition of the CNTs requires some trial and error. The CNTs need to be evenly distributed in a liquid that will quickly evaporate and leave the CNTs attached to the surface of the chip. Acetone, methanol, isopropyl and de-ionized water are all put in small dishes with a pinch of CNTs. The dishes are then sonicated for 5 minutes. The CNTs distribute well in all of the alcohols, but not in the DI water. The acetone evaporates the fastest, but results in clumping of some of the CNTs, as does methanol. Isopropyl reduces clumping, but takes longer to dry. Later in the research, a combination of methanol and DI water as a 1:1 solution is tried and subsequently used for the rest of the CNT deposition.

The CNT/Methanol/DI water solution is deposited on chips with an eye-dropper. The deposition can occur on a spinner rotating at 500 rpm, or on a stationary chip on a flat surface. The spinner results in more uniform CNT distribution, which means that the stationary flat surface shows more evidence of CNT deposition. Chips with CNTs are then coated with Nafion®. CNTs deposited on top of the Nafion® layer are carefully deposited by spreading CNTs over the surface of the Nafion® but are not in a solution.

For one chip, an additional processing step is added to create windows of CNTs. For this chip, after the metal deposition the chip is coated with S1818 photoresist which is exposed with a mask to create windows over the propagation field. A

CNT/Methanol/DI water solution is deposited by eye-dropper on the chip spinning at 500rpm. The chip is then baked at 110˚C for 2 minutes to ensure complete evaporation of the methanol/DI solution. The chip is then cleaned with acetone and methanol for 20 seconds each while spinning at 500rpm and baked again. Some of the propagation fields show evidence of the windows, however during the cleaning, CNTs also adhere to other portions of the chip, so the extra processing does not result in clean IDT fields with no CNTs on the surface.

4.6.2 Nafion® Deposition

Nafion® comes in many different weights and each weight deposits a different thickness of Nafion®. To reduce the number of factors, a 5% wt. Nafion® and methanol is deposited on the SAW device chips used to compare propagation field alterations. Some chips with other weights of Nafion® are tested initially; however, the results of these tests did not affect the selection of using 5% wt. Nafion®. The decision to use 5% wt. is based on previous research at AFIT and AFRL, and a ready supply of 5% wt. Nafion®.

Nafion® is deposited on the chips with a dropper. It is then spun at 500 rpm for 10 seconds and 4000rpm for 30 seconds. The 5% wt. coats chips with approximately a 0.34 micron layer of Nafion®. A 2.5% wt. Nafion® mixture results in a 0.2 micron coat and the 10% wt. of Nafion® is too pooled at the edges to get a good height measurement.

4.7 Nanowire Fabrication

The University of Pittsburgh fabricates nanowires using a Signatone 1160 Series Probe Station and an Agilent B1500A Semiconductor Device Analyzer. Nanowires are grown by running a constant current between 100nA and 800nA with a compliance voltage of 10V between two electrode pads with an e-beam lithography channel 100nm wide on both sides of a 5μm gap, as shown in Figure 24. While the current is run across the two electrodes, a 0.4mL droplet of PPy, PANI, or Pd solution is rolled on and off the channel until a major drop in voltage is seen.

Each nanowire on the sample has a unique resistance, which is measured by the Agilent B1500A immediately after fabrication by a two probe method. The resistance measurement is made by applying a voltage to the nanowire and measuring the complying current. The voltage values range from 1mV to 10mV and 1001 data points are taken.

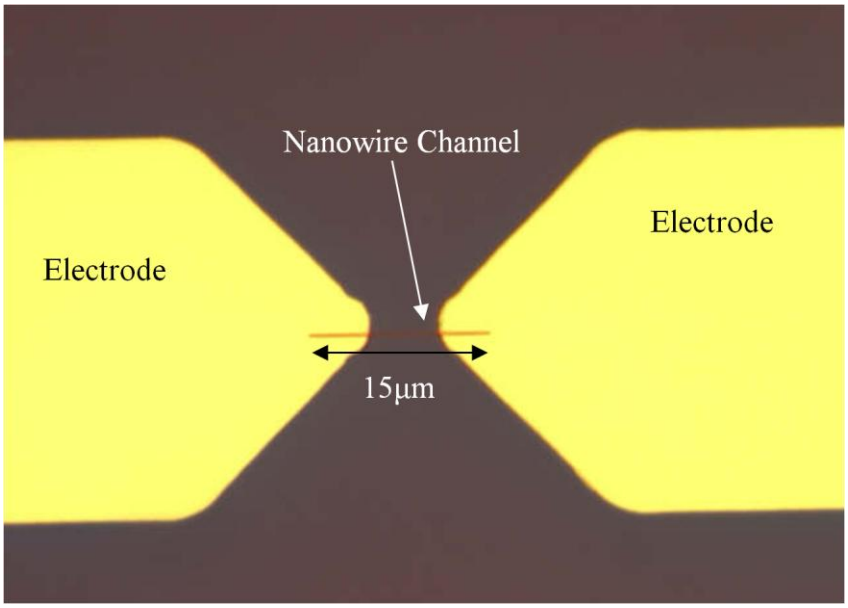

Figure 24 Nanowire Channel and Electrode Gap

The nanowires are made from three different materials. The materials are Pd, PPy and PANI. Pd is a metallic substance and PPy and PANI are conducting polymers. Figure 25 shows a nanowire grown across the channel.

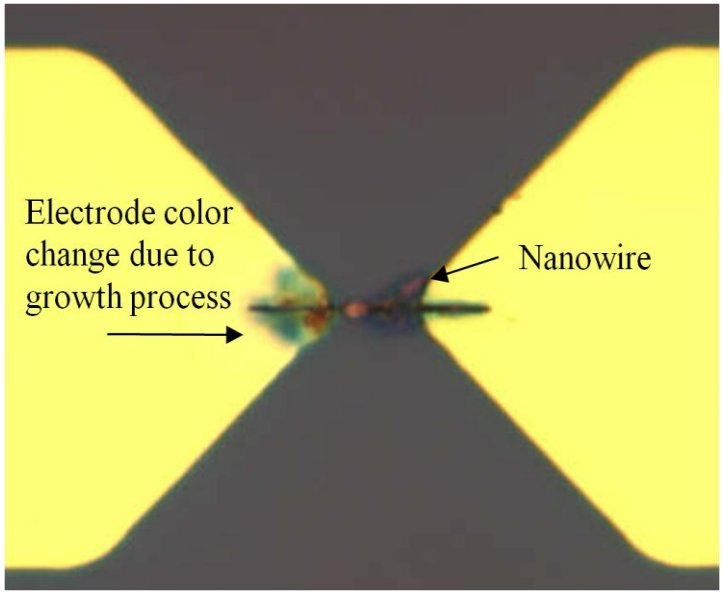

Figure 25 Nanowire of Sample 504, a PANI nanowire

Nanowires grow differently every time and do not have a consistent shape. Some nanowires are better than other for sensing and all have different resistance values. Table 3 shows the sample number for nanowire pieces and the material from which the nanowires on the sample are made.

Table 3 Nanowire Samples

Sample Number	Material
503	Pd
504	PANI
571	PPy
516	PANI
526	PPy
518	PPy
563	Pd

4.8 Fabrication Summary and Results

All of the above described fabrication process result in a number of chips to test, each with slightly different characteristics. Each sample is referred to by the number or letter scratched on the back of the chip. Table 4 lists the samples tested and a description of their coating. These eight chips are the main ones that undergo testing with regulated nitrogen flow. The chips all contain 3μm SAW devices in three different sizes, but the largest size is tested the most. Some other samples are made and tested to show that the process works and ethanol is detected. Figure 26 shows two images of the finished devices.

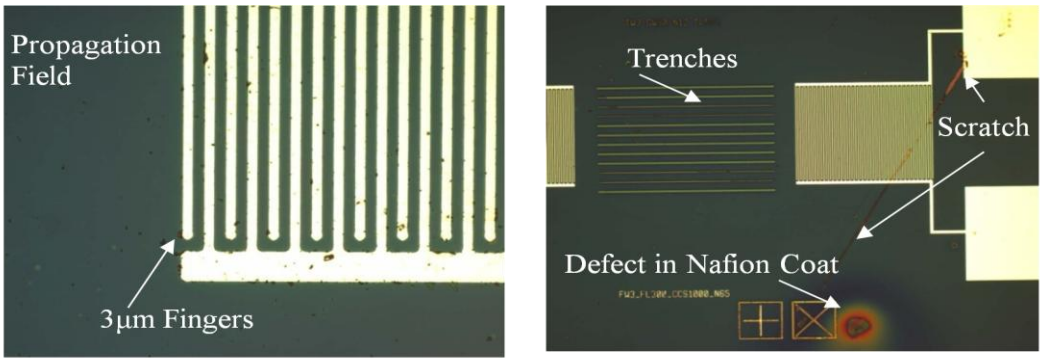

Figure 26 Two images of the final product, devices with a Nafion® coating

Table 4 Samples Tested

Sample	Description
Z1	Coated with zinc oxide, etched before deposition
Z2	Coated with zinc oxide, etched before deposition, was a control with Nafion® for one test
Z4	Coated with zinc oxide, etched after metal deposition
N	No alterations to the propagation field, coated with 5% wt. Nafion®
M	Coated with Nafion® and has CNTs under and on top of Nafion®
F	Sample with CNT window attempt, coated with Nafion®
O	Initially clean, used as a control with no Nafion® coat

Many combinations of fields and coatings can be fabricated, but fabrication takes time and a lot of trial and error. Changes in equipment settings such as bulb power in the mask aligner and ages of chemicals affect exposure and development time, as well as quality.

Researchers at the University of Pittsburgh prepare a number of samples with nanowires fabricated out of three different materials and provide a measurement of the resistance of the nanowire using a two-probe measurement method that is used as a verification of measurements taken during this study.

V. Results and Analysis

5.1 Experimental Set-Up Data Gathering

The testing station uses a sealed probe station chamber, as seen in Figure 27. The station is an MMR Technologies, Inc model LTMP-4, which isolates the sample under test from the environment and provides a path for the flow of nitrogen and ethanol.

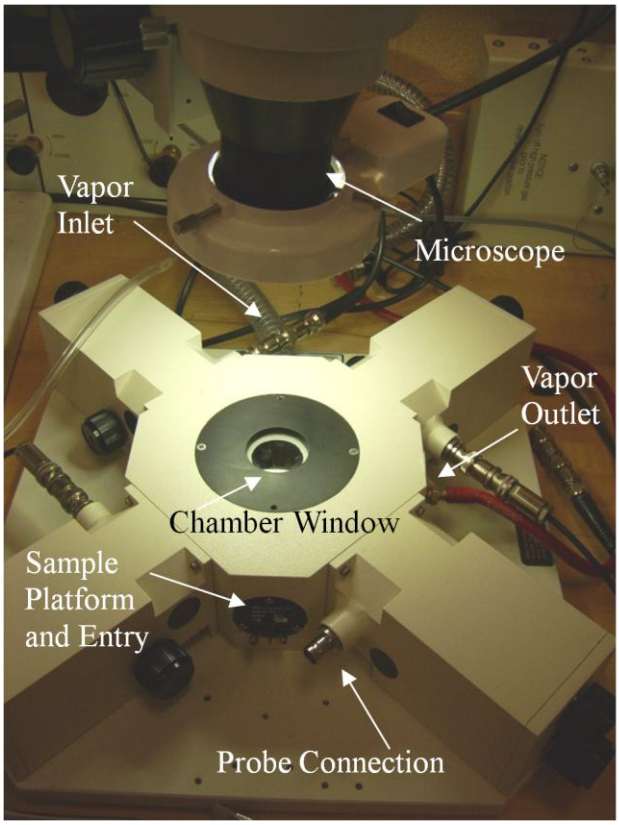

Figure 27 MMR Technologies Inc, probe station chamber model LTMP-4 provides four probes inside a sealed chamber that connects to nitrogen flow

An Owlstone Vapor Generator OVG-4, shown in Figure 28, is used to regulate the nitrogen flow and ethanol flow. Measurements for SAW devices are from the Agilent

Technologies E5070B 300kHz-3GHz Network Analyzer and measurements for the nanowires are from the Keithley 4200 Semiconductor Characterization System.

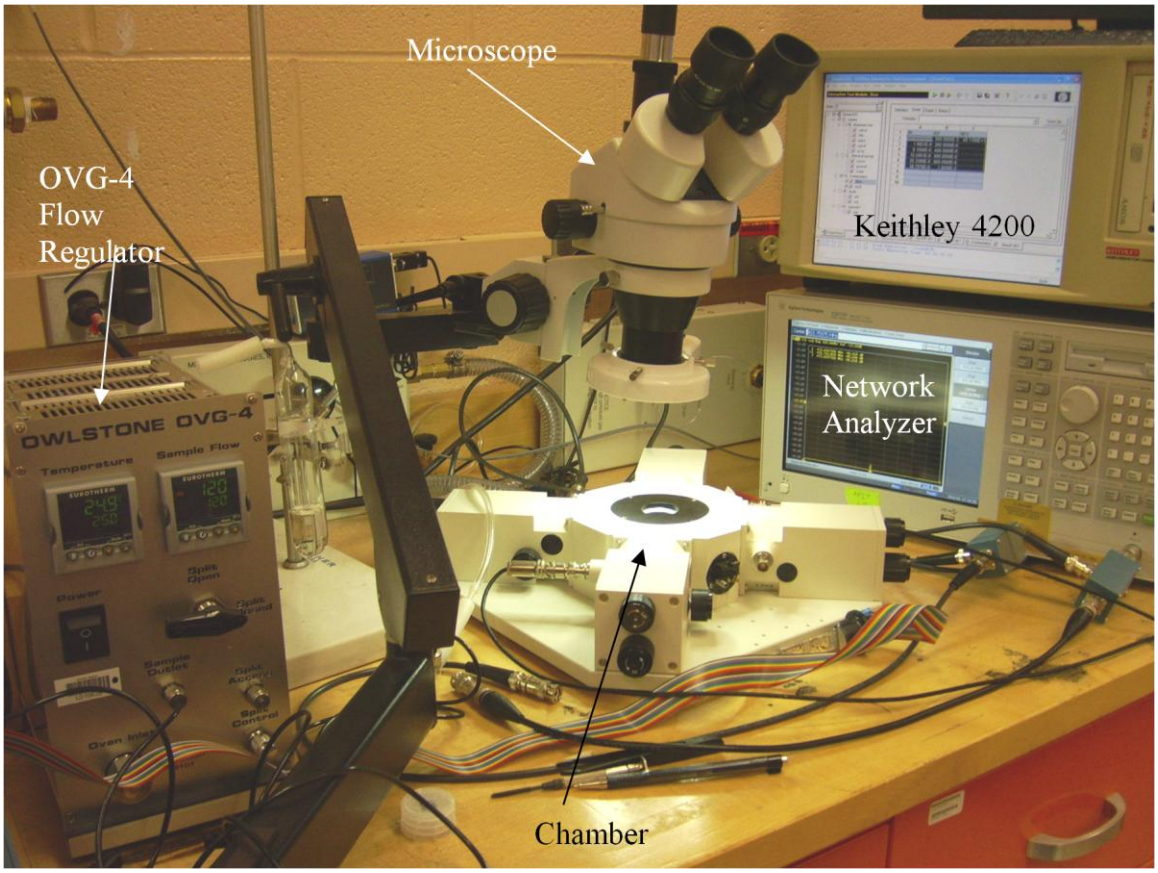

Figure 28 Owlstone OVG, Chamber, Network Analyzer and Keithley 4200 Semiconductor Characterization System

Figure 29 shows a close up of the Owlstone OVG-4 and the tube of ethanol that nitrogen flows through to force ethanol into the chamber. The OVG has a temperature control for its heating chamber and sample flow rate control.

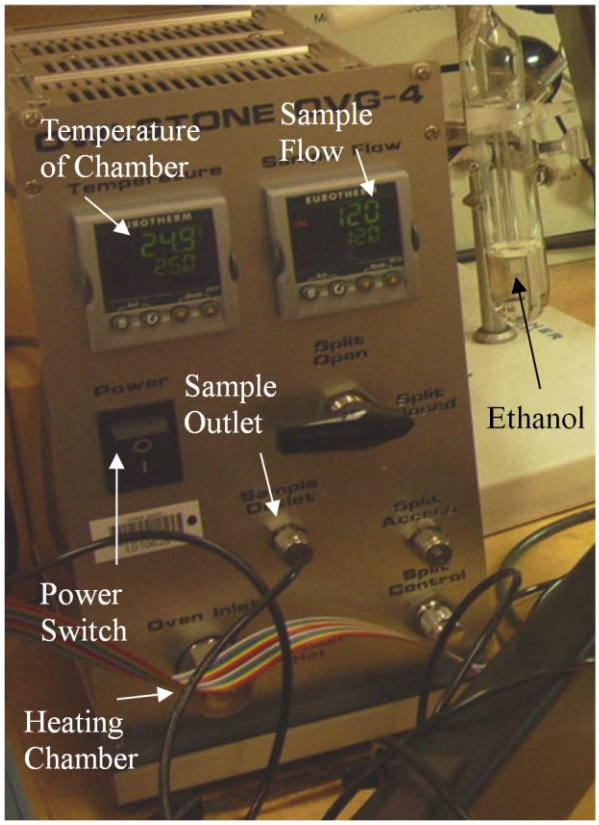

Figure 29 Owlstone OVG-4 used to regulate the flow of nitrogen

The nitrogen flow regulation provides a more direct comparison between how much ethanol and nitrogen is required to produce a change in the frequency characteristics of the SAW. The regulation of nitrogen and ethanol implies that the chamber contains the same concentration of nitrogen or ethanol at the same time when chips are tested. The flow of ethanol is regulated with the OVG set at 85mL/min for ethanol and 500mL/min for nitrogen.

Most of the results appear as graphs in Appendix B: Network Analyzer Data. Section 5.2 shows some partial graphs and some direct comparisons between devices, as well as some notable observations of the devices during testing.

5.2 Results from Large 3µm Devices

Each SAW device is tested individually. SAW activity is verified on each device before testing with chemicals. Measurements of SAW activity are recorded by saving the trace information for phase and magnitude measurements of the S_{12} parameters. The probes are attached to the SAW devices as shown in Figure 30.

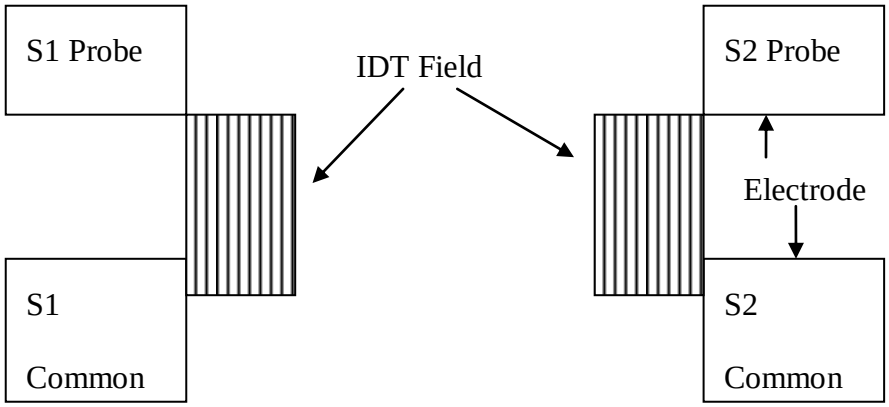

Figure 30 Schematic of SAW connection to network analyzer

All of the devices exhibit similar behavior and shifts in their frequency and phase measurements. An observation not shown on the graph is that the color of the Nafion® visibly changes when the chamber from a blue color to more of a yellow is filled with ethanol.

The magnitude traces exhibit a decrease in peak magnitude and the peak shifts to a lower frequency as ethanol is introduced into the chamber. Figure 31 shows how the trace data changes as ethanol flows into the chamber.

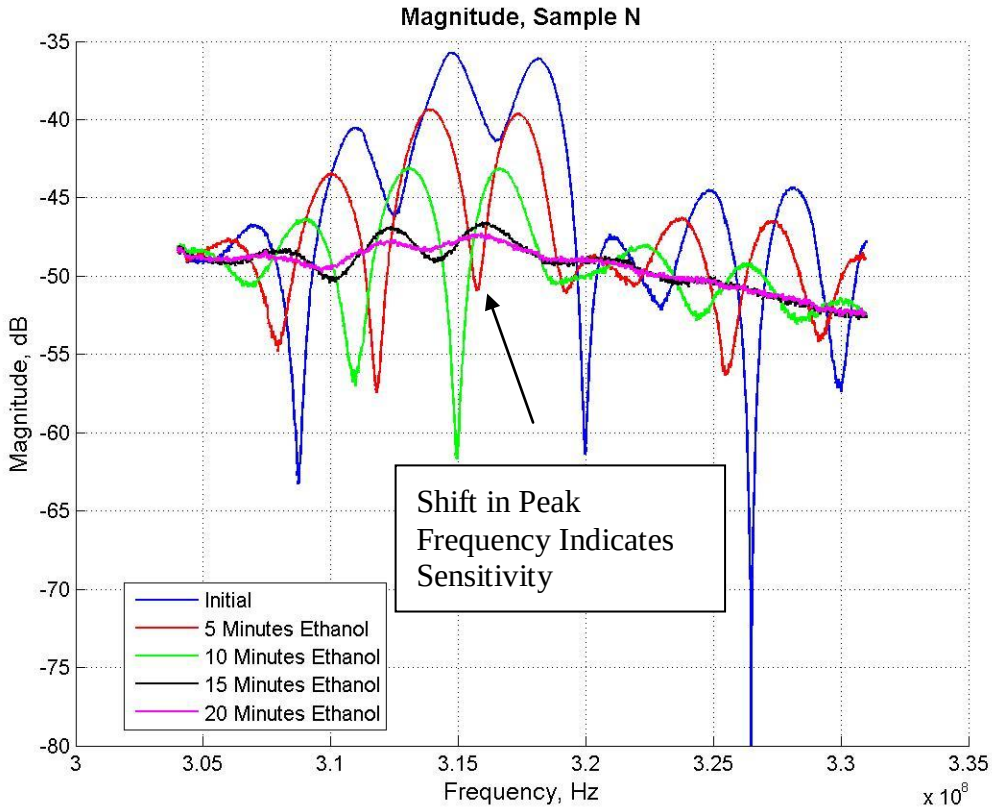

Figure 31 Magnitude traces for an unmodified SAW device during the ethanol exposure process, the shift in the resonant frequency indicates that the device is sensitive to ethanol

The arrow points out the shifting valley and peak in the trace. At 10 minutes of ethanol a sharp valley appears. Such a peak in the valley is observable on all of the devices. The characteristic may be a good way to identify particular concentrations of ethanol, and is a potential signature to look for in the next phase of production for the devices.

The phase traces goes through a similar transition, as seen in Figure 32. The phase ranges from -180 degrees to 180 degrees, which means a spike occurs as the phase

continues to move down. The spike becomes a very identifiable feature to use for comparisons between traces.

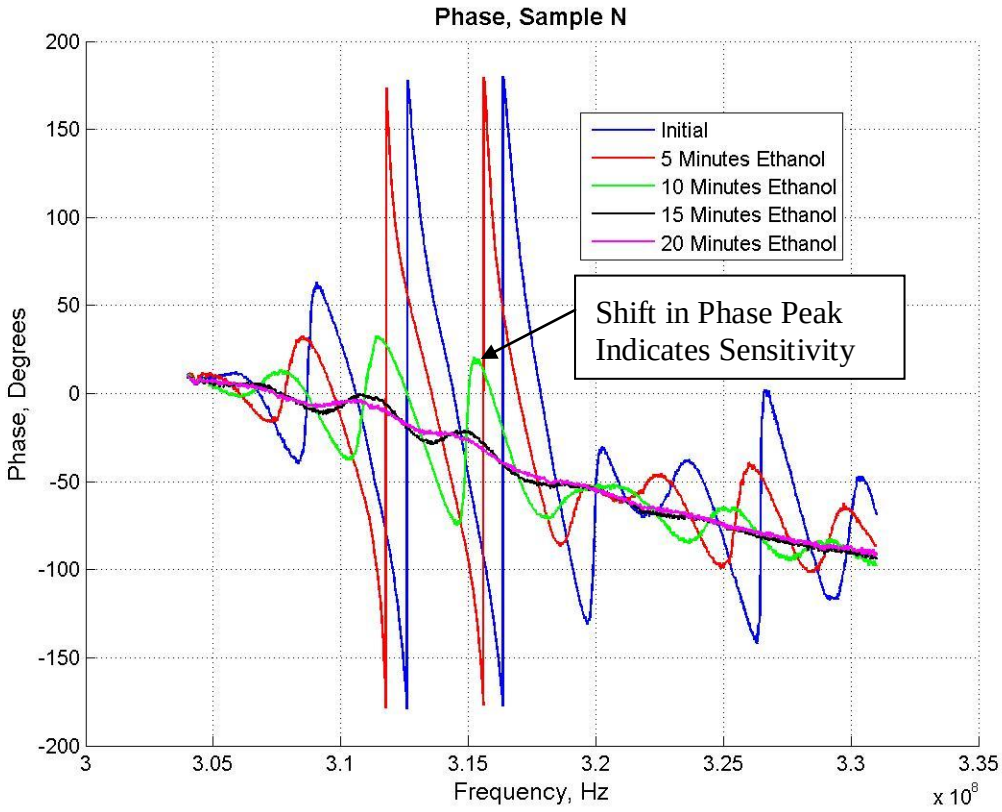

Figure 32 Phase traces for an unmodified SAW device during ethanol exposure, the shift in the frequency at which the phase spikes occur indicate a sensitivity to ethanol

Figure 33 andFigure 34 show the recovery of the device as nitrogen flows back into the chamber to displace the ethanol. The magnitude signal shifts from a subdued trace back to the initial trace that was measured before the introduction of ethanol into the chamber.

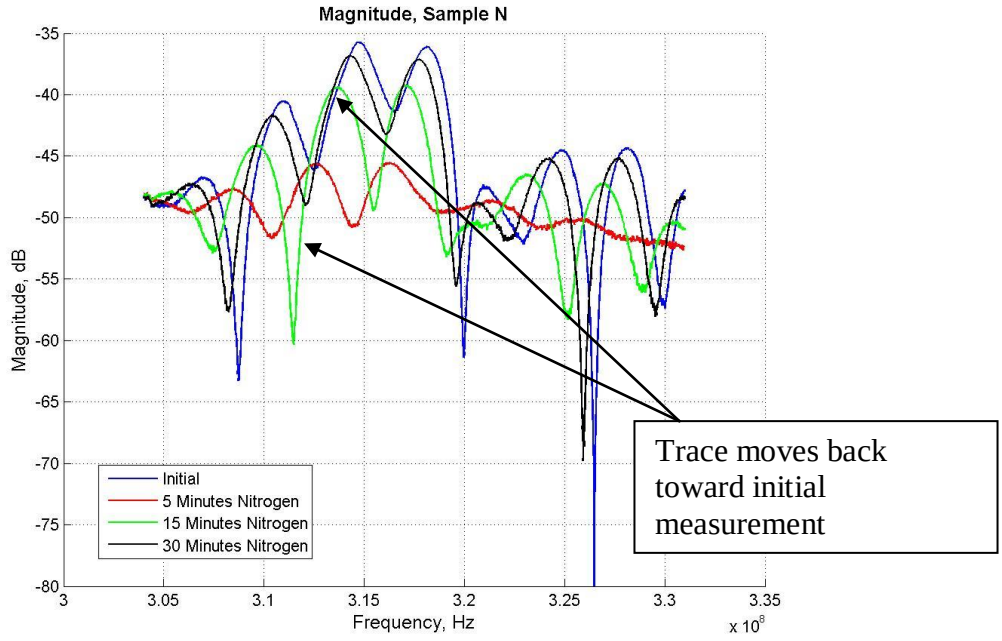

Figure 33 Magnitude traces of an unaltered SAW device recovery, as nitrogen flows into the chamber the frequency signature returns to the initial measurement

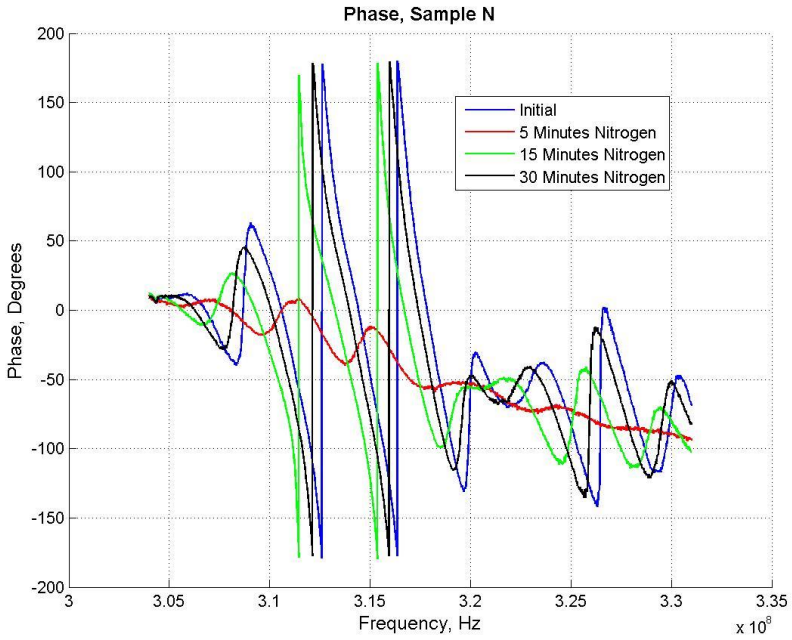

Figure 34 Phase traces of an unaltered SAW device recovery, as nitrogen flows into the chamber the phase signal returns to the initial measurement

As mentioned, all of the devices exhibit similar reactions to the ethanol. The graphs for all of the devices appear in Section B4. The subtle differences between the amounts of shift become the interesting factor for comparison.

5.3 Analysis of SAW Device Tests

Table 5 shows the shifts in frequency for each device at the 5 minutes and 20 minutes of ethanol data sets, as well as the 15 minutes of recovery data. The desired values are large changes in the frequency for ethanol sensing without too much attenuation of the signal. Therefore, large values in the frequency change and smaller numbers in the magnitude change for the ethanol readings are desirable. For the recovery, the device exhibits better recovery if the difference in frequency is small and the difference in magnitude is small. Also notable is that the reading for the sample with the twelve trenches was taken at 12 minutes of ethanol rather than 20 minutes of ethanol because the device reached saturation and with more time would not have distinguishable peaks.

Table 5 indicates that the trenches show a larger shift in frequency after being exposed to ethanol for 5 minutes. The trench propagation also has a larger difference in magnitude after 5 minutes of ethanol. However, the drop in magnitude is expected as sensing occurs and ethanol saturates the Nafion®, which inhibits the SAW propagation. The larger difference in frequency changes are better and indicate that the device senses more ethanol. However, the device also does not recover as quickly. There is still a larger difference in the initial frequency and the peak frequency after 15 minutes of nitrogen flow. The magnitude also does not recover as much on the devices with trenches, which

may be an indication that the device is more sensitive because it is still detecting the level of ethanol. Aanother explanation is that the nitrogen cannot clean the ethanol particles off from the Nafion® in the trenches as well as it cleans the ethanol particles from a smooth propagation field.

Table 5 Frequency and Magnitude Differences for Samples

Sample	Frequency Difference at 5 Minutes Ethanol (MHz)	Magnitude Difference at 5 Minutes Ethanol (dB)	Frequency Difference at 20 Minutes Ethanol (MHz) *12 Min	Magnitude Difference at 20 Minutes Ethanol (dB) *12 Min	Frequency Difference at 15 Minutes Nitrogen Recovery (MHz)	Magnitude Difference at 15 Minutes Nitrogen Recovery (dB)
Unmodified SAW device	0.8	3.61	2.6	12.15	0.7	1.82
CNTs on Nafion®	0.3	0.26	1.6	4.04	0.7	1.15
CNTs under Nafion®	0.6	2.36	2.6	12.47	0.6	2.93
Zinc Oxide, No Trenches	0.4	0.8	2	2.51	0.5	0.81
Zinc Oxide, 6 Trenches	0.9	3.41	3	13.47	1.7	7.21
Zinc Oxide, 12 Trenches	0.9	5.04	2.6*	12.49*	2.3	6.53

*Measurements in 20 Minutes Ethanol Column for the 12 Trenches sample were actually at 12 minutes ethanol because device reached saturation.

Nevertheless, the trenches appear to be more sensitive than an unaltered device and show a larger change in peak frequency. The conclusion that trenches affect the peak frequency is supported by the difference between the frequency changes of the six trench sample and the twelve trench sample. However, once the Nafion® reaches a saturation point, there is little distinction between trenches verses no trenches.

The devices with CNTs show less change in frequency than the trenches. In addition, the device with CNTs coated on the top shows the least changes overall, but recovers the frequency at a rate similar to samples N and F. Sample M keeps its shape better than the other devices and does not exhibit as much decrease in the magnitude of the propagated wave, which could be a desirable attribute because the Nafion® saturation does not completely attenuate the propagating wave. Overall, the CNTs do not show much advantage over an unaltered device, but the trenches do show an advantage in sensing.

Table 6 depicts a similar picture of sample comparisons but uses the phase data from the network analyzer traces. The biggest difference between the magnitude table and the phase table is that the 6 trench device appears to be more comparable to the twelve trench device. The explanation being that the saturation that the twelve trench device experiences at 12 minutes rather than 20 minutes affected its changes. Again, there is no real advantage to adding CNTs to the devices, the normally coated device experiences similar frequency and phase changes to the CNTs. The changes in the normally coated device compare to the trenches, except in the recover phases. As the

samples with trenches recover, they recover the sharp spikes of the average phase plot, but maintain the difference in frequency longer than the unaltered device.

Table 6 Frequency and Phase Differences for Samples

Sample	Frequency Difference at 5 Minutes Ethanol (MHz)	Phase Difference at 5 Minutes Ethanol (Degrees)	Frequency Difference at 20 Minutes Ethanol (MHz) *12 Min	Phase Difference at 20 Minutes Ethanol (Degrees) *12 Min	Frequency Difference at 15 Minutes Nitrogen Recovery (MHz)	Phase Difference at 15 Minutes Nitrogen Recovery (Degrees)
Unmodified SAW device	0.8	4.1	1.9	182.7	0.8	0.1
CNTs on Nafion®	0.2	-1.6	1.1	175.26	0.7	3.4
CNTs under Nafion®	0.4	-60.7	1.7	140.8	0.6	-0.1
Zinc Oxide, No Trenches	0.3	1.7	0.5	142.5	0.5	130.97
Zinc Oxide, 6 Trenches	0.8	-1.9	2.2	196.1	1.4	2.6
Zinc Oxide, 12 Trenches	0.9	0.5	1.9*	202.4*	1.2	-0.9

*Measurements in 20 Minutes Ethanol Column on Z1, 12 Trenches were actually at 12 minutes ethanol because device reached saturation.

The numbers in Table 5 and Table 6 are taken from only one group of data with one device on each different sample tested. No statistical analysis of the data is available, but would be needed for further conclusions and better extrapolation of the findings.

5.4 Nanowire Test Results

Results from the nanowire tests come in the form of current vs. voltage graphs which produce a resistance measurement that relates to the slope of the line. Testing is

done using a four probe method, but the results from a two-probe method are also available. There is typically a 40Ω difference between the two probe measurement and the four point probe measurement. The two probe measurement is the higher resistance value because the two probe method cannot account for the contact resistance the way a four probe measurement does. Figure 35 and Figure 36 show the output graphs of a nanowire measurement with two and four probes, respectively.

The values for the two probe measurements come from the first probe, which is set up to measure the current and voltage values of the probe, as well as the current source for the circuit. The measurements of current and voltage from the first probe are then graphed against one another for the two probe graph. The fourth probe is the ground of the circuit. The second and third probes measure the voltage at a point on either side of the nanowire. The difference between the voltage measurements of the probes is used for the voltage value on the four probe graph.

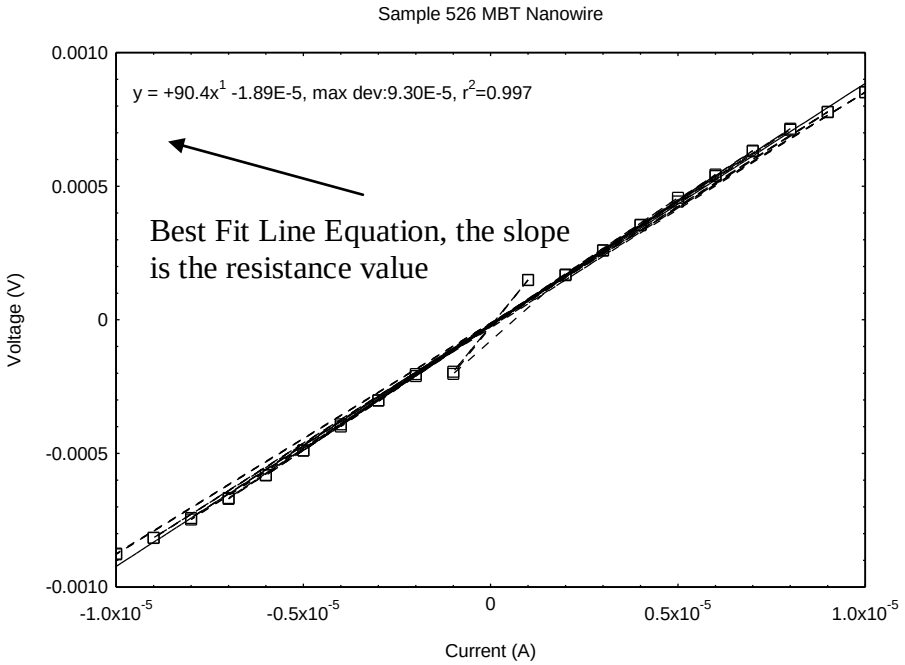

Figure 35 Two point probe measurement of PPy nanowire in the middle bottom top position of sample 526 with best fit line showing a resistance of 90Ω

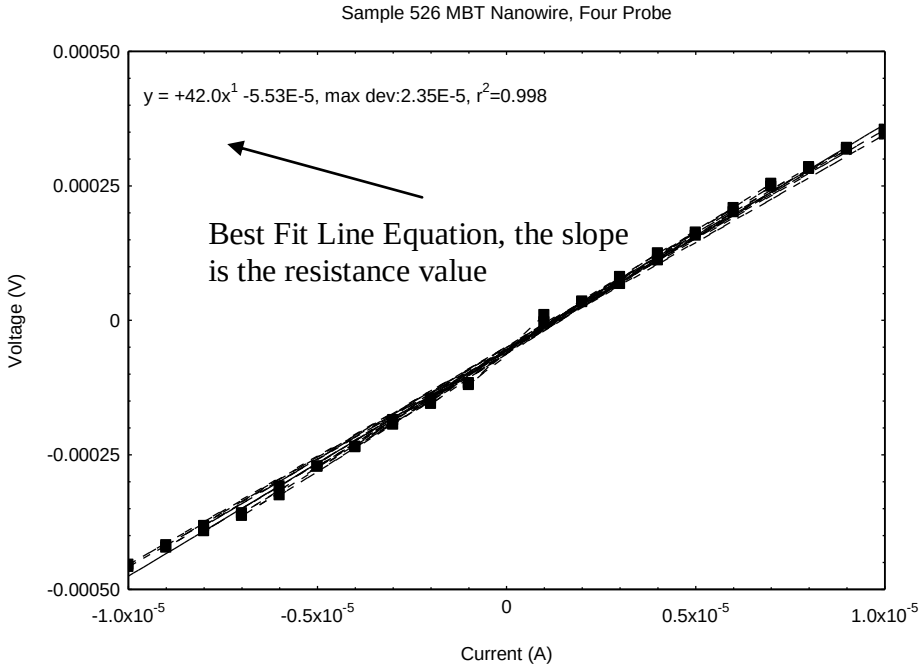

Figure 36 Four point probe measurement of PPy nanowire in the middle bottom top position of sample 526 with best fit line showing a resistance of 42Ω

The nanowires go through the same process as the SAW devices for flooding the chamber with ethanol, but even after 30 minutes of ethanol with a flow rate of 150mL/min no change in the resistance value of any of the nanowires is seen. At the University of Pittsburgh, as methanol is bubbled into the small chamber that contains the nanowire sample the voltage drops significantly for PPy and PANI nanowires. However, the ethanol flow seemed to have no affect on the resistance measurements taken at AFIT on the PPy nanowires on Sample 526 or on the Pd wires of Sample 563.

None of the resistance measurements taken match the measurements of the nanowires that were taken during fabrication. Some of the difference in resistance value is related to the four probe measurement, though the nanowires may experience some change in resistance over time and from transportation factors such as temperature changes. In addition, the chamber at the University of Pittsburgh is much smaller and directs the flow of vapors much better onto the nanowire. The size and nature of the probe station at AFIT could therefore be part of the reason no change in resistance of the nanowires is observed. Some change in resistance is seen when the temperature of the OVG-4 chamber is increased, but even these changes in resistance are not as extreme as the changes seen in the voltage measurement observed at the University of Pittsburgh.

The differences between the results at AFIT and the University of Pittsburgh are attributed to the different test chambers and measurement techniques. Measuring the resistance with a wide range of currents provides a picture of the resistance over a wider range, which is something not available in the Pittsburgh arrangement. Some of the data collected at AFIT seems to show at lower current levels a change in resistance is

apparent, but the change does not happen over a wide enough current spread to change the best fit line that produces the resistance value. Therefore, the research at AFIT shows that there is a characteristic of the nanowires that is not observed through the University of Pittsburgh testing where the measurements are taken at a single voltage and current input level. In addition, the chamber at AFIT provides a more realistic testing arrangement than the more ideal case, a small chamber with a direct chemical flow onto nanowires, that the University of Pittsburgh uses.

5.5 Results of Preconcentrator Tests

The preconcentrators are fabricated using PolyMUMPs™. When the devices are received from the fabricators they are coated with photoresist and still contain the sacrificial oxide. After soaking the devices in acetone for 10 minutes, the sacrificial oxides are removed by submerging the chip in hydrofluoric acid for 3 minutes. The chips are then taken out of the HF and submerged in methanol until they are dried with a CO_2 drier. Chips are dried using AFRL's CO_2 dryer because of unscheduled maintenance on the AFIT CO_2 dryer. After drying, some of the preconcentrators are coated with CNTs.

The CNT coating represents an effort to mimic the carbon coating of other preconcentrators, because the size of the preconcentrators designed limits the ability to use the same carbon coatings. Coating of the preconcentrators is completed by placing CNTs in a 1:1 methanol:DI water solution and sonicating for 5 minutes. The preconcentrators are placed in the solution and then removed by pulling the preconcentrators out under a visible cluster of CNTs, which results in very inconsistent coverage that completely covers preconcentrator devices in some cases. However, the

coating serves the purpose and allows for an investigation of the affect of a CNT coating on a preconcentrator device.

Measuring the concentration capabilities of the preconcentrators is not possible with the test set-ups available because there is no available device that will test the concentration of chemicals in a chamber. There needed to be some way to test if the preconcentrators with CNTs can actually collect particles and then release them when heated. In addition, there are no extra probes for heating the preconcentrator within the chamber while still measuring SAW activity. Testing the devices in the chamber with the preconcentrators requires heating the preconcentrators from the bottom, instead of heating with direct contact as originally intended. The heating method may work, but would use the entire preconcentrator sample device as a preconcentrator. Such a test may be valuable in testing the concentration abilities of the CNTs and the patterns, but was not tried because of complications with the heating arm insert for the probe station. Therefore, tests with the preconcentrators focus on the heating characteristics of the different patterns and the effects of CNTs on heating characteristics.

Tests of heating characteristics of individual preconcentrators show which patterns provide the most uniform heating. The tests also show how carbon nanotubes affect the heating characteristics of the PolyMUMPs™ structures.

The measurements are taken in a QFI Multi-Sensor Microscope System, seen in Figure 37. The system works by heating the background to a specified temperature, 50˚C in this case, and then detecting the difference between the device and the background temperature. The image shows changes in temperature based on a color scale set by the

user. Therefore, the color scale set by the user affects how much temperature change corresponds to the change in color on the image.

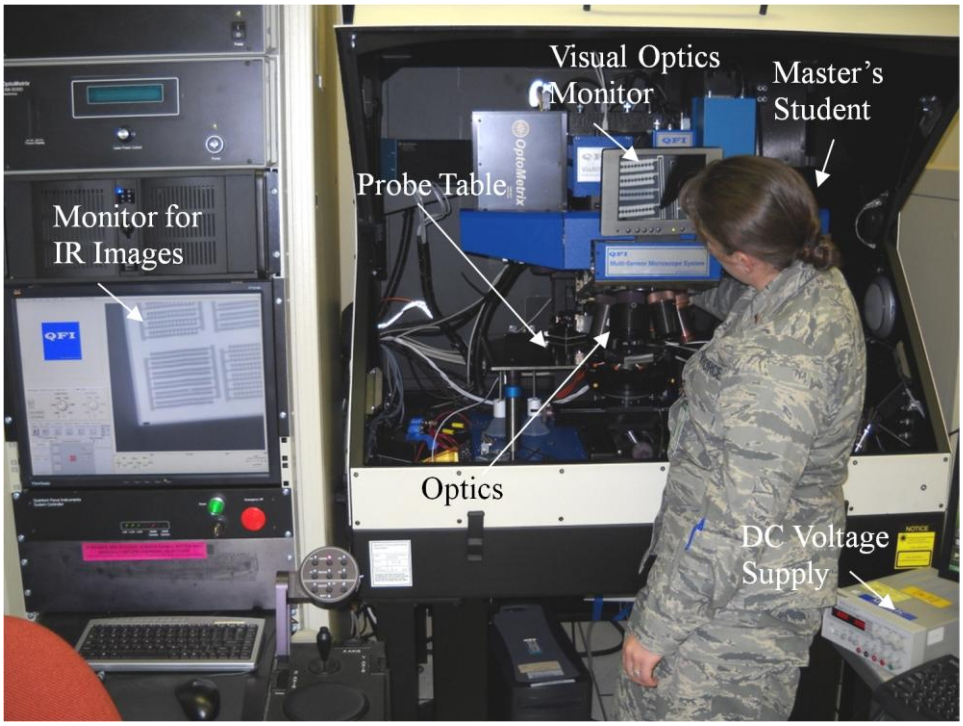

Figure 37 QFI Multi-Sensor Microscope System to provide IR images of preconcentrator prototypes under investigation

5.4.1 Preconcentrators without CNTs

Images of preconcentrator patterns are labeled with the temperature range. Colors range from a dark blue for the lowest temperature to white for the highest temperature. Areas that are out of range on the low side appear as black and temperature out of range on the high side appear as gray.

Figure 38 shows a Poly1-Poly 2 stack in the bars or lines pattern with an input voltage of 2.1V. The low temperatures in the middle are due to bars bent out of plane and resting on the substrate. The temperature range of the image is 46.8˚C to 90.2˚C. The

gray scale image shows how the preconcentrator appears visually, as well as where the probes are connected to the pattern.

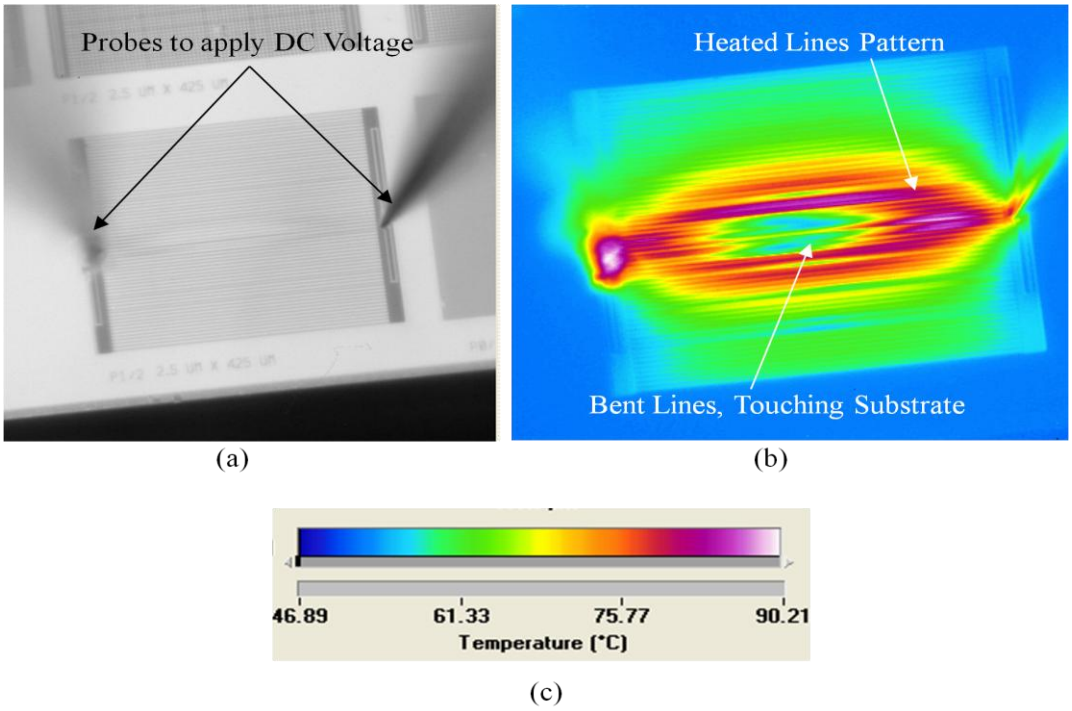

Figure 38 Lines of Poly1-Poly2 stack, 2.1V DC input, temperature range 46.8 to 90.21˚C

Figure 39 shows a bowtie pattern of a Poly1-Poly 2 stack with in input voltage of 2.7V. The temperature range is 51.0˚C to 182.3˚C. The comparison of Figure 39 to Figure 40 shows that placement of the probes affects the heating pattern. The heating pattern is affected by the flow of current through a less direct path through the pattern. Figure 40 shows a Poly1-Poly2 stack in a bowtie pattern with 3.54V input. The temperature ranges from 48.4˚C to 147.2˚C. The second bar of bowties does not heat because it is broken. The two outside bars heat more because as they begin to heat first

due to the current flow, their resistance decreases, causing more current to flow through them than through the other arms of the pattern.

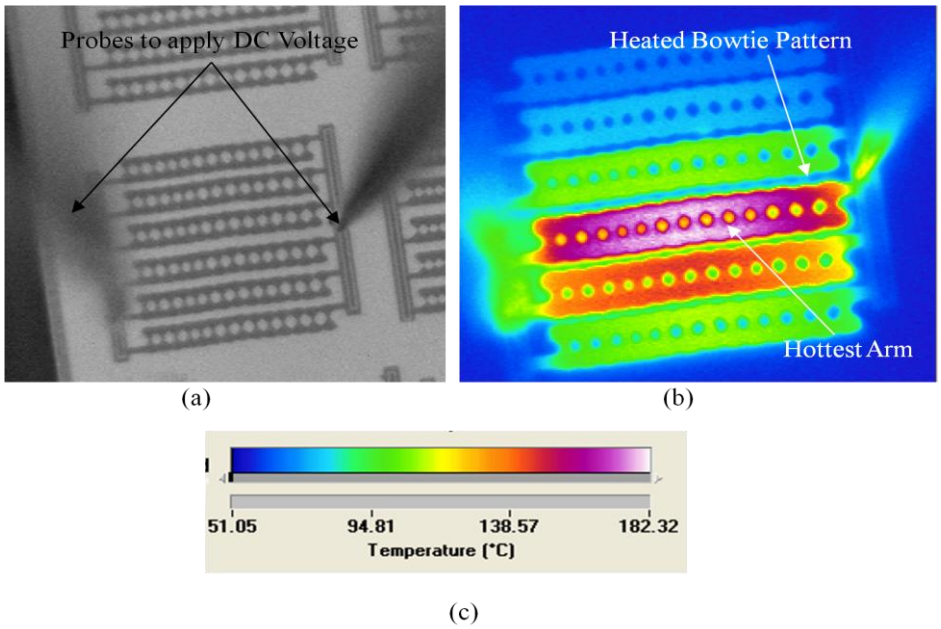

Figure 39 Bowtie Pattern, Poly1-Poly2 stack, 2.7V DC input, temperature range 51.0 to 182.3˚C

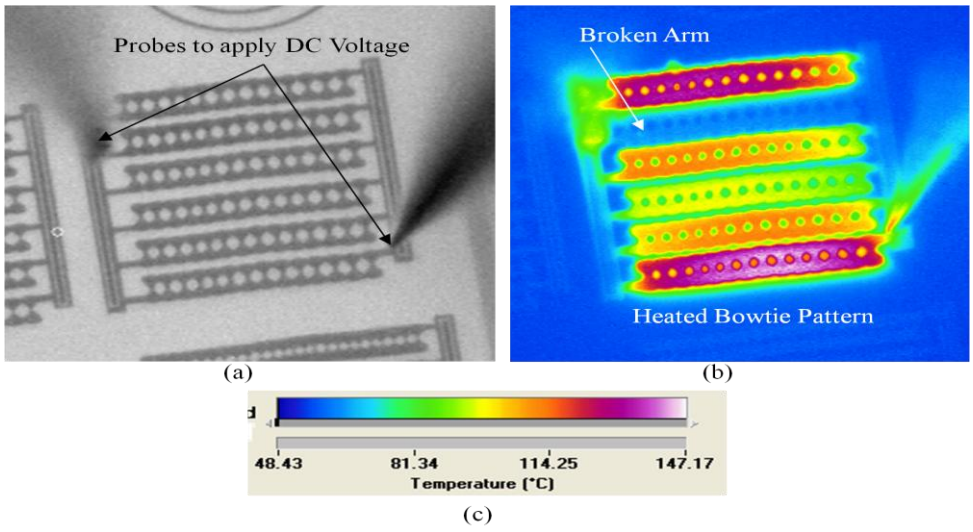

Figure 40 Bowtie Pattern, Poly1-Poly2 stack, 3.54V DC input, temperature range 48.4 to 147.2˚C

Figure 41 shows the grid pattern with 2.44V input. The temperature ranges from 53.8˚C to 214.3˚C. The grid lines are 4µm wide.

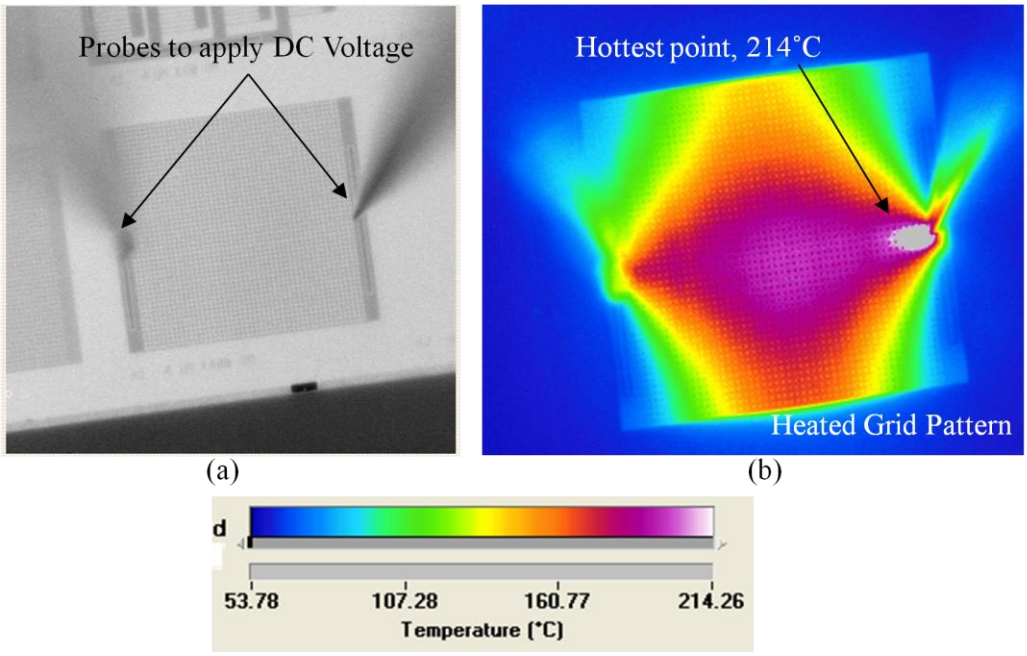

Figure 41 Grid Pattern, Poly1, 2.44V DC input, temperature range 53.8 to 214.3˚C

Figure 42 shows the ladder pattern with a very small temperature range. Part of the small range is due to the fact that the pattern is a Poly0 layer. With 14 V DC input, the temperature range is 75˚C to 82˚C. The rungs of the ladder are 4µm wide, so there is also more material for the voltage to heat than there is in some of the other patterns.

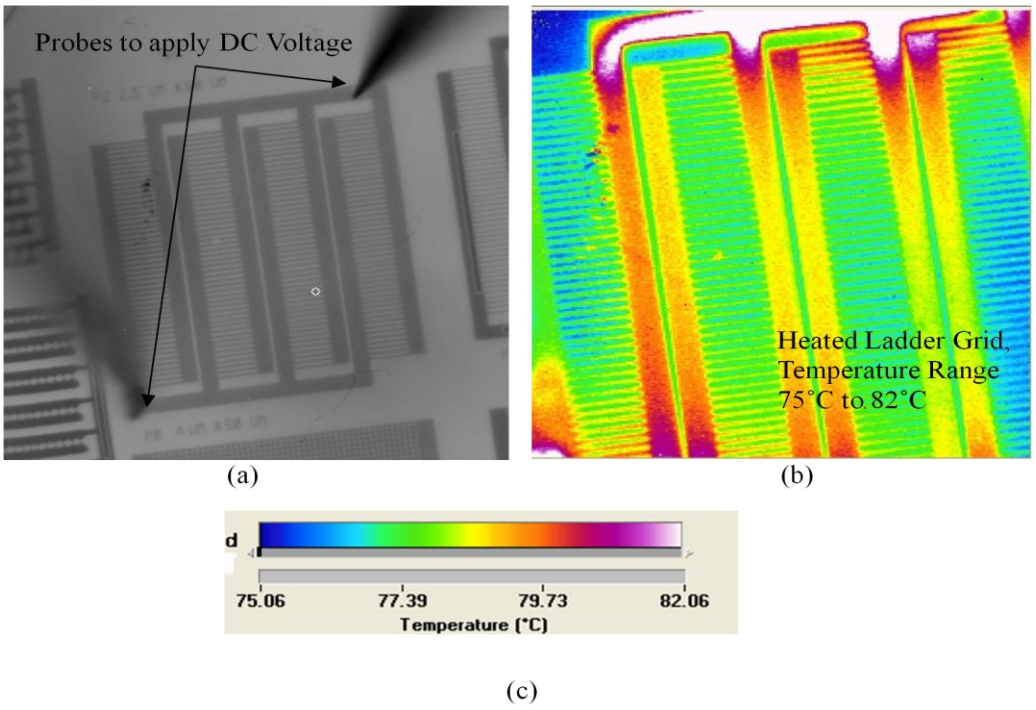

Figure 42 Ladder Pattern, Poly 0, 14V DC input, temperature range 75 to 82˚C

Figure 43 shows the spiral shape. The width of the spiral pieces is 4µm. The pattern is stacked Poly1 and Poly2 and has a temperature range of 49˚C to 93.9˚C. Despite the high voltage, it draws very little current because there is little surface to heat. Spirals that are too long or too skinny easily disconnect from the substrate or become misshapen.

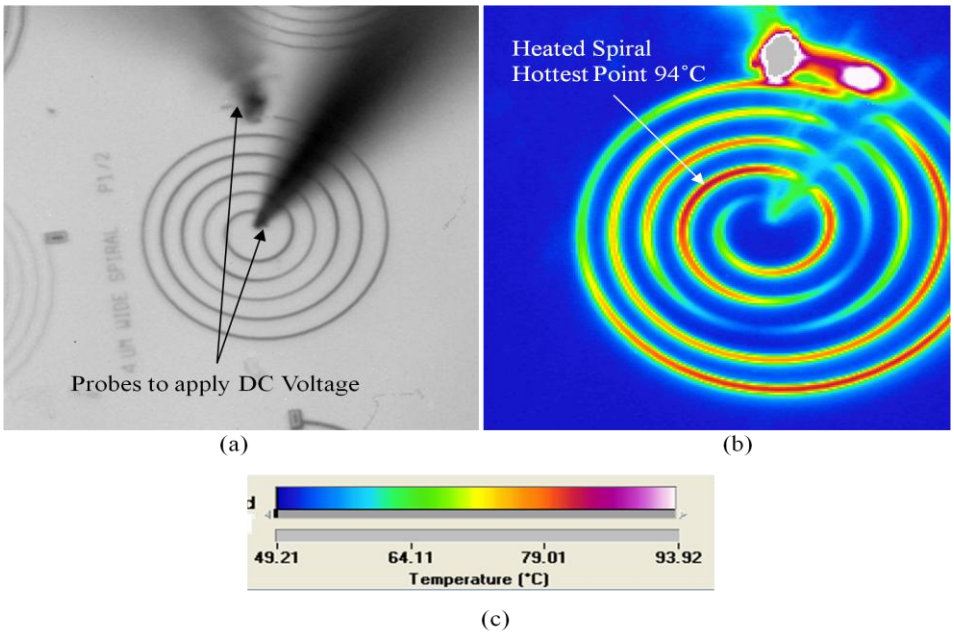

Figure 43 6µm Spiral, Poly1-Poly2 stack, 10V DC, temperature range 49 to 93.9˚C

5.4.2 Preconcentrators with CNTs

There are few good pictures gathered from the preconcentrators with CNTs. Part of this is because of a phenomenon observed during measuring. As the voltage is increased, little change is seen in device temperature, until a threshold is hit. At a certain point, the entire device flashes "white hot" when viewed in the imager. The screen suddenly shows everything is out of the temperature range. The sudden change implies part of the CNT field heats and then the heat is dissipated from one CNT to the next almost instantaneously. The phenomenon is observed repeatedly on the same chip and even on the same pattern, unless the pattern structure breaks. Eventually, the pattern experiences breaking of the polymer structure, and then the phenomenon can no longer be observed. The pictures that follow show some of the observations captured by imaging.

In Figure 44, even though the temperature range is very low, 47.5˚C to 59.3˚C, the grouping of CNTs on top of the pattern are distinctly colder than anything else on the substrate. The CNTs are seen in the gray picture on the left as a white indistinguishable group and appear as black in the colored image on the right, which means that the group is so cold it is outside the temperature range. Even with the low input voltage of 0.3V DC, the pattern heats more uniformly than the patterns did without CNTs based on probe placement.

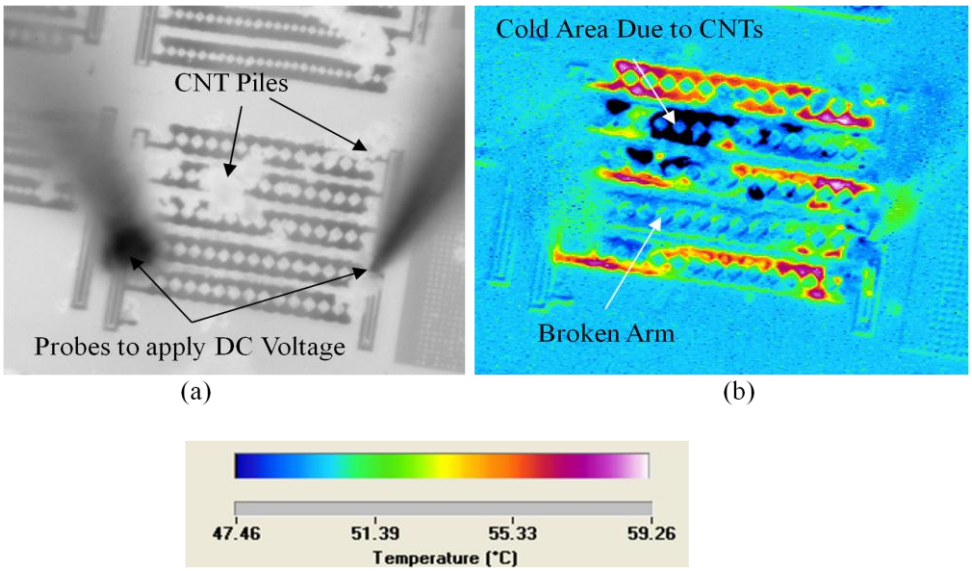

Figure 44 Bowties with CNTs, Poly1-Poly2 stack, 0.3V DC, temperature range 47.5 to 59.3˚C

Figure 45 is as close as any of the images get to capturing the off-the charts heating of the CNTs. The gray figure on the left shows the CNTs in white on top of a ladder pattern and on the right the CNTs are gray, which means way above the

temperature range of 79.3˚C to 152.6˚C. Often, the entire screen would look like the CNT field does in the image on the right of Figure 45.

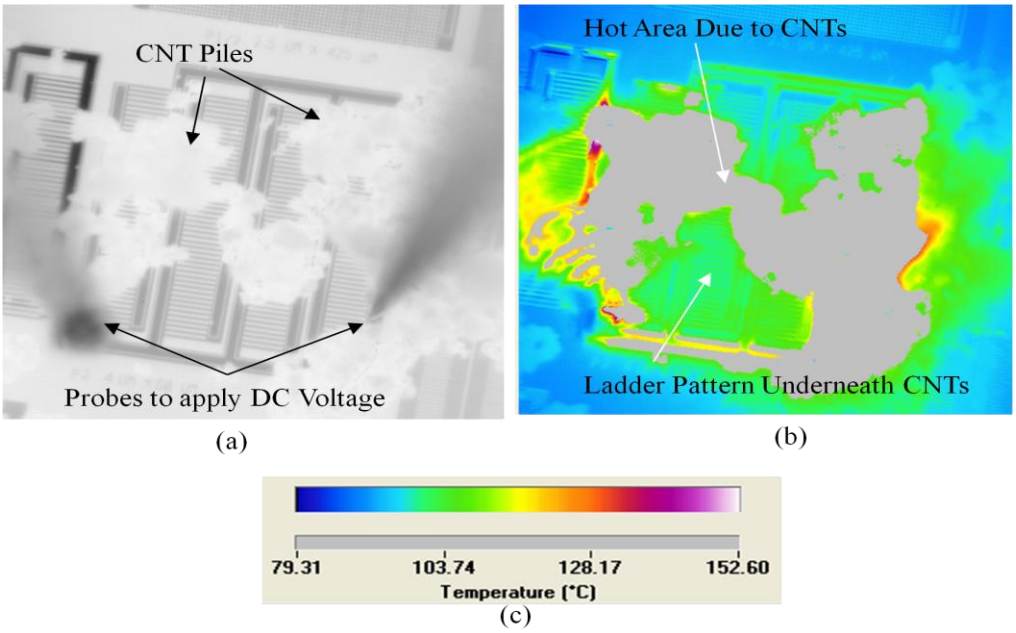

Figure 45 Ladder Pattern, Poly2, 13V DC, temperature range 79.3 to 152.6˚C

After heating the devices, CNTs appear rearranged. In some cases where a clump of CNTs appears at the beginning of testing, the clump would move away entirely or break up into small clumps that adhere to the sides of the structure, as seen in Figure 46. Figure 46 and Figure 47 also show how easily the lines patterns break. The polysilicon layers expand when heated because of the thermal expansion properties of the material; the bending causes the lines to pull away from the anchor and break. Some of the breaking could be due to the post-processing step of depositing CNTs; however, the patterns look fine under visual inspection during probe placement.

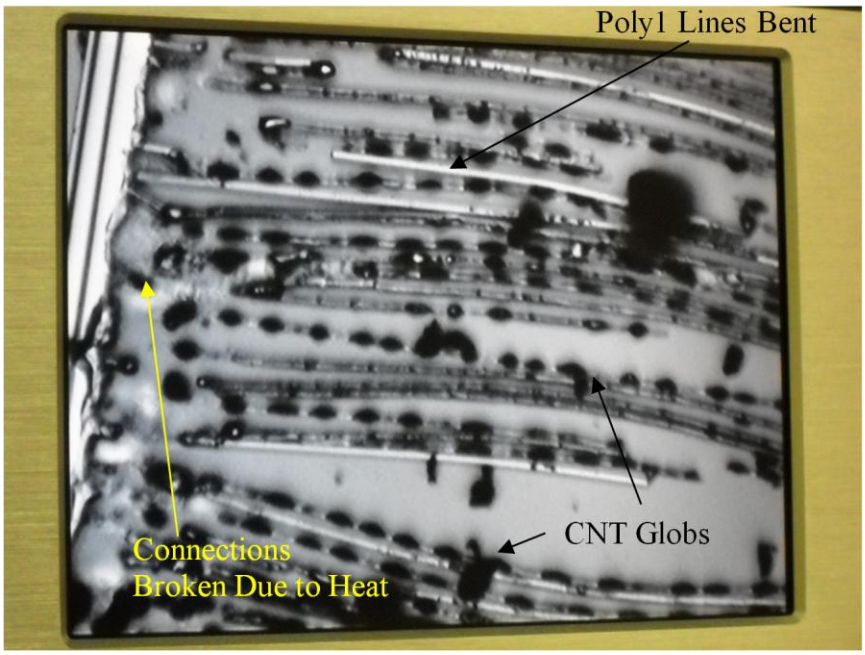

Figure 46 Bars pattern, Poly1 after heating, clumps of CNTs appear as black and poly layer structure is white

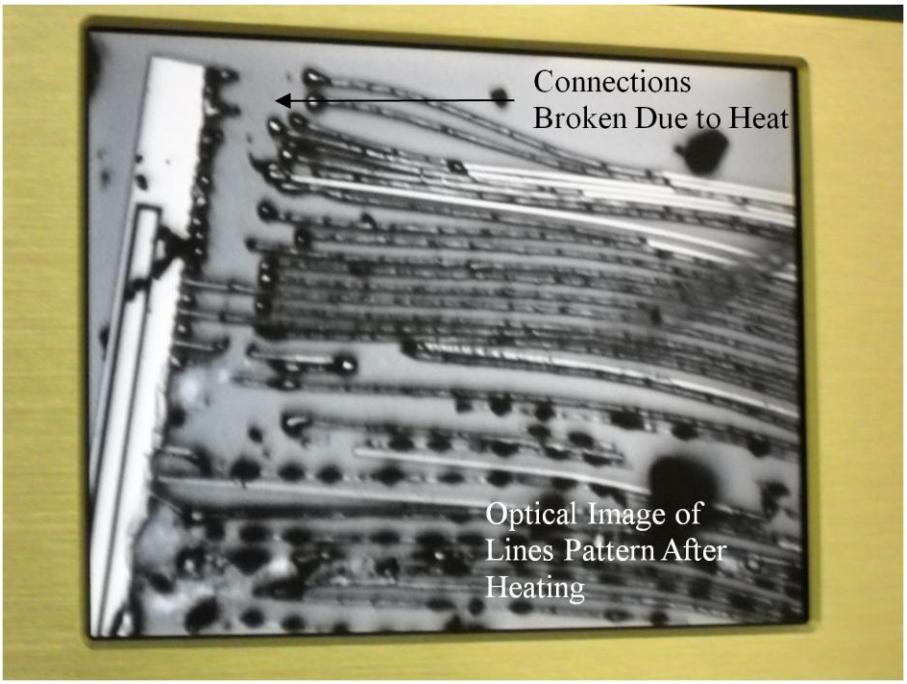

Figure 47 Broken Poly1 bars due to heating and bending of Poly1 layer

5.4.3 Analysis of Preconcentrator Heating

The grid pattern heats the most uniformly of the patterns observed. The power consumption is not very different between patterns, however is lower in spiral shapes. Poly0 layers tend to cause heating to the substrate as well as heating to the pattern because Poly0 is not isolated from the substrate. The larger feature sizes allow for more heating before bending out of shape too much and breaking.

The flash of heat from the CNTs is related to the thermal and electrical conductivity of CNTs [27]. Other researchers have also found uniform heating of CNTs in a preconcentrator setting [3, 4]. The large difference in heating characteristics between the devices with and without CNTs is because the same current and voltage fed into heats the small feature sizes of the CNTs much more than the polysilicon. CNTs have conductive properties similar to metals, so they will heat to a higher temperature than the polysilicon once the power source reaches a CNT field [27].

VI. Conclusions and Recommendations

SAW devices are one way to detect chemicals. There are a wide variety of possible polymer coatings that make the devices sensitive to many different chemicals. The creation of an array of devices with different coatings introduces the possibility for a handheld device that is sensitive to many hazardous chemicals. Making the devices more sensitive decreases the risk to human and animal life.

The work in this document focuses on making SAW device chemical sensors more sensitive by altering the propagation field of the surface wave and investigating the sensitivity of nanowires as chemical sensors. All tests on the SAW devices involve sensing with ethanol with a Nafion® coating, but the principle of increased sensitivity expands to other chemicals. The devices are fabricated in the AFIT cleanroom and tests are done at an AFRL facility with a sealed MMR Technologies Inc. probe station chamber. The research includes altering the design of SAW devices to increase the sensitivity. The modifications aim to increase the surface area of the field, therefore increasing the amount of sensitive coating on the propagation field.

Changes to the field include etching trenches along the propagation field and coating devices with CNTs both under and on top of the sensitive layer. The results show that increasing the surface area with trenches etched in the propagation field does increase the amount of change seen at each concentration of ethanol. However, the trenches also slow the recovery response of the device because the propagation continues to be affected by the ethanol as the chamber fills with nitrogen. The CNT coatings also affect the changes due to ethanol.

Nanowires are also a possible solution for chemical sensing. Nanowires fabricated at the University of Pittsburgh show sensitivity to methanol, hydrogen and nitrous oxide. The chemicals cause a change in nanowire resistance. Work at AFIT on the nanowires involves testing them in the MMR Technologies Inc. chamber to show the sensitivity of wires to ethanol. The nanowires are less rugged than SAW devices because of their small size. To date the nanowires show no measurable sensitivity to ethanol in the MMR Technologies Inc. chamber; but the measurements at the University of Pittsburgh are very promising. The University of Pittsburgh has repeatedly observed changes in the current and voltage readings across a nanowire. Explanations for the difference in observations are that the chamber at AFIT is a more realistic testing arrangement because the chamber at the University of Pittsburgh is much smaller and the flow of vapor is much more directed onto the nanowires. The MMR Technologies Inc chamber is more of an ambient air simulation, which may be part of the difference in sensitivity observations. Additionally, the measurements of resistance at AFIT use a wide range of current values by using a semiconductor analyzer, which provides a broader picture of what happens to the nanowire resistance where as the measurements at the University of Pittsburgh use a single current level and measures the changes in the voltage drop across the resistor.

The preconcentrator prototypes of PolyMUMPs™ fabricated devices provide insight to the heating of PolyMUMPs™ structures and the effects of a CNT coating. The aspects researched include heating characteristics and the effect of CNT coating on the devices. PolyMUMPs™ structures heat quite uniformly in a grid pattern and have a low power consumption that is good for preconcentrators. However, small features in

PolyMUMPs™ layers do not have the ability to reach high temperatures without deforming because of expansion. For a device to reach the 300°C needed for heating preconcentrator coatings, larger structures than the ones tested here must be used, especially for the lines patterns because the lines bridges deformed enough to break the structure before reaching 300°C, other patterns did not exhibit the same weaknesses at the same temperatures. Additionally, the carbon coating on the structures helps the structures heat quickly and uniformly.

6.1 Summary of Contributions

Contributions to the chemical sensing field of study include the investigation of altering the propagation field of a SAW device. The alterations appear to result in a higher sensitivity of SAW devices. The samples with trenches in the propagation field show a shift in frequency peak faster than unaltered devices and faster than devices with CNTs. The samples with CNTs both on and under the Nafion® coating are comparable to unaltered devices and show little advantage. A disadvantage of the trenches is that the recovery of the device takes twice as long as an unaltered device. The length of recovery time may be related to the sensitivity of the device, or may be because the nitrogen does not clean out the trenches as well as an unaltered propagation field.

Testing on the nanowires does not show any convincing chemical sensing results from the AFIT testing, which highlights the need for testing devices in various environments because the testing at University of Pittsburgh shows that the nanowires are quite sensitive to various vapors. This work also presents some preconcentrator prototypes that can be added to SAW devices to increase their sensitivity.

6.2 Suggestions for Future Study

Some areas of this work that are possibilities for future work are introducing ethanol into the chamber so that the concentrations of ethanol are more precise and the comparisons between changes in the signal are more comparable. Running more tests on the SAW devices will provide a more statistical analysis of the observations made in this study. Another direction is to continue researching different structures for sensing devices such as trench sizes, the inclusion of preconcentrators or using nanowire devices and arrays. More data points and measurements of devices with trenches would allow for a more statistical analysis of the difference caused by the trenches vs. the difference caused by the individual SAW devices, each of which is unique and has a unique frequency signal.

The nanowires need more testing and more convincing results; one thing that would add to the results is measuring current and voltage values that show the resistance changes. Testing the nanowires with both ethanol and DNT is another area for future study. The observation of testing at the University of Pittsburgh implies that there is a difference between the testing environments and a change in resistance over a wide range of current values does not explain the phenomenon that the University of Pittsburgh observes. The difference between the two sites and the specific current levels at which the nanowires need to be measured needs investigation.

Also, taking the preconcentrators a step further and finding a way to measure the concentration factors of preconcentrators. The preconcentrator work is a project of its own and may benefit from some use of commercial preconcentrators and known

preconcentrator structures for comparison. Further study into CNT absorption of chemicals may show that CNTs are a good alternative for preconcentrator coatings [27, 28].

The creation of a circuit for an array of SAW devices is another project. A circuit would focus on the signal processing and relation of particular changes in the propagating wave to particular chemicals and concentrations. Another possible direction is experimenting with various biological and polymer films and how the films react to the different structures. The study of polymer and chemical reactions is much more of a research area for chemical engineers and chemists. However, the application of new and different polymers and applying the thin films and seeing their interaction with the MEMs devices is an intriguing area and shows a lot of promise for various electronic nose technologies and sensors to detect hazardous biological and chemical threats.

Appendix A: SAW Fabrication Process

Section A1: L-edit Patterns

2µm Finger Pattern

The L-edit patterns are difficult to show because of their small feature sizes. In Figure A1, the large rectangular areas have 2µm fingers alternating with 2µm spaces. The fingers are 400µm long and total to 100 on each side. The center to center spacing is 2000µm. The four smaller rectangles are bond pads. The upper rectangle connects to half of the fingers and the lower rectangle attaches to the other half, in an alternating fashion. See Figure A2 for a larger image of the intersection. The alignment marks are for aligning the pattern later with the trench patterns. Aligning the marks with the trenches' alignment marks places the trenches in the middle of the propagation field.

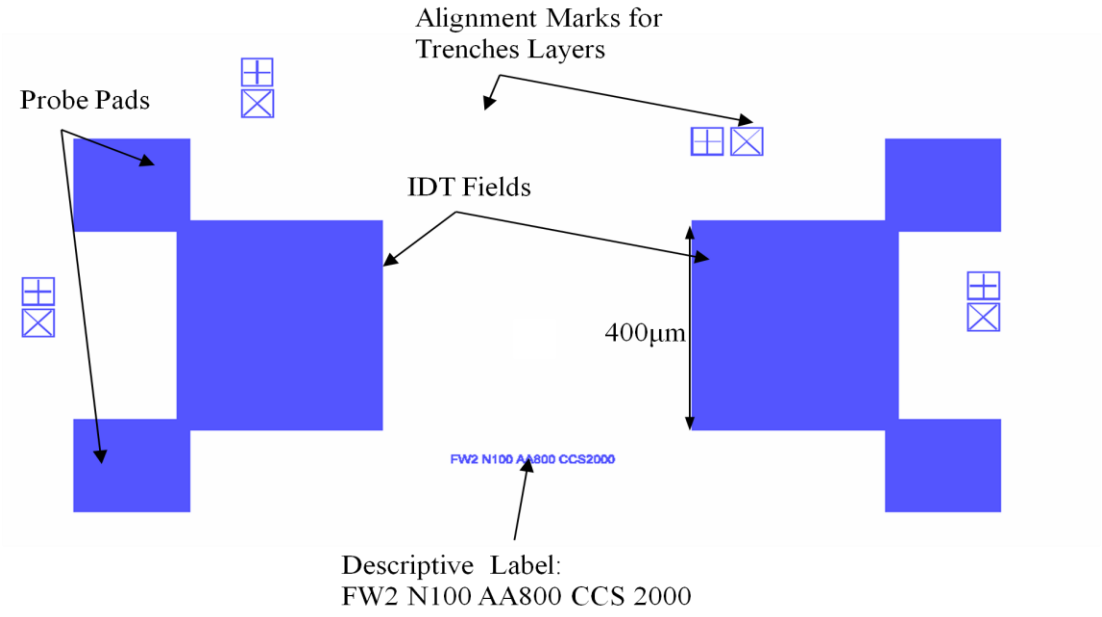

Figure A1 2µm Finger SAW Device Pattern

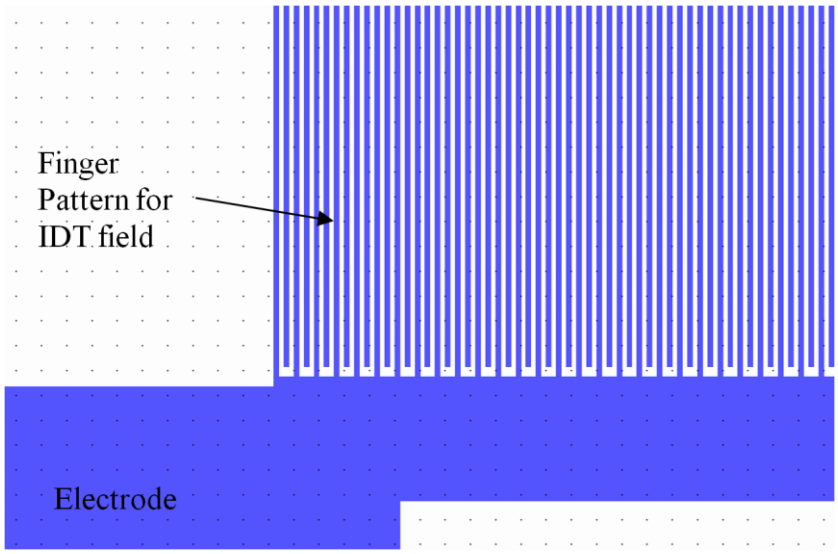

Figure A2 2µm Finger Device, Bond Pad and Finger Intersection

3µm Finger SAW Device Patterns

Three different sizes of 3µm finger SAW devices exist on the mask used for this research. Most of the data is from the largest of the three patterns. The smallest version has 17 fingers that are 85µm long and a center to center spacing of 400µm. The medium pattern has 33 fingers that are 150µm long and has a center to center spacing of 500µm. The largest 3µm finger design has 65 fingers on each side that are 300µm long and a center to center spacing of 1000µm. Figure A3 shows the basic shape of all three of the 3µm SAW devices. The mask labels each device with the finger width, finger length, center to center spacing and number of fingers.

The 3µm patterns included traces to the bond pads, instead of directly connecting as the 2µm pattern does. The difference makes no big difference, merely space usage and drawing preferences. Some problems also occur with the traces to bond pads being scratched off, however.

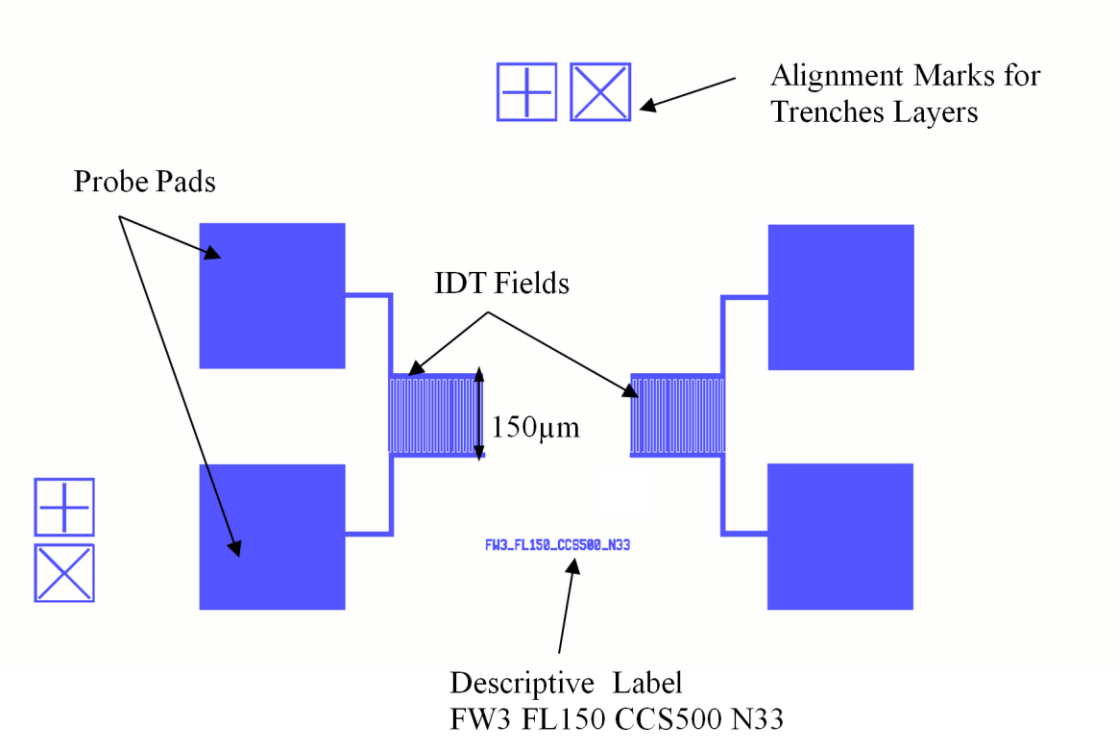

Figure A3 Medium 3µm Finger SAW Device Pattern, Finger width 3µm, finger lenths 150µm, center to center spacing 500µm, number of fingers 33

Scratch a line to indicate flat edge of wafer for propagation direction Scratch a number or letter as identifier for chip
Clean Sample Spray sample with acetone for 30 seconds with spinner at 500 rpm Spray sample with methanol for 20 seconds with spinner at 500 rpm Dry with nitrogen for 10 seconds with spinner at 500 rpm Bake sample on hotplate at 110˚C for 2 minutes
Deposit Photoresist Deposit S1818 photoresist on clean sample without the spinner moving Using ramp of spinner, spread the 1818 at 500 rpm for 5 seconds Spin sample for 30 seconds at 3000 rpm Bake on 110˚C hotplate for 2 minutes
Exposure with AFIT EVG620 Clean the mask with acetone and methanol, then dry the mask with nitrogen Place mask in mask aligner Align flat edge of wafer mark so that one end of SAW device pattern is toward mark Expose photoresist for 5 seconds
Development Develop the photoresist with spinner at 500 rpm Spray with 351 developer for 5 seconds Stop the spinner and continue spraying for 5 seconds Stop spraying and let the developer puddle on chip for 5 seconds. Begin spraying chip again and start spinner at 500 rpm, continue for 10 seconds Spray chip with water for 30 seconds with spinner at 500 rpm Dry chip with nitrogen for 15 seconds with spinner at 500 rpm Dry back of chip with nitrogen and inspect development, adjust development time and process as needed for desired results
Metal Deposition Plasma ash sample for 4 minutes with power at 75 Watts Using evaporation, deposit metals in the following order: 100 Å Titanium 750 A Aluminum 100 A Nickel 150 A Gold
Metal Liftoff Use tape to remove a majority of the metal Soak chip in acetone for 20 seconds, or bubbles form under metal to be removed Place dish with acetone and chip in sonicating machine and sonicate for 3 to 5 minutes, until pattern of metal looks well defined Clean chip with acetone and methanol using cleaning steps

Deposit Nafion®
Nafion® is at the AFRL facility, but any spinner will work Deposit desired weight of Nafion® on stationary chip Start spinner with spread speed of 500 rpm for 10 seconds, then spin at 4000 rpm for 30 seconds Let sample dry for more than 24 hours

An important consideration is the age of the photoresist. After about 3 months photoresist starts to age and the exposure and developing processes do not provide usable patterns or consistent exposure and development results. Chips that exhibit patterns that are over or underdeveloped can be cleaned off and coated with photoresist again. Pictures of photoresist coatings after development are shown in Figure A4.

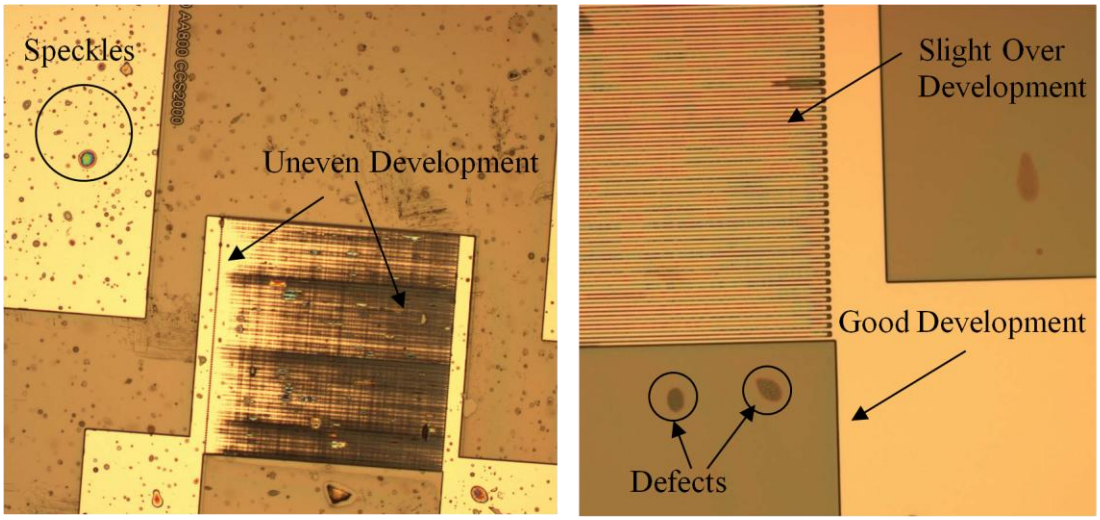

Figure A4 Development Photographs: (a) is an example of poor development, the speckles are probably due to old photoresist. (b) is an example of good development, however the color variation of the fingers indicates that the fingers are slightly over developed

Figure A5(a) shows poor adherence of the metal to the substrate. One of the problems with the sample is that it was not plasma ashed before metal deposition.

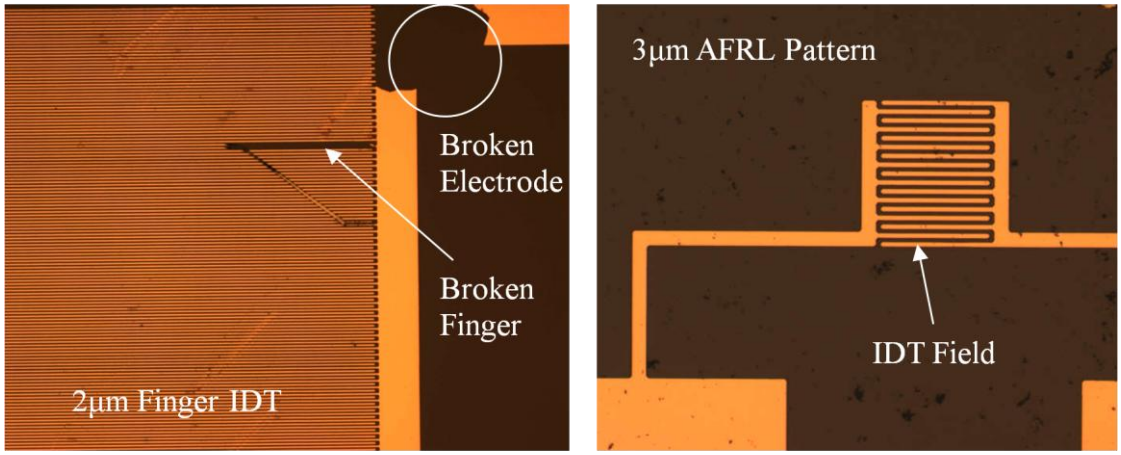

Figure A5 Metalized Sample Images (a) shows a finger that did not adhere to the substrate and part of the bondpad connection that did not adhere to the substrate. (b) shows one complete side of a SAW device from the AFRL mask with 3µm fingers with good metal liftoff

The nanowires are grown on a slice of silicon that has a number label and then each nanowire has a corresponding position label, such as left bottom top (lbt) or right bottom top (rbt), etc. for the 16 possible spaces for nanowires.

One thing that may help with the fabrication of the fingers is to create a mask with more space between the end of the fingers and the connecting electrode, as shown in Figure A6.

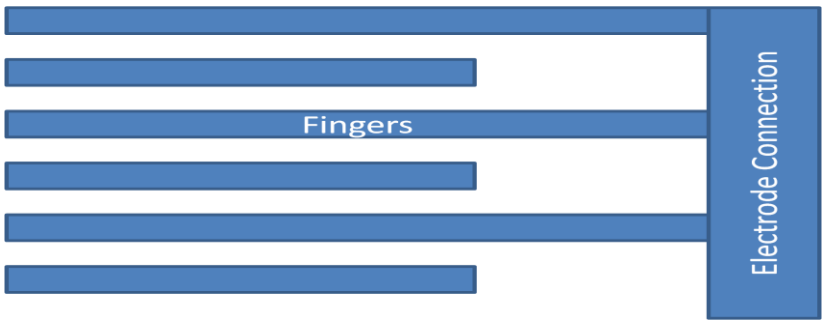

Figure A6 Example of IDT Pattern

Appendix B: Network Analyzer Data

Images are from tests performed on various samples. Each chip has a letter or number scratched on the back. The letters help keep track of which chip is which so that the configuration can be paired with the chip. The numerical designation indicates if the device was the first, second or third and so on sample tested on the chip on the particular day. No notes exist for where the device is located on the chip, but some visual inspection of the chip when absorbing ethanol suggests that device placement in the chamber may have a small affect on how the device is exposed to ethanol.

The measurement results are labeled based on the day the data was collected, whether the trace is phase or magnitude, if the device being tested is the first test of a device on the particular sample, and the sample from which the traces came. The traces are labeled based on how much time has elapsed with the ethanol or nitrogen filling the chamber.

Section B1: 3µm Size Comparisons

There are differences in the trace data between different devices and samples. Sample M is coated with CNTs and then a 5% Nafion® solution. The Nafion® thickness averages 0.30 microns. The data for the sets of sample M in Figure B1, Figure B2, Figure B3, and Figure B4 come from tests performed on 23 November 2009, before CNTs are dry coated on top of the Nafion®. Figure B5 and Figure B6 data comes from tests performed on 3 December 2009.

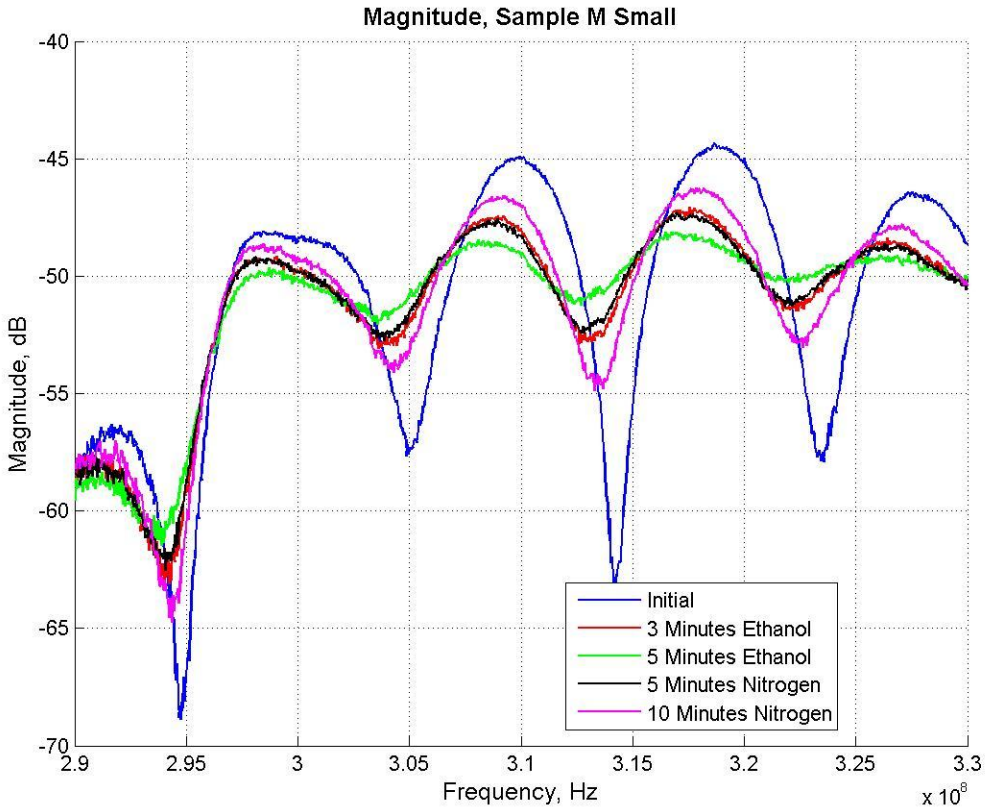

Figure B1 3µm Small, Sample M, 5% wt Nafion®, Magnitude

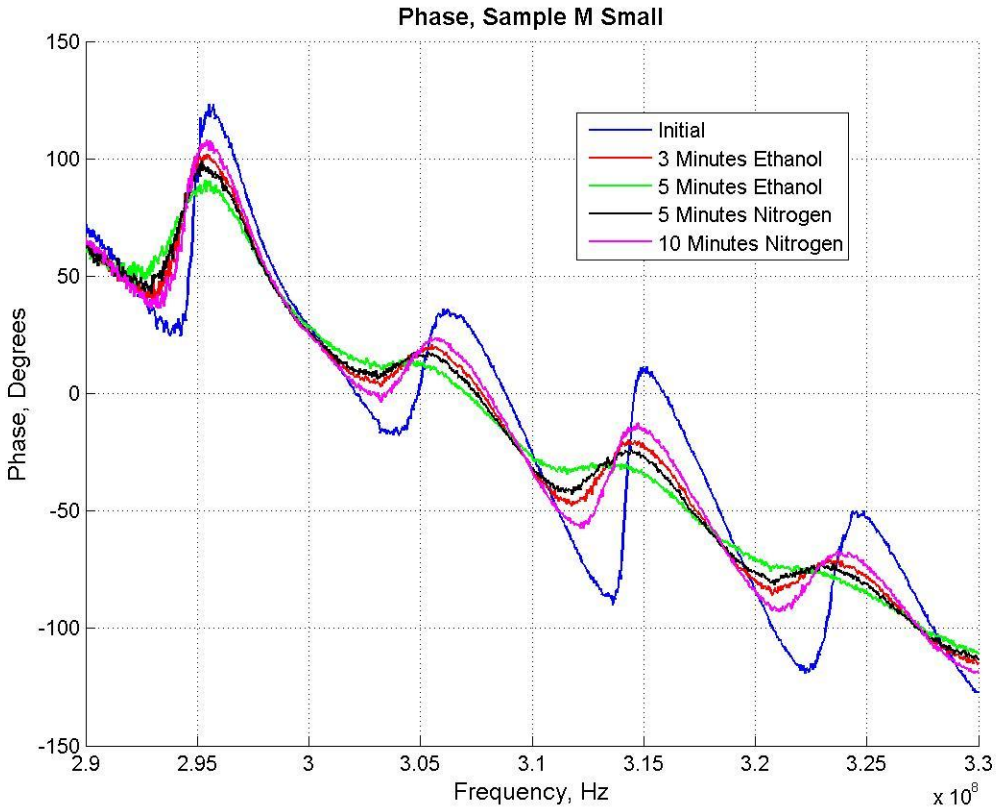

Figure B2 3µm Small, Sample M, 5% wt Nafion®, Phase

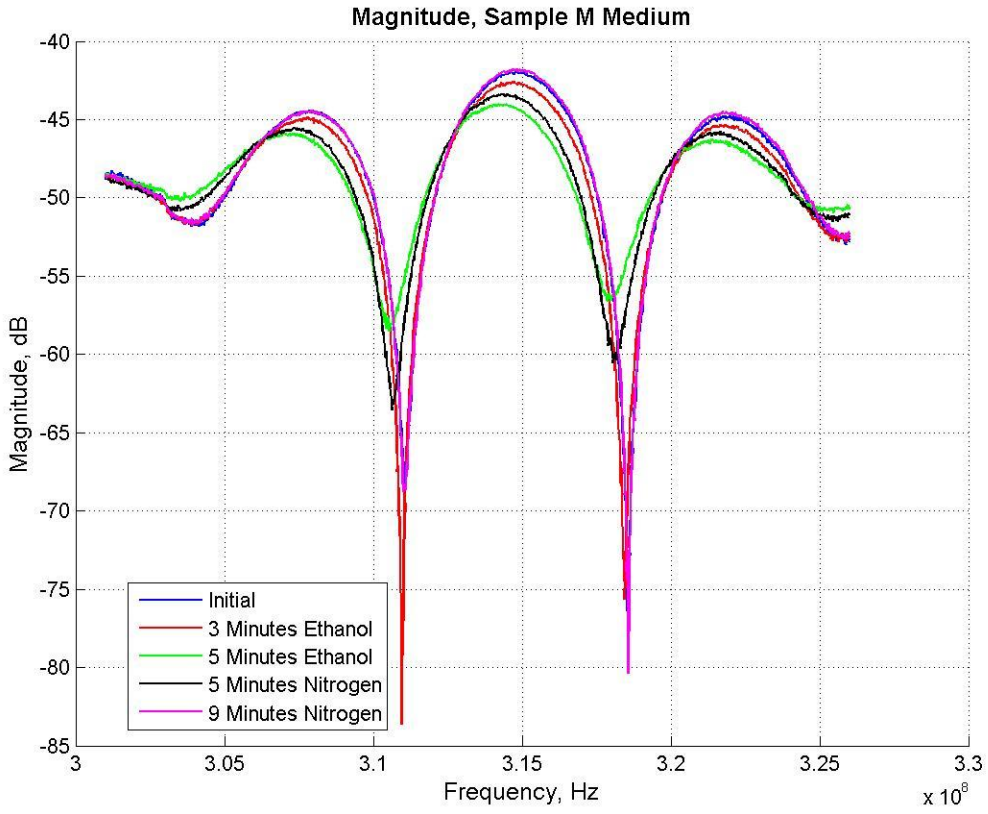

Figure B3 3µm Medium, Sample M, 5% wt Nafion®, Magnitude

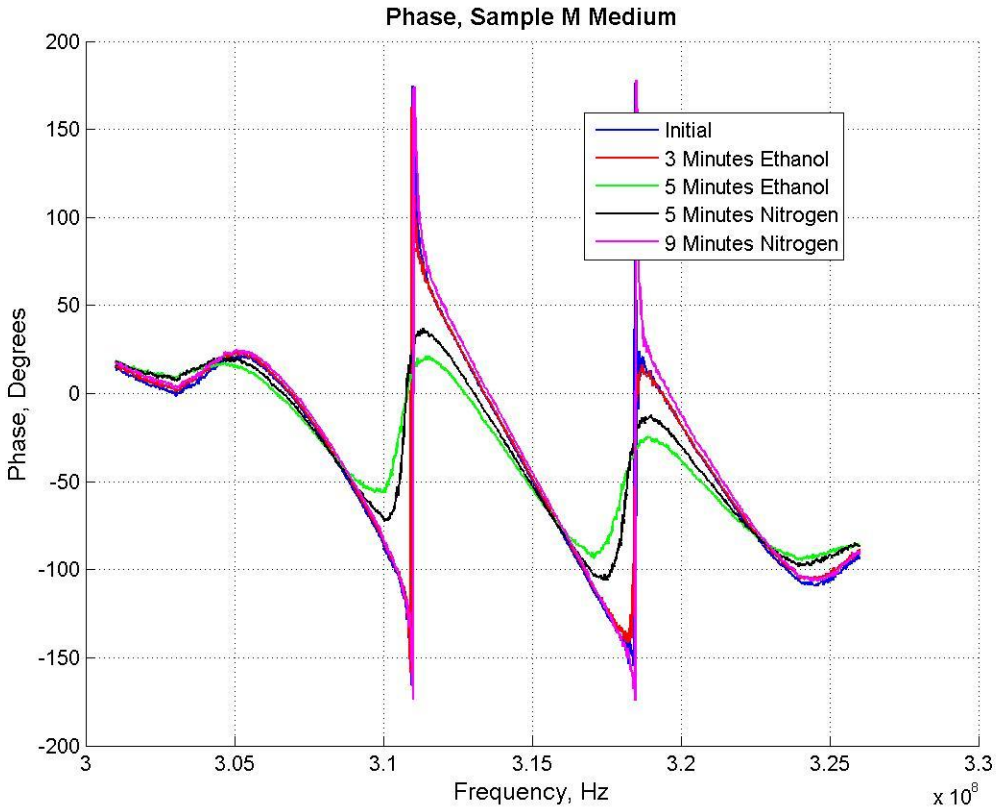

Figure B4 3µm Medium, Sample M, 5% wt Nafion®, Phase

Data for the large devices shown here is from tests conducted on 3 December 2009. The first large device traces do not how the actual typical trace information.

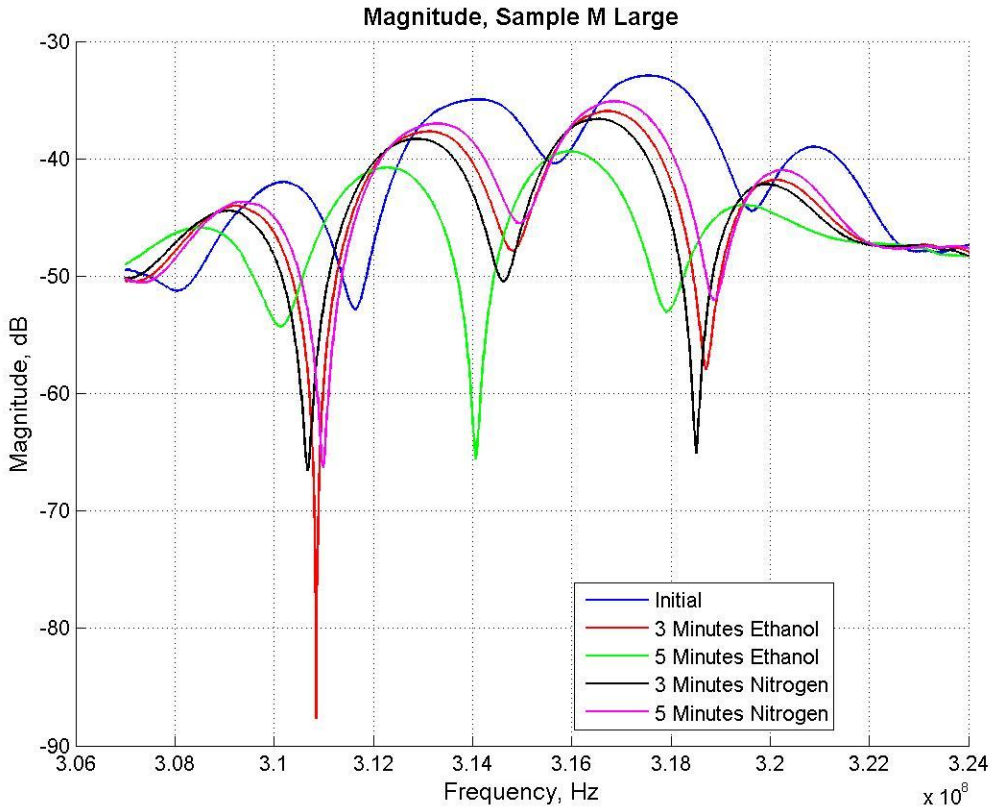

Figure B5 3µm Large, Sample M, 5%wt Nafion®, Magnitude

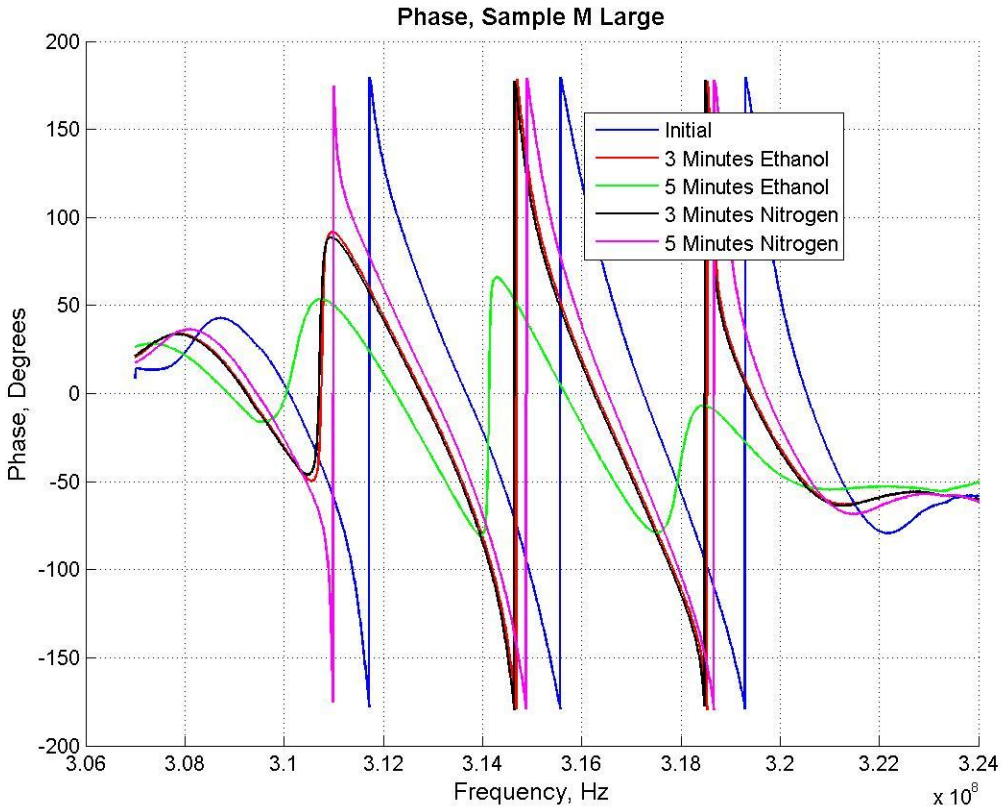

Figure B6 3µm Large, Sample M, 5% wt Nafion®, Phase

The graphs show that the magnitude traces from the medium and large devices are comparable in bandwidth and magnitude differences. Later tests focus on the large devices because they should have the more measurable change and the trenches for the large devices etched the best. The negative peaks of the large samples show a larger shift down in frequency than the shifts in the medium devices. Therefore, the changes in the traces are easier to see. Additionally, the longer fingers and larger center to center spacing produce a narrower bandwidth. One may ask, then, why the different patterns were made. Part of it was that as the fingers get longer, they become more difficult to fabricate. In addition, the different devices allow for an interesting comparison of patterns

and show that at some point there is a significant difference, such as between the small and the medium devices. But the difference between the medium and the large is not as significant. The sizes and their specific signatures is not the focus of this study, so there is no indepth comparison between the signatures. Most tests are performed on the large devices because it is predicted at the larger surface area of their propagation field provides the most opportunity for seeing the effects of the alterations to the propagation field.

Section B2: 2μm Device Graphs

Not much data from the 2μm devices exists. Below is a graph of three devices tested without Nafion® on the chip. The lines are thick because in order to graph the information a scatter plot is used because different windows for frequency were used. The graph shows that the first device is exhibiting surface acoustic wave activity, and the trace for the second device does not extend far enough to show any activity. The data from the 2μm finger device was collected on 18 November 2009. The trace data on Sample 1 can be seen to alter based on ethanol exposure and starts to reset after nitrogen cleans the system. The SAW activity almost disappears because of the amount of ethanol in the chamber and the saturation of the Nafion®. The high flow rate of the unregulated nitrogen bubbling through the ethanol caused the signal saturation in a very short period of time. The same flow rate of nitrogen does not clean off the surface as fast as the ethanol affects it. Also, because of the low magnitude values of the initial signal, very little ethanol is needed to negate the signal. It is likely that because the 2μm devices are so difficult to make not all of the fingers are aiding in forming the SAW, which makes

the signal weak and not as useful for making measurements. The SAW activity that does appear is at a much higher frequency, around 425MHz than the 3µm devices, which have SAW activity at the 311MHz region. The difference is because of the finger width.

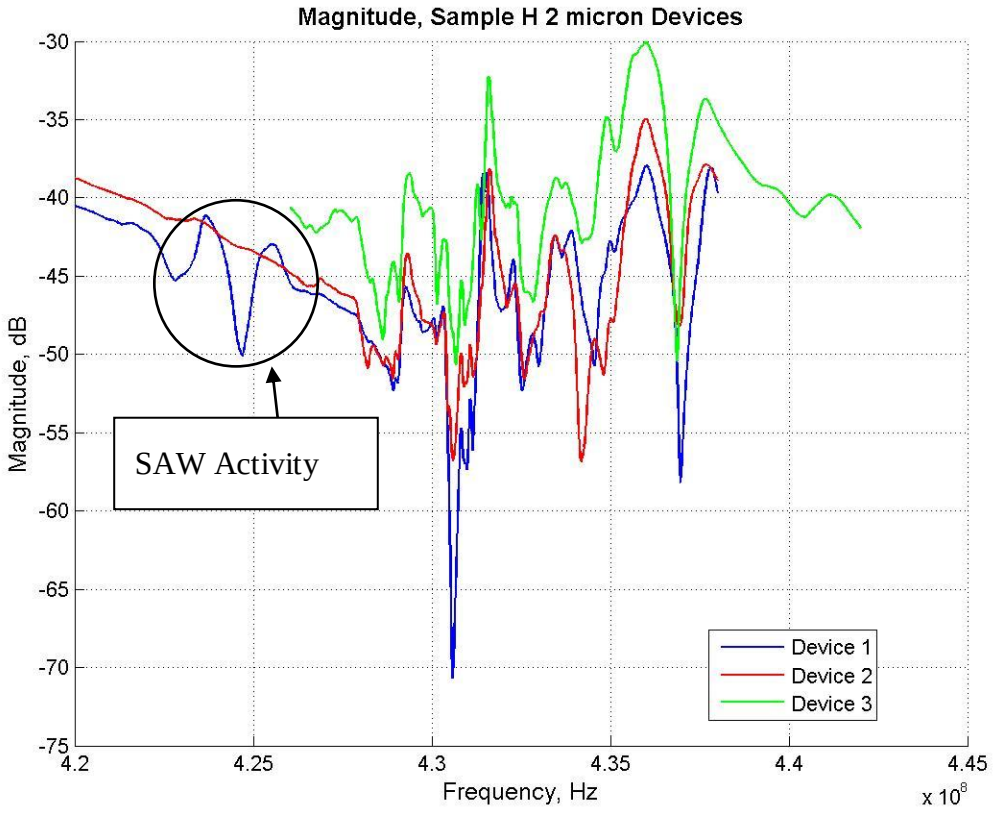

Figure B7 2µm Fingers, Sample H, no Nafion®, Magnitude

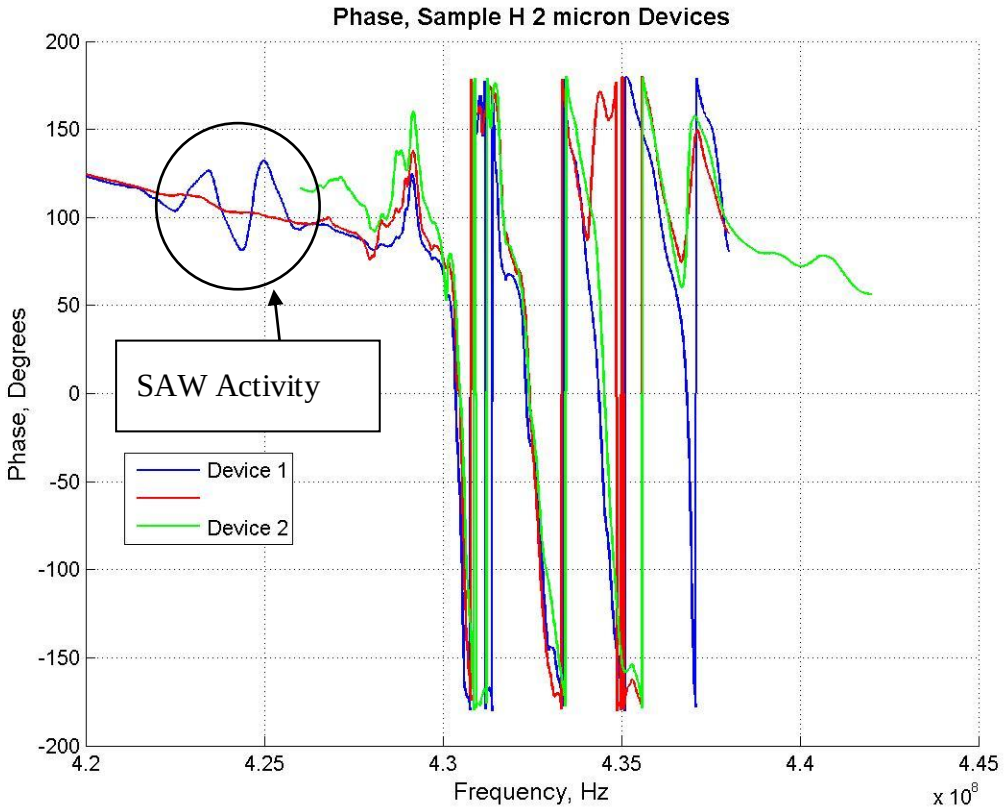

Figure B8 2µm Fingers, Sample H, no Nafion®, Phase

Section B3: AFRL Device Data

AFRL patterns of 3µm and 6µm fingers are used to start the research and work with the fabrication process while the mask for other 3µm finger devices is designed and developed. Learning how long to expose the chips to ethanol and learning what sorts of signatures represent SAW activity are the lessons taken from testing the AFRL devices. The 6µm and 3µm devices are easier to make than the 2µm devices that were also available for production at the beginning of the research. The AFRL devices are much smaller than the later designs. AFRL devices have fewer and shorter fingers.

The tests from the 3μm AFRL designs were done early in the testing process to show some sensing and get used to the test set up. The 3μm devices show better surface activity signals than the 6μm devices. The tests are only run for 5 minutes of ethanol, which is not long enough to provide enough ethanol to the device for it to produce an apparent sensing shift.

Section B4: Large 3μm Devices, Propagation Field Alterations

Sample N is the unaltered sample with a normally coated Nafion® layer. The traces show two major areas where the SAW propagates. One is around the 315MHz region and the other is at the 325MHz region. An interesting point is that a sharp downward spike occurs during sensing, seen in Figure B9. The spike is observed on multiple devices and may be a good marker to look for in identification.

Nitrogen traces with a label of "plus #" indicate that after regulating the flow for a period of time, the flow of nitrogen is unrestricted for the number of "plus" minutes specified. An unregulated nitrogen flow lets the chamber reset completely for the next test and proves that the piece entirely recovers if given enough time.

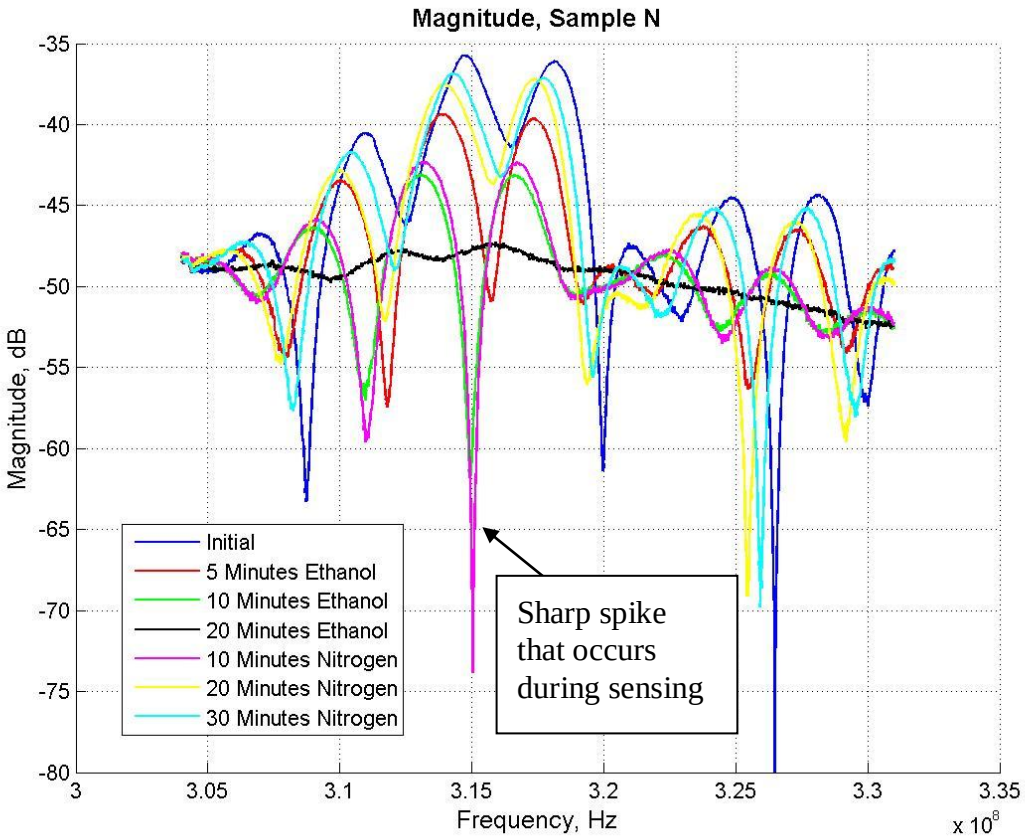
Magnitude, Sample N
Magnitude, dB
-35
-40
-45
-50
-55
-60
-65
-70
-75
-80
3
3.05
3.1
3.15
3.2
3.25
3.3
3.35
Frequency, Hz
x 10^8
Initial
5 Minutes Ethanol
10 Minutes Ethanol
20 Minutes Ethanol
10 Minutes Nitrogen
20 Minutes Nitrogen
30 Minutes Nitrogen
Sharp spike that occurs during sensing

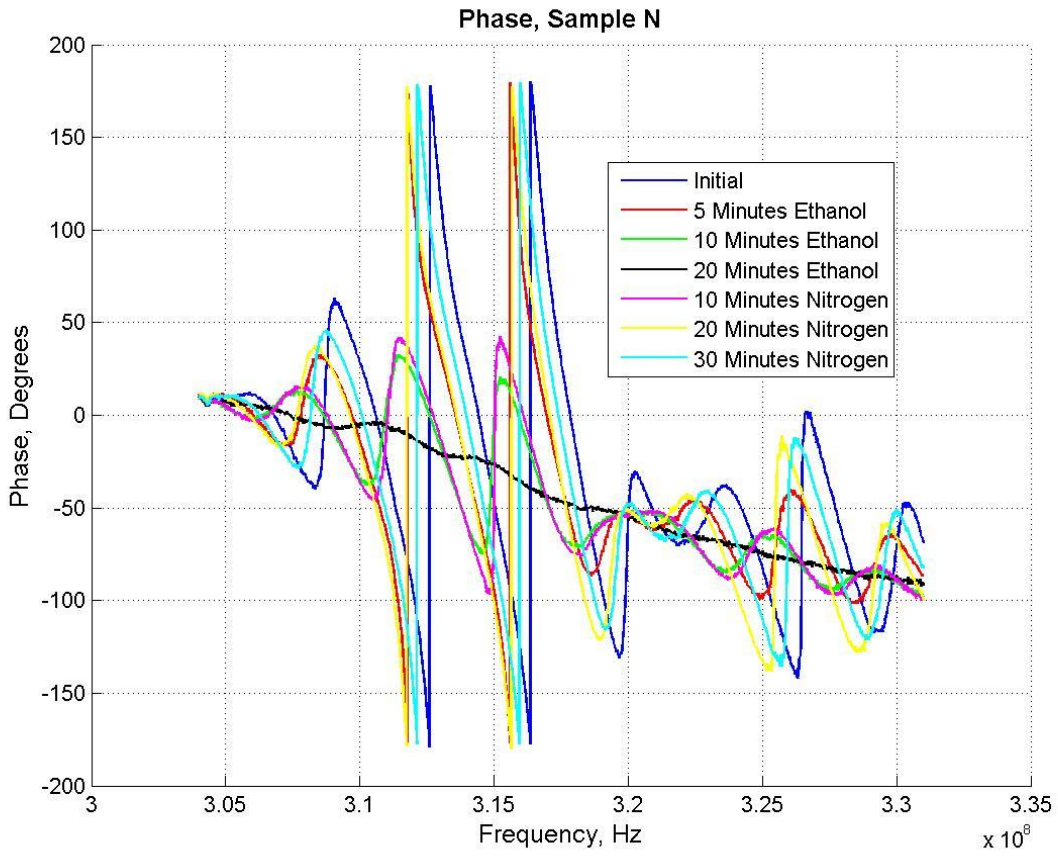

Figure B9 Sample N Magnitude and Phase Traces

Sample F, shown in Figure B10 is the device with CNTs under the Nafion®. Depositing CNTs in windows of photoresist and then cleaning off the photoresist cleans off the CNTs as well, so instead, a solution of methanol and DI water with CNTs is deposited on the chips and as the methanol and water evaporate leaves CNTs on the surface. There appears to be no significant advantage of having CNTs under the Nafion®.

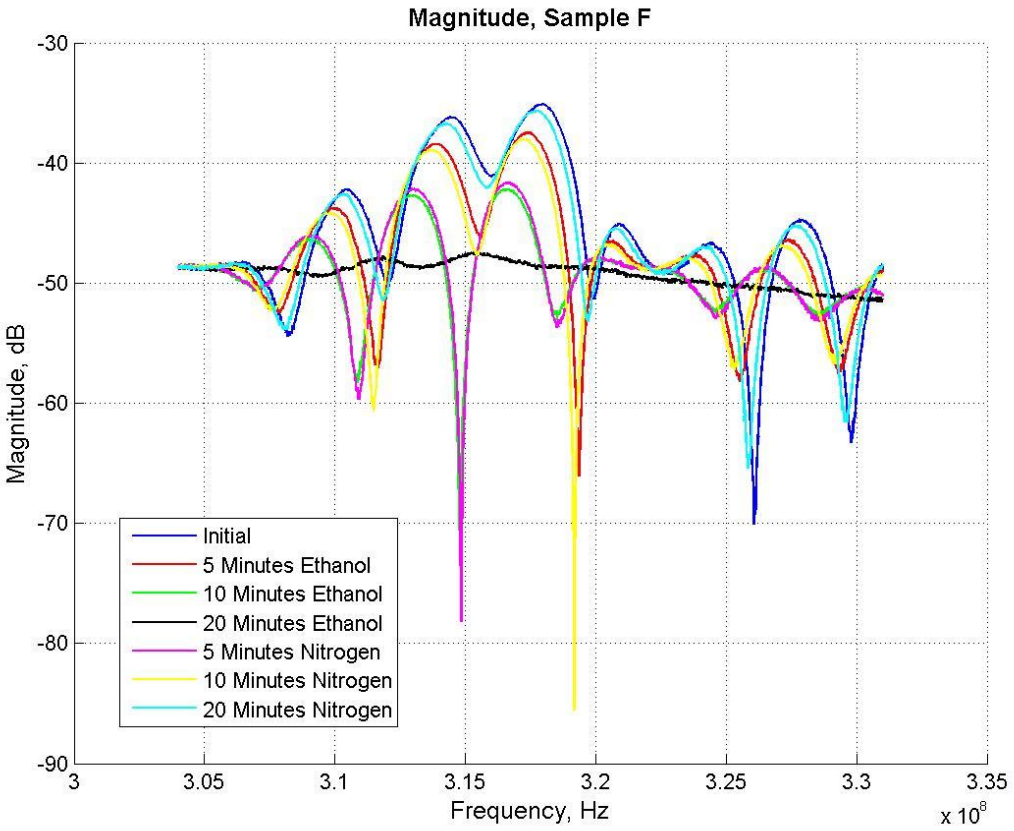
Magnitude, Sample F
-30
-40
-50
-60
-70
-80
-90
Magnitude, dB
3
3.05
3.1
3.15
3.2
3.25
3.3
3.35
Frequency, Hz
x 10^8
Initial
5 Minutes Ethanol
10 Minutes Ethanol
20 Minutes Ethanol
5 Minutes Nitrogen
10 Minutes Nitrogen
20 Minutes Nitrogen

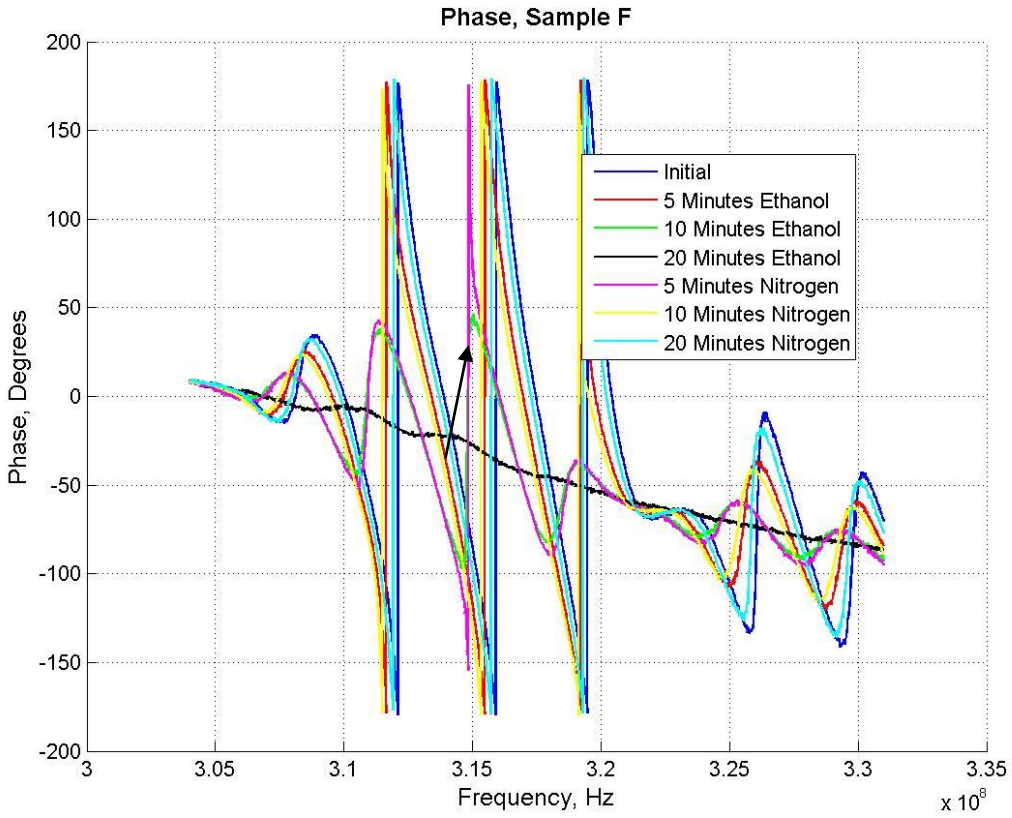

Figure B10 Sample F Magnitude and Phase Plots

Sample M contains CNTs on the surface of the Nafion®. One possible advantage of the CNTs on the surface is that the signal appears to keep its shape better and does not become saturated enough to dampen the signal seen in Figure B11. However, there did not appear to be more shifting that would occur in the trace after the typical saturation point.

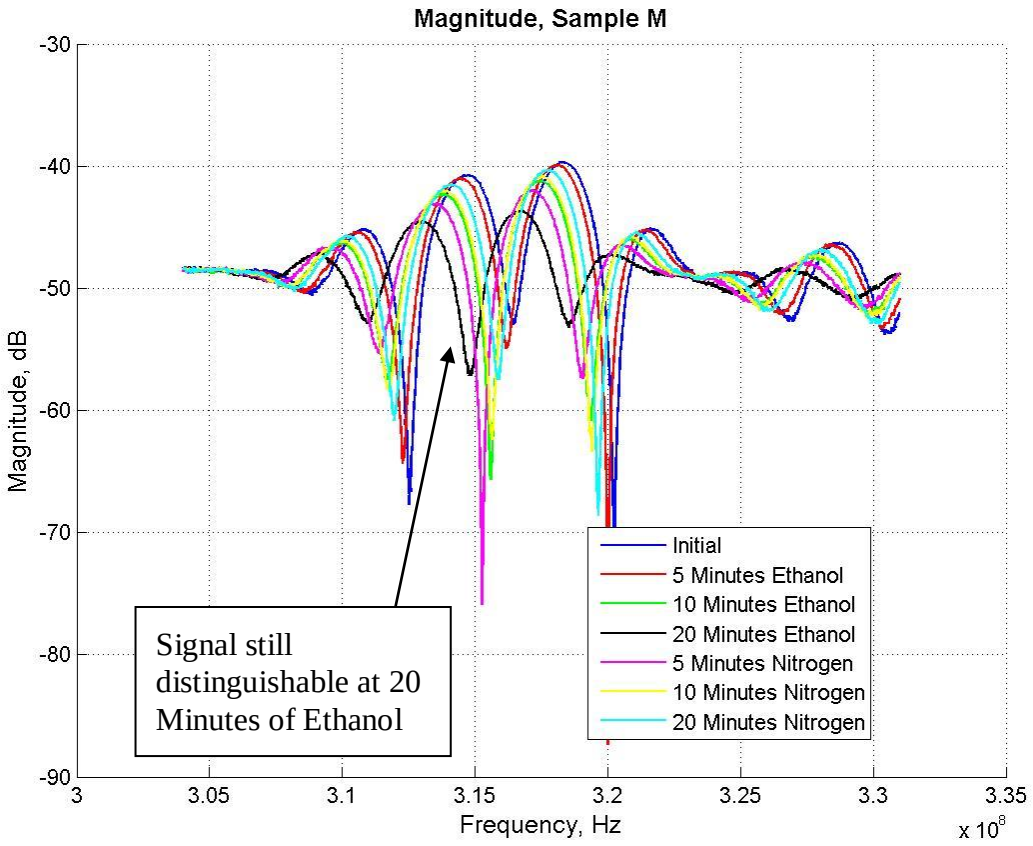
Magnitude, Sample M
-30
-40
-50
-60
-70
-80
-90
Magnitude, dB
3
3.05
3.1
3.15
3.2
3.25
3.3
3.35
Frequency, Hz
x 10^8
Initial
5 Minutes Ethanol
10 Minutes Ethanol
20 Minutes Ethanol
5 Minutes Nitrogen
10 Minutes Nitrogen
20 Minutes Nitrogen
Signal still distinguishable at 20 Minutes of Ethanol

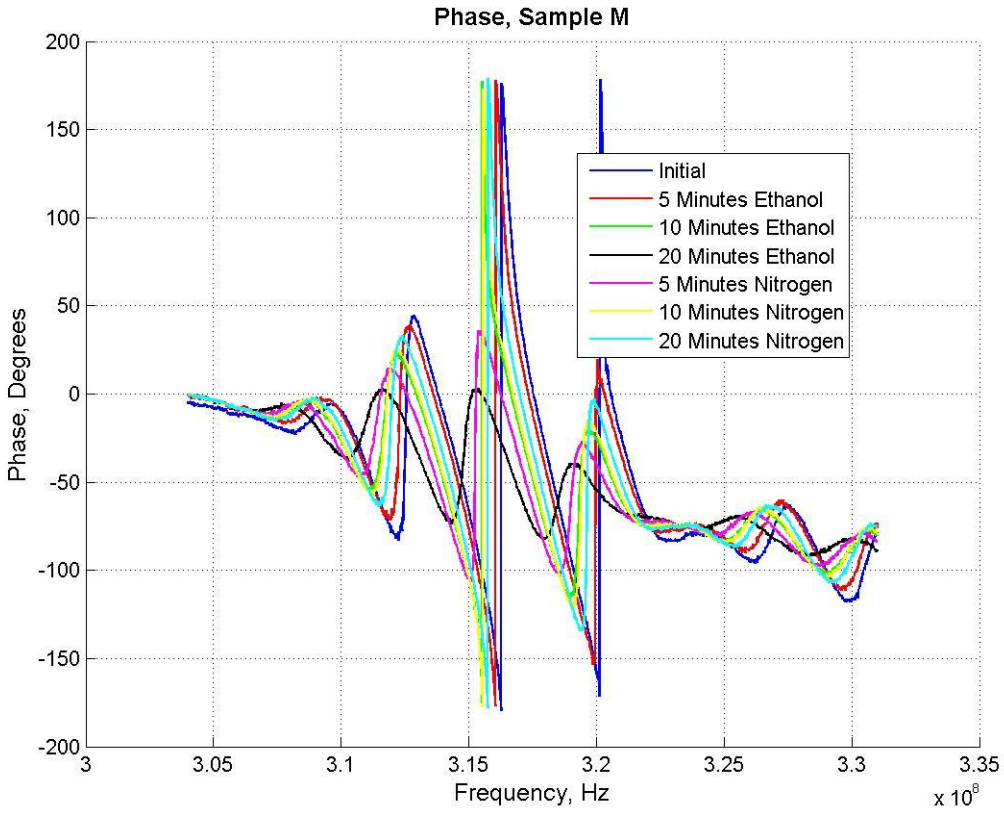

Figure B11 Sample M Magnitude and Phase Plot

Sample Z4 is coated with zinc oxide and contains the devices with no trenches etched in the zinc oxide. The zinc oxide allows for SAW propagation, but appears to dampen the signal slightly so that the downward spikes are not as prominent. In addition, the phase plot, shown in Figure B12 shows less spikes with no trenches than the samples with zinc oxide trenches.

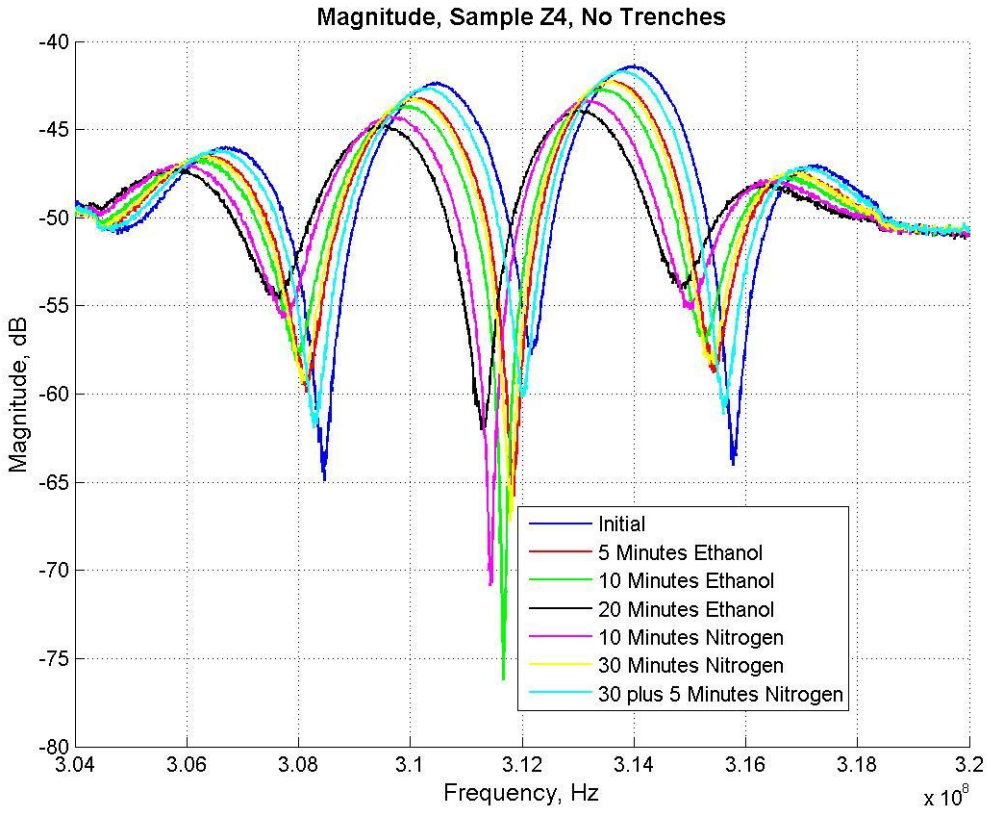
Magnitude, Sample Z4, No Trenches
-40
-45
-50
-55
-60
-65
-70
-75
-80
Magnitude, dB
3.04
3.06
3.08
3.1
3.12
3.14
3.16
3.18
3.2
Frequency, Hz
x 10^8
Initial
5 Minutes Ethanol
10 Minutes Ethanol
20 Minutes Ethanol
10 Minutes Nitrogen
30 Minutes Nitrogen
30 plus 5 Minutes Nitrogen

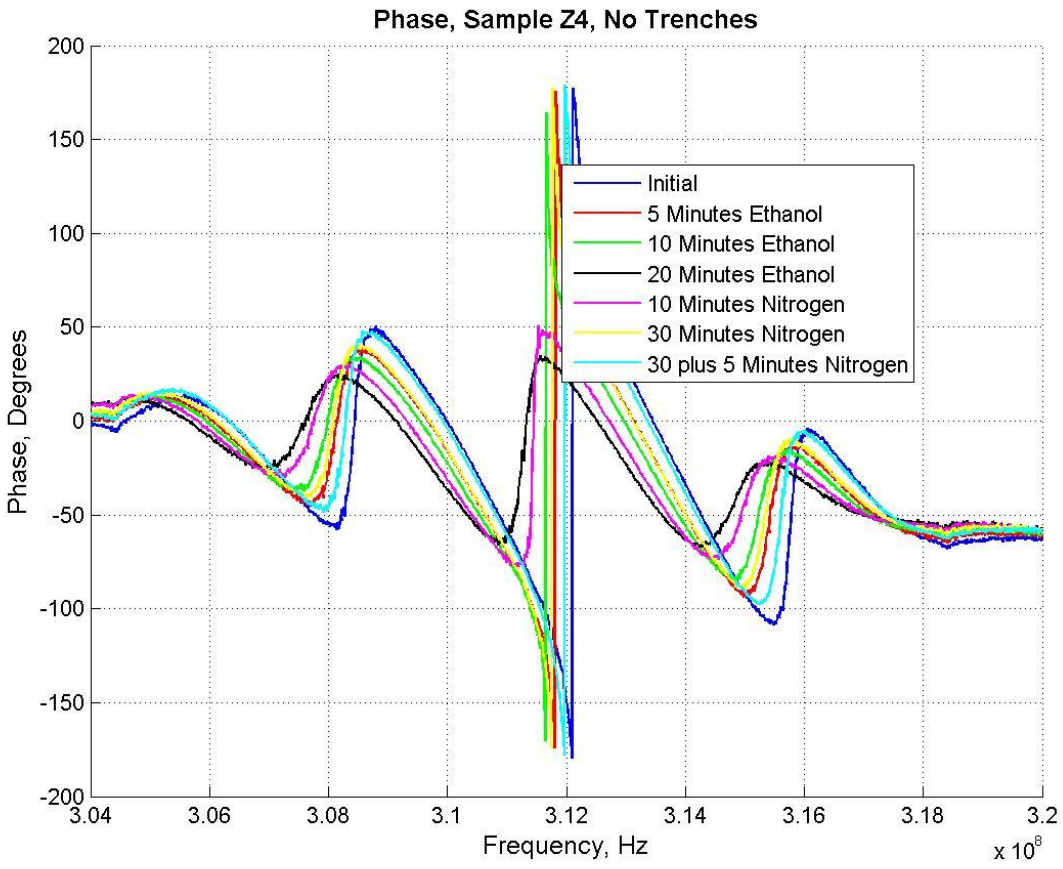

Figure B12 Sample Z4, a zinc oxide sample with no trenches

The zinc oxide layered samples with trenches show a wider spread in the frequency plots, which indicates that the signal shifts more with the trenches. The phase plots, shown in Figure B13 and Figure B14 show a much larger shift in the location of the phase spikes than Figure B12. One disadvantage of the trenches is that it takes a longer period of time for the signal to return to the initial location. The amount of time needed may be related to the sensitivity of the device, but it could also be that the nitrogen does not clean the surface of the trenches as well as it cleans the surface of an unaltered device. In other words, the ethanol particles are able to cling to the Nafion® within the

trenches better, which means that the Nafion® continues to affect the wave propagation for a longer period of time.

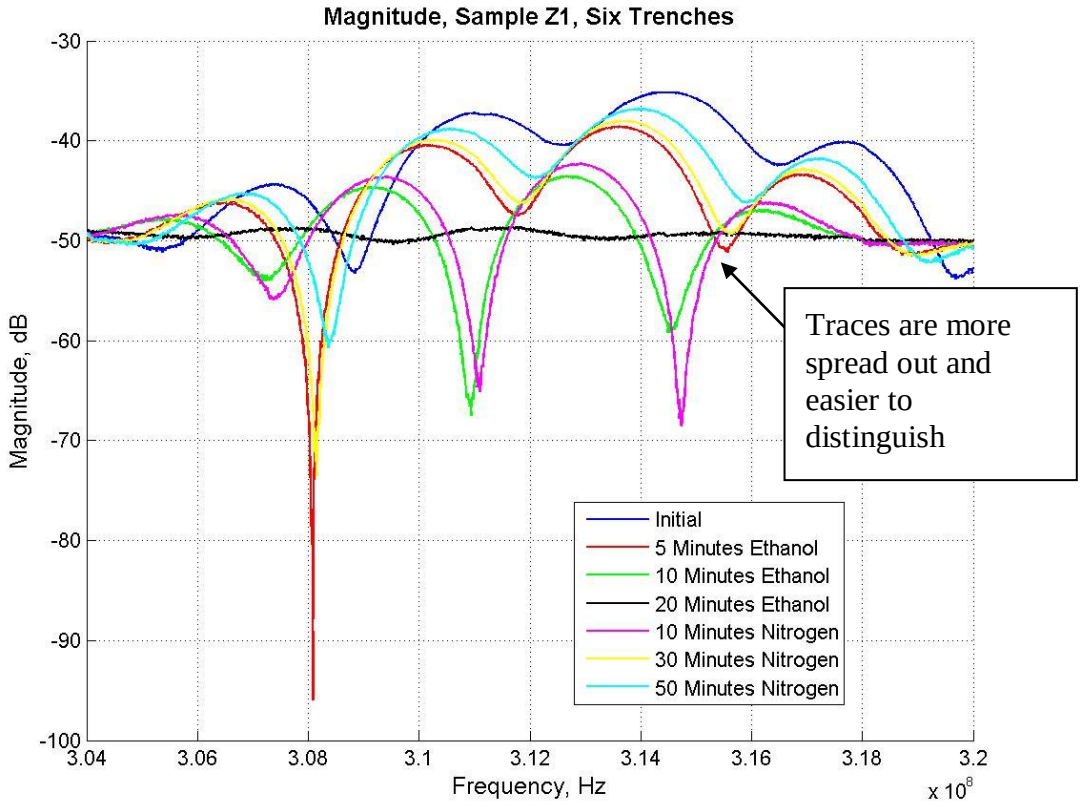

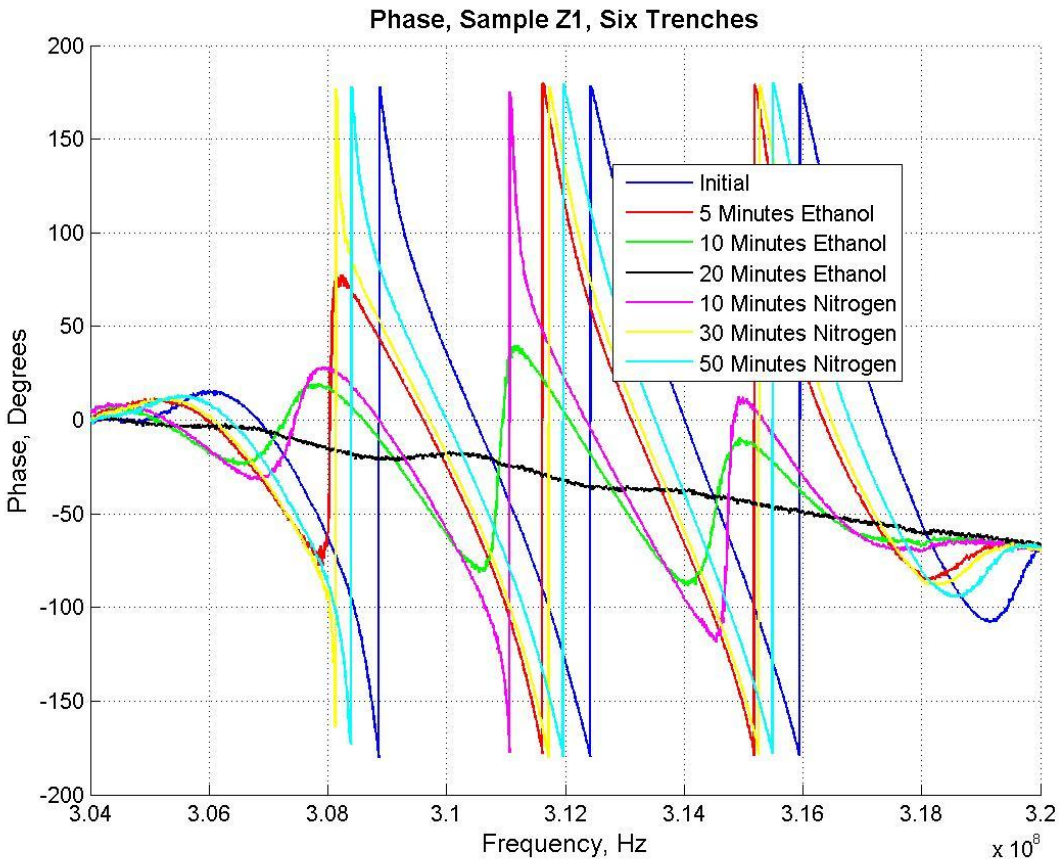

Figure B13 Sample Z1, Six Trench Device

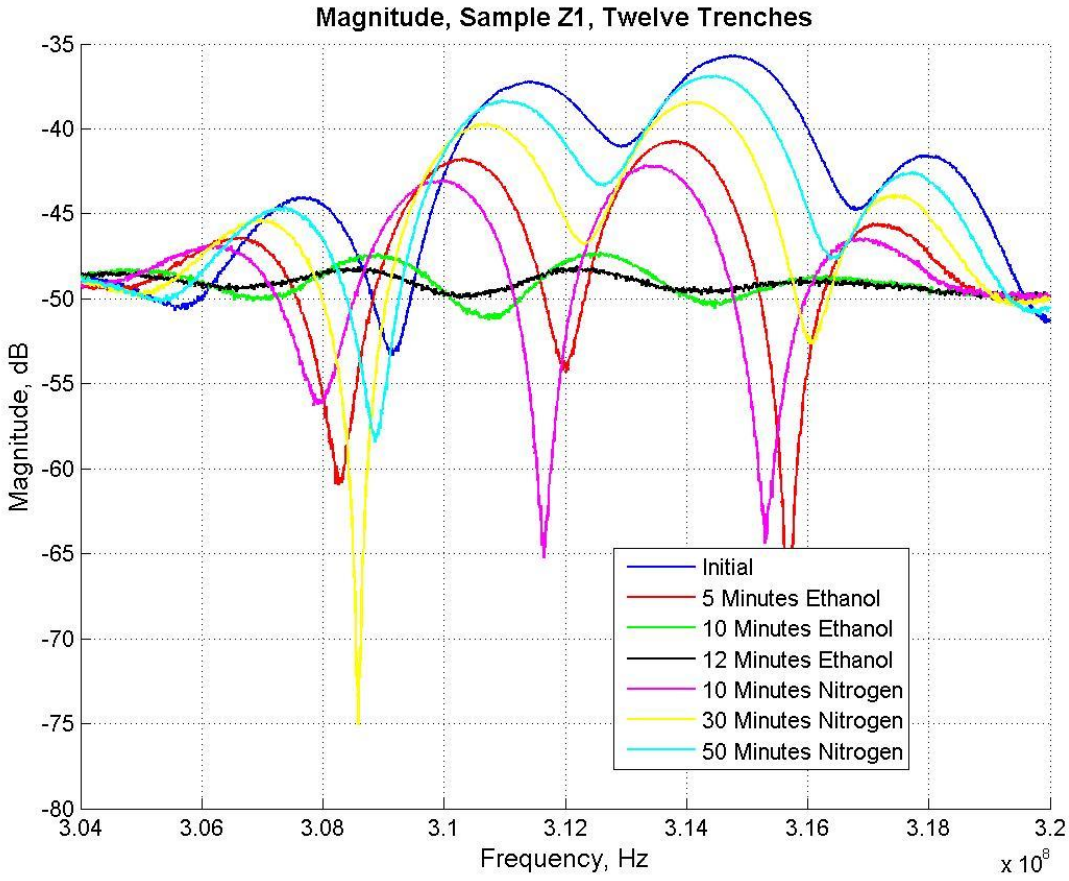
Magnitude, Sample Z1, Twelve Trenches
Magnitude, dB
-35
-40
-45
-50
-55
-60
-65
-70
-75
-80
3.04
3.06
3.08
3.1
3.12
3.14
3.16
3.18
3.2
Frequency, Hz
x 10^8
Initial
5 Minutes Ethanol
10 Minutes Ethanol
12 Minutes Ethanol
10 Minutes Nitrogen
30 Minutes Nitrogen
50 Minutes Nitrogen

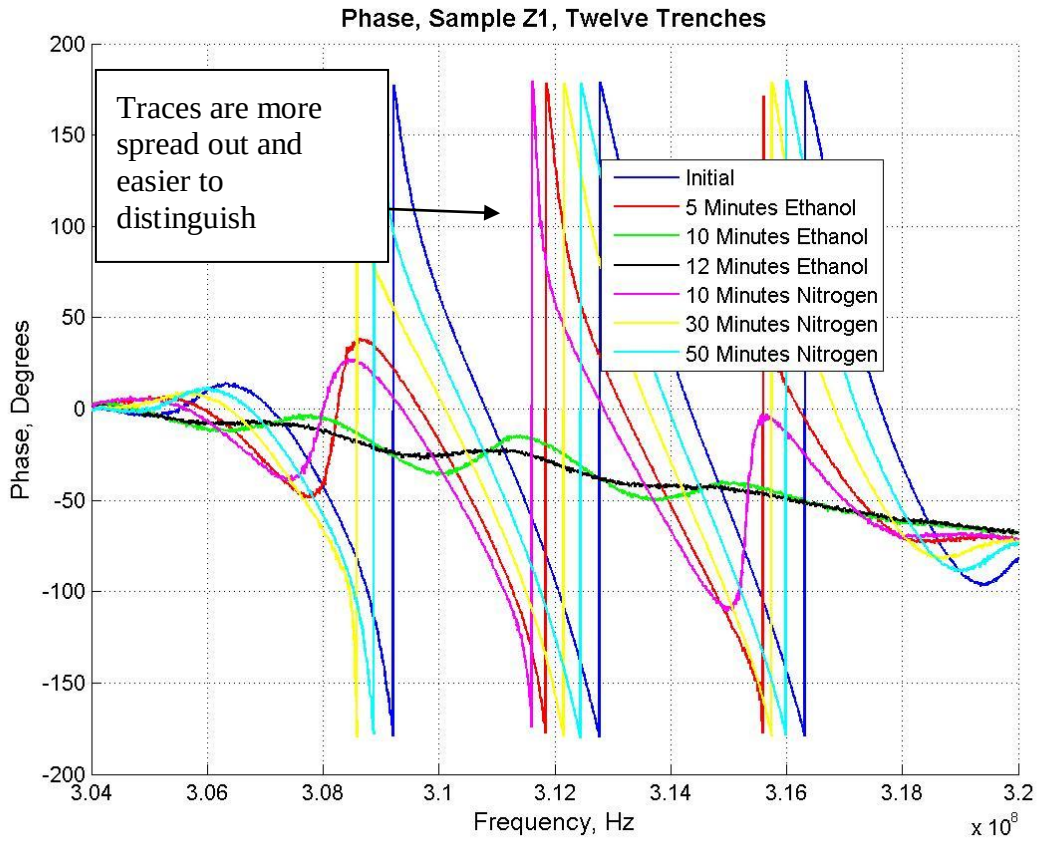

Figure B14 Sample Z1 a Twelve Trench Device

Appendix C Lessons Learned

Testing takes a lot of time; it requires time to get used to the set up and figure out what exactly is going on with the devices and what the best way to test them and record the data is. The testing takes a long time for each individual device (almost an hour and a half in some cases), especially if the data needs to reflect how the traces change with respect to different levels of ethanol because the flow rate needs to be so low. Identifying the proper flow rates to use is very important, but the same flow rate must be used on each device so that comparisons can be made between the data.

The nanowires need to be tested with a range of currents, but currents below 0.1μA do not return good results. At least 20 points are needed for a good resistance line for the nanowires. However, more is better. The resistance tests do not take long if the timing delays are turned way down on the Keithley 4200. However, flooding the chamber with ethanol or DNT still takes time. Switching between DNT and ethanol using the OVG is not easy if the temperature needs to be adjusted because the OVG takes time to change temperature.

Learning the ins and outs of fabricating and the cleanroom also takes time. Fabrication always takes longer than expected and never seems to work as well as it should. There must be tricks of the trade or simple things that go wrong every time until they are learned. Making multiple samples also takes time because of the cleaning and baking processes involved.

Bibliography

1. D. Gallagher, "Surface Acoustic Wave Devices As Chemical Vapor Sensors," 2009.

2. Yushi Hu, D. Perello, U. Mushtaq and Minhee Yun. (2008) A single palladium nanowire via electrophoresis deposition used as a ultrasensitive hydrogen sensor. *Nanotechnology, IEEE Transactions on 7(6),* pp. 693-699.

3. D. Kazachkin, "Investigation of Chemical and Adsorption Properties of Carbon Nanotubes: Building a Bridge for Technological Applications of Carbon Nanotubes," 2009.

4. X. Feng, "Application of Single Walled Carbon Nanotubes in Environmental Engineering: Adsorption and Desorption of Environmentally Relevant Species Studied by Infrared Spectroscopy and Temperature Programmed Desorption," 2005.

5. M. L. P. da Silva and J. G. Gameiro, "Pre-Concentrators: Trends and Future Needs," *Revista Brasileira De Aplicações De Vácuo,* vol. 25, pp. 123-130, 2006.

6. D. W. Hannum. (2000, Miniaturized explosives preconcentrators for use in man-portable explosives detection systems. *IEEE Annual International Carnahan Conference on Security Technology, Proceedings* pp. 222-227.

7. J. W. Judy, "MEMS Design Lecture: MEMS Foundries: Features/Consequences and the MUMPS Process," 2005.

8. D. S. Ballantine, R. M. White, S. J. Martin, A. J. Ricco, E. T. Zellers, G. C. Fry and H. Wohltjen, *Acousitc Wave Sensors Theory, Design, and Physico-Chemical Applications.* Sandiego: Academic Press, 1997, pp. 435.

9. T. C. Pearce, S. S. Schiffman, H. T. Nagle and J. W. Gardner, *Handbook of Machine Olfaction Electronic Nose Technology*. Federal Republic of Germany: Wiley-VCH, 2003, pp. 577.

10. Microsensor Systems Inc., "VaporLab Questions and Answers," vol. 2009, 2004.

11. Electronic Sensor Technology. Model 4500 mobile ultra-fast GC analyzer.

12. P. R. Lewis, P. Manginell, D. R. Adkins, R. J. Kottenstette, D. R. Wheeler, S. S. Sokolowski, D. E. Trudell, J. E. Byrnes, M. Okandan, J. M. Bauer, R. G. Manley and C. Frye-Mason. (2006) Recent advancements in the gas-phase MicroChemLab. *Sensors Journal, IEEE 6(3),* pp. 784-795.

13. J. Simonson, "Micro Analytical Systems Department Technology - MicroChemLab Fact Sheet," 2001.

14. B. Drafts. (2001) Acoustic wave technology sensors. *Microwave Theory and Techniques, IEEE Transactions on 49(4),* pp. 795-802.

15. S. J. Martin, G. C. Frye, J. J. Spates and M. A. Butler. (1996) Gas sensing with acoustic devices. *Ultrasonics Symposium, 1996. Proceedings. , 1996 IEEE 1*pp. 423-434 vol.1.

16. I. Voiculescu, M. Zaghloul and N. Narasimhan. (2008, 4). Microfabricated chemical preconcentrators for gas-phase microanalytical detection systems. *TrAC Trends in Analytical Chemistry 27(4),* pp. 327-343.

17. C. Heitner-Wirguin. (1996, 10/30). Recent advances in perfluorinated ionomer membranes: Structure, properties and applications. *J. Membr. Sci. 120(1),* pp. 1-33.

18. W. -. Tian, H. K. L. Chan, S. W. Pang, C. -. Lu and E. T. Zellers. (2003) High sensitivity three-stage microfabricated preconcentrator-focuser for micro gas chromatography. *TRANSDUCERS, Solid-State Sensors, Actuators and Microsystems, 12th International Conference on, 2003 1*pp. 131-134 vol.1.

19. Wei-Cheng Tian, H. K. L. Chan, Chia-Jung Lu, S. W. Pang and E. T. Zellers. (2005, Multiple-stage microfabricated preconcentrator-focuser for micro gas chromatography system. *Microelectromechanical Systems, Journal of 14(3),* pp. 498-507.

20. Wei-Cheng Tian, S. W. Pang, Chia-Jung Lu and E. T. Zellers. (2003) Microfabricated preconcentrator-focuser for a microscale gas chromatograph. *Microelectromechanical Systems, Journal of 12(3),* pp. 264-272.

21. J. W. Gardner and J. Yinon, *Electronic Noses & Sensors Detection of Explosives.* vol. 159, Dordrecht: Kluwer Academic Publishers, 2004, pp. 308.

22. Yun, Minhee and Coutu, Ronald, "Collaborative research explosive detection using an integrated single nanowire array sensor on a chip and a surface-modified-based single nanowire field-effect-transistor." University of Pittsburgh, 2009.

23. Y. Hu, A. C. To and M. Yun. (2009) The controlled growth of single metallic and conducting polymer nanowires via gate-assisted electrochemical deposition. *Nanotechnology (28),* pp. 285605. Available: http://stacks.iop.org/0957-4484/20/285605

24. C. Liu, *Foundations of MEMS.* Upper Saddle River, NJ: Pearson Prentice Hall, 2006, pp. 530.

25. R. Lake, 2010.

26. D. Gallagher, "Surface Acousitic Wave Devices as Chemical Vapor Sensors,"

27. J. Hone, "Carbon Nanotubes: Thermal Properties," *Dekker Encyclopedia of Nanoscience and Nanotechnology,* 2004.

28. R. E. Majors and P. W. Carr, "Glossary of HPLC/LC Separation Terms," vol. 2009, pp. 1, February 1, 2008.

REPORT DOCUMENTATION PAGE

Form Approved
OMB No. 074-0188

1. REPORT DATE *(DD-MM-YYYY)*	**2. REPORT TYPE**	**3. DATES COVERED** *(From – To)*
19-02-2010	**Master's Thesis**	August 2008-March 2010

4. TITLE AND SUBTITLE
Increasing the Sensitivity of Surface Acoustic Wave (SAW) Chemical Sensors and other Chemical Sensing Investigations

5a. CONTRACT NUMBER

5b. GRANT NUMBER

5c. PROGRAM ELEMENT NUMBER

6. AUTHOR(S)

Smith, Nina R., 2nd Lieutenant, USAF

5d. PROJECT NUMBER
Intentionally left blank

5e. TASK NUMBER

5f. WORK UNIT NUMBER

7. PERFORMING ORGANIZATION NAMES(S) AND ADDRESS(S)
Air Force Institute of Technology
Graduate School of Engineering and Management (AFIT/EN)
2950 Hobson Way, Building 640
WPAFB OH 45433-8865

8. PERFORMING ORGANIZATION REPORT NUMBER
AFIT/GE/ENG/10-28

9. SPONSORING/MONITORING AGENCY NAME(S) AND ADDRESS(ES)
Air Force Research Laboratory
Attn: Daniel Gallagher, AFMC AFRL/RXBN Daniel.Gallagher@WPAFB.AF.MIL 937-785-9106
3005 Hobson Way, Building 654
WPAFB, OH 45433

10. SPONSOR/MONITOR'S ACRONYM(S)
AFRL/RXBN

11. SPONSOR/MONITOR'S REPORT NUMBER(S)

12. DISTRIBUTION/AVAILABILITY STATEMENT
Approved for Public Release; Distribution Unlimited

13. SUPPLEMENTARY NOTES

14. ABSTRACT

The work involves the fabrication and testing of three different surface acoustic wave (SAW) device designs, an investigation of nanowires sensitive to chemicals and preconcentrator prototypes to include with chemical sensors. The SAW chemical sensor designs include modifications to a basic SAW device to see if the sensitivity of the SAW device is increased. The modifications consist of etched trenches along the propagation field, coating the device with carbon nanotubes (CNTs) under the chemically sensitive layer and coating CNTs on top of the chemically sensitive layer. SAW devices are coated with Nafion®, a polymer sensitive to ethanol. The tests indicate that trenches etched between the transducer fields increase the sensitivity of the SAW devices. The increase of sensitivity is signified by a shift of peak frequency of an extra 100kHz over the unaltered device after five minutes of flowing ethanol.

Testing of the nanowires involves measuring the resistance of palladium, polypyrrole and polyaniline nanowires. Investigation of the nanowires indicates that they are less suited to detecting chemicals in a non-ideal measurement circumstance than SAW devices. Preconcentrators are another way to improve the sensitivity of chemical sensors. Some preconcentrator prototypes fabricated in the PolyMUMPs™ system are tested and evaluated for heating characteristics and abilities.. A grid pattern presents the best way to heat a large surface area the most uniformly. Coating the devices with CNTs also increases the heat to which devices can be heated and decreases the amount of time that it takes to heat the devices.

15. SUBJECT TERMS
Surface Acoustic Wave, Chemical Sensor, Nafion®, nanowires, preconcentrators, MEMS, vapor sensor, electronic nose, piezoelectric

16. SECURITY CLASSIFICATION OF: Unclassified			**17. LIMITATION OF ABSTRACT**	**18. NUMBER OF PAGES**	**19a. NAME OF RESPONSIBLE PERSON**
REPORT	**ABSTRACT**	**c. THIS PAGE**			**Ronald Coutu, PhD**
U	**U**	**U**	**UU**	145	**19b. TELEPHONE NUMBER** *(Include area code)* 937-255-3636(x7230) ronald.coutu@afit.edu

Standard Form 298 (Rev: 8-98)
Prescribed by ANSI Std. Z39-18